Semaphorin receptors in the immunological synapse: regulation and measles virus-driven modulation

Semaphorinrezeptoren in der immunologischen Synapse: Regulierung und masernvirusgesteuerte Modulation

Doctoral thesis for a doctoral degree
at the Graduate School of Life Sciences,
Julius-Maximilians-Universität Würzburg

Section: Infection and Immunity

Submitted by

HIEU TRAN-VAN
from
Nha Trang, Viet Nam

Würzburg 2010

Submitted on:.....

Members of the *Promotionskomitee*:

Chairperson: Prof. Dr. Thomas Dandekar

Primary Supervisor: Prof. Dr. Sibylle Schneider-Schaulies

Supervisor (Second): Prof. Dr. Peter Friedl

Supervisor (Third): Prof. Dr. Marie Christine Dabauvalle

Date of public defence:.....

Date of Receipt of Certificates:.....

For the Hs,
H2 and CC

I hereby declare that my thesis entitled “Semaphorin receptors in the immunological synapse: regulation and measles virus-driven modulation” is the result of my own work. I did not receive any help or support from commercial consultants. All sources and/or materials applied are listed and specified in the thesis.

Furthermore; I verify that this thesis has not yet been submitted as part of another examination process neither in identical nor in similar form.

Würzburg, ...September 2nd, 2010.....Hieu Tran-Van.....

Date Signature

I would like to acknowledge my supervisor committee for their tutoring and mentoring. My grateful thank goes to Prof. Sibylle Schneider-Schaulies, my first supervisor as well as my boss, for her education and expert guidance on my project that help me to be more "mature" in term of scientific abilities. For funding support and program mentoring, I would like to express my appreciation to the Graduate school of Life Sciences, Graduate college of Immunomodulation, which is now renamed Graduate program of Immunomodulation, and their staff as well.

I am indebted to my lab mates, 'Spiderman' Ibo, 'mafia-in' Eve, 'Snow White' Elita, 'süße' Susi, 'nachbar' Andi, Meena, Alice, for their nice support at my very first days in Germany. I am also grateful to Babara, Bea, 'Sonnenschein' Charlene and Caro for their expert technical assistance. Others I would like to thank are Katrin and the neighbor group for their willing to swap materials and eagents, Dr. Avota for her infinite patience to explain and give suggestions.

I would like to express my gratitude to Dr. Harry Harms and Dr. Nora Müller for their invaluable work on imaging documentation, Dr. Rik de Swart, Dr. Martin Ludlow and Rory in Erasmus MC, Rotterdam, The Netherlands for their help in monkey tissue samples, Dr. Michael Sixt in MPI of Biochemistry, Munich for an interesting collaboration, Dr. Luca Tamagnone in IRCC, Turin for his generosity in providing me with human plexA1 constructs using in this project and last but not least, Prof. Jürgen Schneider-Schaulies and Prof. Georg Kohne for their useful comments and creative discussion.

For non-scientific life, I wish to thank the ladies in Guest House of University of Würzburg for showing me how wonderful Germans and Germany are by their willing to organize weekly excursions and culture events.

Thank my friend Duy Phan for his not only critical help in linguistics but also precious advice in scientific activities. I wish to acknowledge any anonymous whose useful projects and information do not include here due to limited space and many thanks to blood donors who made this project possible.

My final but most honest thanks go to Huy Phan for his resolution to computer related issues as well as advice in image and software difficulties and my family for their unconditional love and support that make my life enjoyable.

Akt	serine/threonine-specific protein kinase
BSA	bovine serum albumin
CDK	cyclin-dependent kinase
CFSE	carboxyfluorescein succinimidyl ester
CIITA	class II transactivator
CPE	cythopathic effect
CQ	chloroquine
CRMP	collapsin response mediator protein
CUB	complement binding
DC	dendritic cell
DRM	detergent-resistant membrane microdomain
ER	endoplasmic reticulum
ERM	ezrin/radixin/moesin
FASC	fluorescence activated cell sorting
FCS	fetal calf serum
FIP	fusion inhibitory peptide
GAP	GTPase-activating protein
GEF	guanyl nucleotide exchange factors
ICAM	inter-cellular adhesion molecule
IF	Immunofluorescence
Ig	immunoglobulin
IL	interleukin
IP	immunoprecipitation
IS	immunological synapse
LARG	leukemia-associated Rho GEF
LFA	leukocyte function associated antigen
LIMK	LIM domain kinase
LPS	lipopolysaccharide
MAM	merphin A5
MDDC	monocyte-derived dendritic cells
MHC	major histocompatibility complex

MICAL	molecule interacting with CasL
MLR	mixed lymphocyte reaction
MTOC	microtubulin organizing center
MV	measles virus
NP	neuropilin
PAK	p21- activated kinase
PAO	phenylarsine oxide
PBL	peripheral blood leukocyte
PDZ	PSD-95/Dlg/ZO-1
PFA	paraformaldehyde
PI3K	phosphatidylinositol-3 kinase
PKC	protein kinase C
plex	plexin
PLL	poly-L-lysine
R18	octadecyl rhodamine B chloride
RNP	ribonucleoprotein
ROCK	Rho-associated coiled-coil containing kinase
SCR	short consensus repeats
SEMA	semaphorin
SHIP	Src homology domain 2 containing inositol-5-phosphatase
SLAM	signaling lymphocytic activation molecule
SMAC	supramolecular activation cluster
TCR	T cell receptor
Th	T helper
TIM	T-cell immunoglobulin domain and mucin domain
TLR	Toll-like receptor
TRAIL	TNF-related apoptosis-inducing ligand
UV	ultraviolet
VSV	vesicular stomatitis virus
WASp	Wiskott-Aldrich Syndrome protein
WAVE	WASP family Verprolin-homologous protein
WB	Western blot
ZAP	ζ-chain associated protein

Declaration i
Acknowledgement ii
Abbreviation iii
Contents vi

1. Introduction 2
1.1. Measles 2
1.1.1. MV morphology and genome structure 3
1.1.1.1. Virus morphology 3
1.1.1.2. Genome structure 3
1.1.2. MV receptor usage 7
1.1.2.1. CD46 7
1.1.2.2. CD150 8
1.1.2.3. Unidentified cellular receptor(s) 9
1.1.3. MV-induced immunosuppression 9
1.1.3.1. Lymphopenia 10
1.1.3.2. MV-driven modulation of DC viability and function 10
1.1.3.3. MV-infected DC-induced T cell suppression 11
1.1.3.4. Viral proteins modulating or silencing T cells 11
1.1.3.5. Surface receptor(s) involved in silencing of T cells 13
1.1.3.6. Signaling pathways targeted by MV 13
1.2. DC-T cell interaction 14
1.2.1. Immunological synapse 14
1.2.2. Termination of immune response 17
1.3. Semaphorins and their role in cell morphology and immune modulation 17
1.3.1. SEMA receptors 18
1.3.1.1. The plex family 18
1.3.1.2. The NP family 18
1.3.2. Cellular morphology regulation 19
1.3.2.1. SEMA-mediated cellular detachment to ECM via plexin 20
1.3.2.2. Induction of cytoskeletal dynamics by plexin-mediated SEMA 20
1.3.3. Immunomodulatory semaphorins 22

1.3.3.1. Semaphorin in DC functions 22
1.3.3.2. Semaphorin-mediated T cell activation, differentiation and termination response 22
1.4. Aims 23
2. General methodologies 26
2.1. Laboratory safety 26
2.2. Chemical reagents 26
2.3. Sterilization 26
2.4. Commonly used solutions and buffers 27
2.4.1. Water 27
2.4.2. Standard buffers 27
2.5. Tissue Culture 27
2.5.1. Solutions and media 27
2.5.1.1. Growth media 27
2.5.1.2. Serum 28
2.5.1.3. Anticoagulant solution 28
2.5.1.4. Trypsin solution 28
2.5.1.5. Freezing medium 28
2.5.2. Miscellaneous 29
2.5.2.1. Poly-L-lysine 29
2.5.2.2. Lubria-Bertani broth (LB broth) 29
2.6. Tissue culture techniques 29
2.6.1. Cultured cell lines 29
2.6.1.1. B95a 29
2.6.1.2. BJAB 29
2.6.2. Maintenance and sub-culturing of B95a and BJAB 30
2.6.3. Maintenance of stocks of frozen cells 30
2.6.4. Recovery of cells from storage at -80˚C 30
2.6.5. Cultured primary cells 31
2.6.5.1. Maintenance and sub-culturing of human T cells 31
2.6.5.2. Maintenance and sub-culturing of human monocyte-derived dendritic cells (MDDCs) 31
2.6.6. Culturing cells on coverslips 32

2.6.7. Trypan blue staining 33
2.7. Viruses 33
2.7.1. Virus strains 33
2.7.2. Virus stock preparation 33
2.7.3. Tissue culture infectious dose assay 34
2.7.4. Inhibition of MV mediated cell-to-cell fusion 35
2.7.5. Infection of MDDCs 35
2.7.6. Virus exposure assay 35
2.8. Detection of molecules of interest by flow cytometry 36
2.8.1. Solutions 36
2.8.1.1. Paraformaldehyde (PFA) fixation buffer 36
2.8.1.2. FACS buffer 36
2.8.1.3. Saponin buffer 36
2.8.2. Monoclonal antibodies and polyclonal antisera 36
2.8.3. Immunofluorescent staining of primary T cells or MDDCs 38
2.8.3.1. Immunofluorescent staining of live cells 38
2.8.3.2. Immunoflourescent staining of fixed cells 38
2.8.4. Immunocytochemical staining of human primary T cells or MDDCs 39
2.8.4.1. Paraformaldehyde fixation 39
2.8.4.2. Immunocytochemical staining of fixed cells 40
2.8.4.3. Detection of filamentous actin in fixed cells 40
2.9. Tracker and inhibitors 40
2.10. Semaphorin treatment 41
2.11. Mixed leukocyte reaction (MLR) 41
2.12. Scanning electron microscopy 41
2.13. Conjugate formation between DC and T cells 42
2.14. Pseudo immunological synapse formation using CD3/28 DYNAL® bead 43
2.15. Western blotting 43
2.15.1. Sample preparation 43
2.15.2. Gel electrophoresis 44
2.16. Amplification of Plasmids 44
2.16.1. Transformation 44
2.16.2. Endo-free plasmid preparation 45

2.17. Handling and disposal of ethidium bromide 45
2.18. Spectrophotometry 45
2.19. DNA gel electrophoresis 45
2.20. Documentation of gel images 46
2.21. Preparation of total RNAs from MDDCs 46
2.22. RT-PCR amplification of SEMA3A 47
2.22.1. Primers 47
2.22.2. RT-PCR 47
2.23. Immuno-precipitation of soluble SEMA3A in supernatants 48
2.24. Under agarose assay 48
2.24.1. Experimental setups 48
2.24.2. Tracking and quantification of migrating cells 49
2.25. FACS-based conjugate analysis 49
2.26. siRNA-mediated plexA1 knockdown 50
2.27. Statistic 50
3. Results 52
3.1. Expression of SEMA3A prototypic receptors on human primary T cells is not grossly altered by MV exposure 52
3.1.1. Expression profile of plexA1 and NP-1 52
3.1.2. PlexA1 and NP-1 expression patterns is not grossly altered by MV exposure 53
3.2. Polyclonal CD3/28 stimulation causes short-term translocation of plexA1 to the T cell surface and increases the percentage of plexA1 as well as NP-1 expressing cells on long-term culturing 55
3.3. PlexA1 is involved in DC-induced T cell proliferation 56
3.3.1. Exogenous blockage of plexA1 directly inhibits T cell proliferation 57
3.3.2. siRNA-mediated knockdown of plexA1 significantly decreases T cell proliferation 57
3.3.3. Ectopic expression of cytoplasmic tailless, but not full length, plex-A1 reduces T cell proliferation 58
3.4. PlexA1 and NP-1 are recruited to the IS 59
3.4.1. PlexA1 translocates towards the interface formed between T cells and DCs 59
3.4.2. NP-1 on T cells is recruited to the IS 60
3.5. MV-driven abrogation of plexA1/NP-1 translocation to the IS 62

3.6. PlexA1 and NP-1 surface expression on maturing DCs is regulated by endocytosis . 63
3.7. Upregulation and early secretion of SEMA3A by MV-DCs 66
3.8. SEMA3A and, to a greater extent, SEMA6A causes a transient loss of F-actin and microvillar extension in T cells 69
3.8.1. SEMA3A and -6A cause a transient loss of F-actin, while front-rear polarization remains unaffected 69
3.8.2. SEMA3A and SEMA-6A cause transient loss of microvillar extensions in T cells. 70
3.9. SEMA3A reduces the mean velocities of DCs but not T cells under "semi-3D" migratory condition 72
3.10. DC/T cell conjugate formation decreases in the presence of SEMAs 74
4. Discussion 78
4.1. Basic regulation of plexA1 and NP-1 79
4.1.1. Basic regulation of plexA1 and NP-1 in T cells 79
4.1.2. Basic regulation of plexA1 and NP-1 in DCs 81
4.2. MV-driven modulation and consequences 82
5. Summary 89
6. Zusammenfasung 91
7. Reference 93
8. Publication 107
9. Curriculum vitae 108

CHAPTER I
INTRODUCTION

1. Introduction

1.1. Measles

Measles is a highly transmittable disease that is mainly related to childhood. Acute measles is associated with high mortality rates. It can lead to rare but severe, even lethal, complications such as pneumonia, encephalitis, acute measles post-infection encephalitis (AMPE), and subacute sclerosing panencephalitis (SSPE). Although vaccine-preventable, measles is still a major challenge for global healthcare. According to WHO's 2008 annual report, the disease causes approximately 164,000 deaths worldwide per annum and most of the cases occur in low-income countries where healthcare infrastructure is lacking (WHO 2009). Humans are the only existing reservoir for MV (Gerlier, Varior-Krishnan et al. 1995). Although the virus can infect monkeys, primates are not main vectors of transmission (Topley, Wilson et al. 2005; de Swart 2009). It has been estimated that the vaccination of over 90 percent of community is required for prevention of transmission-free condition (Peltola, Heinonen et al. 1994; Biellik, Madema et al. 2002).

The introduction of the global vaccination program against MV has shifted susceptible hosts from infants to teenagers in industrialized countries. The scenario is still different in developing and low-income countries, where children up to 4 years of age are the main target of MV. In addition, malnutrition plus poor healthcare system increases the relative frequency of MV infection in children under 2 year-old there (Bellini, Rota et al. 1994). Therefore, maintaining high vaccine coverage is an accomplishable and efficient step to prevent measles outbreaks and spead.

1.1.1. MV morphology and genome structure

1.1.1.1. Virus morphology

The MV particle consists of a lipid envelope, acquired from the host cell membrane during the budding process, which encloses the viral RNP complex. The complex is comprised of N, P and L proteins associated with viral RNA genome. Surface spike-like projections are made by the transmembrane fusion F and haemagglutinin H proteins (Figure 1-1). It has been shown that the cytoplasmic tails of both F and H functionally and physically interact with matrix proteins M (Cathomen, Mrkic et al. 1998; Cathomen, Naim et al. 1998; Moll, Klenk et al. 2001; Moll, Klenk et al. 2002). The full encapsidation of viral genome makes it resistant to RNase degradation.

The viral virions are pleomorphic with size range from 100 to 300nm and can package more than one genome per particle accounts for its diversity in size (Rager, Vongpunsawad et al. 2002).

1.1.1.2. Genome structure

MV is a prototypic species of *Morbillivirus* genus. It has a single negative stranded RNA genome of about 16kb, which encodes for six structural proteins, in order: 3', nucleoprotein (N), phosphoprotein (P), matrix protein (M), fusion protein (F), haemagglutinin protein (H) and large protein (L) (Dowling, Blumberg et al. 1986), as well as three non-structural (V, R, C) proteins transcribed from the P gene.

1.1.1.2.1. Nucleocapsid protein N

The most abundant 60kDa nucleocapsid protein encapsidates viral genomic and antigenomic RNA in a 'rule of six' manner (Calain and Roux 1993).

In the RNP complex, the N protein is phosphorylated at both serine and threonine in

contrast to the free N which has only phosphorylated serine. The amino terminus of N is highly conserved among MV strains and its conservation was experimentally proven to be required for promoting binding to P protein and for self-assembling of RNP complex (Bankamp, Horikami et al. 1996). In stark contrast, the carboxyl terminus is highly diverse and officially used for genotype assignment.

1.1.1.2.2. Phosphoprotein P and non-structural proteins V, C and R

The 72kDa P protein is abundant in infected cells and a small amount is packed the into infectious virion. Phosphorylation is mediated by cellular casein kinase II (Das, Schuster et al. 1995) and has been shown to be important for P function as polymerase cofactor (Horikami and Moyer 1995). The N interacting domains locate at both amino and carboxyl termini (Harty and Palese 1995) while the central region is shown to be crucial for cytoplasmic retention of N protein (Huber, Cattaneo et al. 1991).

The role of the three non-structural proteins V, C and R is not fully elucidated, particularly the R protein. The V protein contains the amino-terminal region of P but a different, cysteine-rich carboxy-terminal motif. This protein is translated from mRNAs in which one non-templated G residue has been inserted after three genomically encoded Gs (Cattaneo, Kaelin et al. 1989). The 40kDa V protein diffusely distributes in MV-infected cells, distinct from viral nucleocapsids (Wardrop and Briedis 1991).

The 28kDa C protein is translated from an overlapping P reading frame. This protein is abundantly located in the nucleus and in cytoplasmic inclusions of infected cells (Bellini, Englund et al. 1985). Its role in MV replication is not fully characterized. Silencing of this gene doese not affect virus growth in culture (Radecke and Billeter 1996). However, it may contribute to viral pathogenicity and virulence *in vivo* (Valsamakis, Schneider et al. 1998) as also seen in other closely related viruses (Young, Didcock et al. 2000). The defect in MV

protein C and/or protein V interferes with the cellular interferon response (Shaffer, Bellini et al. 2003; Yokota, Saito et al. 2003) as well as virus growth (Baron and Barrett 2000).

1.1.1.2.3. Matrix protein M

The 37kDa M protein is translated from an 1,450 nt mRNA which contains 400 non coding nucleotides at its 3' ends (Bellini, Englund et al. 1986). In infected cells, it locates below the plasma membrane and interacts with the cytoplasmic tail of both glycoprotein F and H (Cathomen, Mrkic et al. 1998; Cathomen, Naim et al. 1998; Moll, Klenk et al. 2001; Moll, Klenk et al. 2002). Its interaction with nucleocapsid is thought to negatively regulate transcriptional activity of RNP complex (Suryanarayana, Baczko et al. 1994). In addition, restricted expression of M by rapid posttranslational degradation or mutational disruption is typically associated with persistent infections *in vivo* (Sheppard, Raine et al. 1986; Billeter, Cattaneo et al. 1994).

1.1.1.2.4. Fusion protein F

The type I glycoprotein F is synthesized as a precursor, then proteolytically cleaved by a host trans-Golgi resident protease to yield a disulfide-linked, biologically functional F_1/F_2 heterodimer. In addition to proteolytical cleavage, glycosylation is also required for its activity (Sato, Kohama et al. 1988; Bolt, Pedersen et al. 1999).

The fusion inhibitory peptide (FIP), which has a similar sequence as polypeptide F1 at the amino terminus, inhibits virus-induced cell fusion (Richardson and Choppin 1983). Moreover, interaction of a central, linear region of F with H is required for virus-induced fusion (Fournier, Brons et al. 1997) and hetero-dimerization of F and H in the ER (Plemper, Hammond et al. 2001). The strength of F/H dimerization and fusogenicity are modulated by their cytoplasmic tail interaction with M protein (Moll, Klenk et al. 2001; Moll, Klenk et

al. 2002; Plemper, Hammond et al. 2002).

1.1.1.2.5. Haemagglutinin H

The type II transmembrane glycoprotein H together with F presents on the surface of the virion as a spike-like protrusions. It mediates viral attachment to receptors (section 1.1.2) and F-dependent fusion. Unlike that of paramyxovirus, MV H has no neuraminidase activity (Colf, Juo et al. 2007). The crystal structure of the wild type H ectodomain reveals a membrane distal orbicular-shaped beta-propeller homodimer. Widely distributed N-linked glycosylation in the globular domain vertically bends the dimer apart and exposes the unshielded putative receptor binding site outwards (Hashiguchi, Kajikawa et al. 2007). Besides its receptor binding function, H has a helper function for F-induced fusion (Billeter, Cattaneo et al. 1994; Fournier, Brons et al. 1997; Plemper, Hammond et al. 2002). Furthermore, epitopes for neutralizing antibodies mostly contain putative binding sites for CD150, but not for CD46 explaning the lymphotropsim of the wild-type strain (Hashiguchi, Kajikawa et al. 2007; Santiago, Celma et al. 2010).

1.1.1.2.6. Large protein L

The 220kDa protein L combined with P protein is a multifunctional RNP-specific RNA polymerase. It produces mRNA, replicative intermediates and progeny viral genomic RNAs (Bankamp, Kearney et al. 2002).

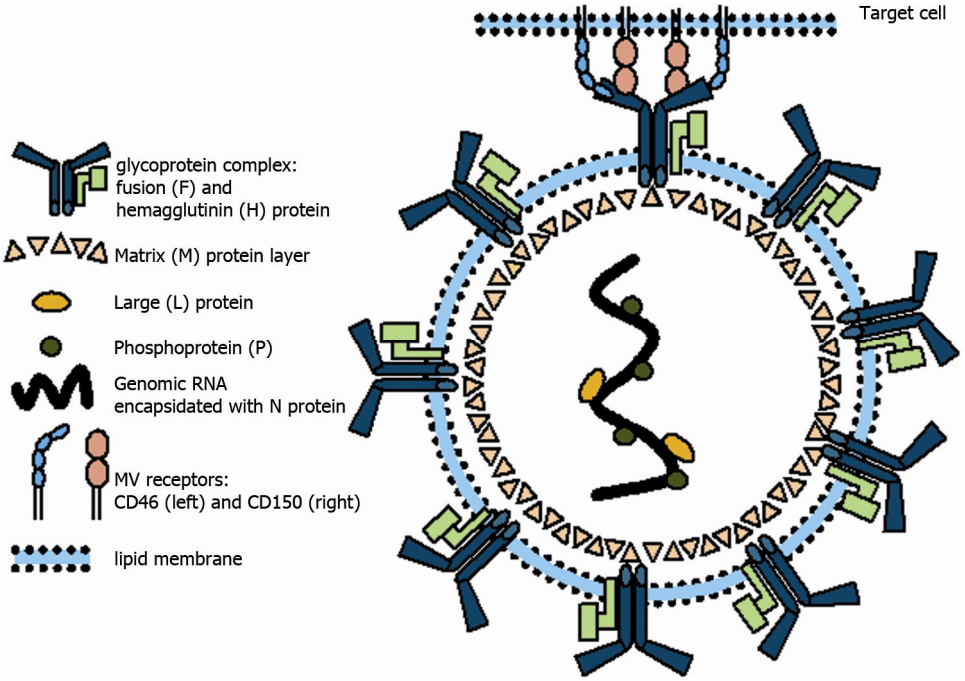

Figure 1-1: An *en face* scheme of MV.

An MV virion is shown next to a target cell. MV consists of a single stranded, N-encapsidated genomic RNA and associated proteins, including phosphoprotein (P) and polymerase (L) protein, packaged in a pleomorphic core composed of matrix (M) protein, all surrounded by a lipids membrane envelope derived from host cell. Virally encoded membrane glycoproteins (fusion F and hemagglutinin H) are spanning the envelope. CD46 or CD150 on the host cell surface function as MV receptors.

1.1.2. MV receptor usage

The key parameter determining viral tropism is receptor distribution. Unlike other members of *Paramyxoviridae*, MV does not utilize a sialic acid moiety for virus attachment and entry. *In vivo* MV pathogenesis largely segregates with CD150 as expressed on hematopoetic cells, while late in infection other recptor might also be used (Figure 1-1).

1.1.2.1. CD46

CD46 was first identified as MV binding receptor (Naniche, Wild et al. 1992). This molecule is expressed on all cells except for human erythrocytes, which explains the inability of MV to agglutinate such cells. CD46 belongs to the regulator of complement activation (RCA) gene cluster, which plays a crucial role in innate immunity.

CD46 consists of 4 N-terminal short consensus repeats (SCRs), 1-3 serine/threonine-rich domains, a transmembrane domain and a cytoplasmic tail (Seya, Hirano et al. 1999). Only the first two membrane-distal SCR1 and SCR2 participate in MV-H protein binding (Manchester, Liszewski et al. 1994; Casasnovas, Larvie et al. 1999). Particularly, two sequential proline residues (PP motif) on the protruding loop of SCR1 deeply penetrate into a hydrophobic pocket in MV-H protein (Santiago, Celma et al. 2010). CD46 requires N-glycans on SCR2 to serve as virus receptor (Maisner, Schneider-Schaulies et al. 1994; Maisner, Alvarez et al. 1996). Furthermore, CD46 is down-modulated from the surface of MV-infected cells (Krantic, Gimenez et al. 1995; Bartz, Brinckmann et al. 1996) or uninfected cells contacted by MV particles (Schneider-Schaulies, Schnorr et al. 1996). It is clear that CD46 serves as entry receptor for mostly attenuated MV strains or wild-type strains that were adapted to grow on Vero cells. Lymphotropic wild-type and freshly isolated strains do not interact with and do not down-modulate CD46 (Bartz, Firsching et al. 1998; Hsu, Sarangi et al. 1998).

1.1.2.2. CD150

Based on a cDNA library approach, human signaling lymphocytic activation molecule (SLAM-CD150) was identified as MV-receptor on lymphoid cells (Ono, Tatsuo et al. 2001; Tatsuo, Ono et al. 2001; Erlenhofer, Duprex et al. 2002). This molecule is a CD-2 like molecule of the Ig superfamily and is upregulated upon T or B cell activation (Browning, Woodliff et al. 2004). CD150 is also found on mature DCs (Kruse, Meinl et al. 2001), memory T and B cells, but not on freshly isolated monocytes and immature DCs (Minagawa, Tanaka et al. 2001). The induction of CD150 on monocytes involves interaction with both wild-type MV-H and Toll-like receptor 2 (TLR2), which is not a MV entry receptor (Bieback, Lien et al. 2002).

CD150 consists of two Ig superfamily domains: a membrane-distal V and a membrane-proximal C. The former domain mediates MV-H binding (Ono, Tatsuo et al. 2001). The molecule is down-modulated upon infection or exposure of cell to MV. Although mediating MV-H binding to lymphocytes, CD150 of T cell is not involved in contact-mediated proliferation inhibition (Erlenhoefer, Wurzer et al. 2001). The interactive site of CD150 forms a positively charged area complementary to the negatively charged patch on MV-H β5 blade (Hashiguchi, Kajikawa et al. 2007). In contrast, the CD46 binding site locates on the β4 blade, establishing a steric hindrance for coincident engagement of CD150 (Colf, Juo et al. 2007). Though positionally different from that of CD46, the PP motif on CD150 extends into the hydrophobic MV-H pocket just as efficiently as CD46, which is a likely explanation why the vaccine strains can use both structurally unrelated receptors (Santiago, Celma et al. 2010).

1.1.2.3. Unidentified cellular receptor(s)

There is accumulating evidence that wild-type MV infects CD150-negative epithelial, endothelial and neuronal cells (Hashimoto, Ono et al. 2002; McQuaid and Cosby 2002). In other words, the ability of MV to infect CD150-negative cells, albeit with low efficacy, suggests the existence of unidentified MV-receptor(s).

1.1.3. MV-induced immunosuppression

The term anergy was first coined by Von Pirquet in 1908 to describe the loss of delayed-type hypersensitivity (DTH) to tuberculin in individuals infected with MV. Immunosuppression induced by MV can be described by several features: 1) lymphopenia, which is quickly resolved (Ryon, Moss et al. 2002); 2) a Th2-dominated response suppressing a Th1 response (Griffin and Ward 1993); and 3) unresponsiveness of PBL to mitogenic or polyclonal activation *ex vivo* (Schneider-Schaulies, Bieback et al. 2002).

1.1.3.1. Lymphopenia

MV-induced lymphopenia is transient, but severe, and lymphocyte loss mainly occurs by apoptosis (Okada, Sato et al. 2001) which may involve soluble Fas-Ligand (FasL) (Ryon, Moss et al. 2002) or surface expression of apoptosis-related molecules such as TNF-related apoptosis-inducing ligand (TRAIL), TRAIL-receptors, CD95 (Fas) and FasL (Okada, Sato et al. 2001; Ryon, Moss et al. 2002).

However, the loss of T cells could also take place in secondary lymphatic organs via trans-infection mediated by productively infected DCs or DCs carrying infectious virus (de Witte, de Vries et al. 2008).

1.1.3.2. MV-driven modulation of DC viability and function

Bridging innate and adaptive immunity, DCs are thought to be the first targets conveying MV to lymphoid tissues. There are several reasons making DCs the most MV-exploited vehicle. They are strategically located at sites of viral entry including epithelia of the skin and respiratory tract, which is primarily natural site for air-borne virus entry. In contrast to epithelial cells, DCs or Langerhans cells do express MV-receptor CD150 both *in vitro* and *ex vitro* (de Witte, Abt et al. 2006; de Witte, de Vries et al. 2008). Moreover, their capacity to migrate to draining lymph nodes upon virus encounter is another advantage for the virus spread. In line with the hypothesis of MV being carried by DCs for transmission, MV-infected $CD11c^+$ myeloid DCs were seen in lymphoid tissues of experimentally infected monkeys (de Swart, Ludlow et al. 2007) as well as in human cryosections of tonsil and lymph node (de Witte, de Vries et al. 2008).

MV infection induces DC maturation comparable to that by LPS or TNF-α in terms of surface markers such as CD40, CD80, CD83, CD86 and cytokine release (Klagge, ter Meulen et al. 2000; Servet-Delprat, Vidalain et al. 2000). However, the infection affects

CD40L-mediated cytokine synthesis as seen in weak induction of IL-12p35 and IL-12p40 and strong enhancement of IL-10 transcription (Servet-Delprat, Vidalain et al. 2000; Bieback, Lien et al. 2002). This, thereby, polarizes the Th response towards a Th2-type.

Albeit only subtly different from LPS-matured DCs with regard to integrin activation, morphological and adhesive properties, MV-infected DCs showed a failure in CCR5 to CCR7 switching and chemotaxis which may result in prolongation of tissue residency and impairment of parafollicular zone migration (Shishkova, Harms et al. 2007; Abt, Gassert et al. 2009).

1.1.3.3. MV-infected DC-induced T cell suppression

DCs have a pivotal role in initiating naïve T cell responses. Virus can highjack DCs as a Trojan horses since the cells are able to actively migrate to draining lymph nodes where T cells recirculate. Whether DCs support MV transmission to T cells is not fully understood as CD150 is barely detectable on naïve T cells (Browning, Woodliff et al. 2004). MV-infected DCs are unable to stimulate allogeneic T cell proliferation. Actively replicating virus was claimed for this allogeneic inhibition (Grosjean, Caux et al. 1997; Servet-Delprat, Vidalain et al. 2000; Vidalain, Azocar et al. 2000).

1.1.3.4. Viral proteins modulating or silencing T cells

Although the percentage of infected PBMCs differs from stage to stage and does not exceed 5% (Schneider-Schaulies, Kreth et al. 1991; Forthal, Aarnaes et al. 1992), total PBLs are unresponsive to mitogenic or polyclonal stimuli *ex vivo*. There is evidence supporting the role of viral proteins in T-cell modulating or silencing. Proliferative arrest can be reversed using antibodies against MV-proteins, but not IL-2,-10 or INF-γ (Dubois, Lamy et al. 2001; Laine, Bourhis et al. 2005).

1.1.3.4.1. The N protein

Cytosolic nucleocapsid protein (N), together with P protein, constitutes the major part of RNP complex which encapsidates the viral genome. Unexpectedly, upon release into the extracellular compartment after apoptosis and/or secondary necrosis of MV-infected cells *in vitro*, N protein becomes an inhibitory factor inducing cell proliferation and apoptosis via FcγRIIB (CD32) or an uncharacterized nucleocapsid receptor (Laine, Trescol-Biemont et al. 2003; Laine, Bourhis et al. 2005). FcγRIIB is exclusively expressed on B cells as an inhibitory feedback receptor, thus it apparently explains the negative effect of antibody production seen on the B lymphocytes (Ravanel, Castelle et al. 1997). The immunosuppression role of N protein, however, is still a matter of debate since its putative receptor is not expressed on T cells.

1.1.3.4.2. The gp complex

There is evidence of the immunosuppressive role of MV glycoproteins *in vitro*. *Bona fide* MV-gp, but not VSV-G, induced proliferation arrest in α/β T lymphocytes in dose- and contact-dependent manner (Schlender, Schnorr et al. 1996; Bieback, Breer et al. 2003). The gp complex, but neither single protein, led to immunosuppression. Neither glycosylation nor fusogenicity is required for proliferative inhibition effect (Weidmann, Fischer et al. 2000; Weidmann, Maisner et al. 2000) and human sera or polyclonal antibodies against H, and to a lesser extent F, reversed immunosuppression induced by MV-infected DCs in mixed lymphocyte reactions (MLRs) (Dubois, Lamy et al. 2001).

In line with *in vitro* findings, intraperitoneal inoculation of cells transiently expressing MV glycoproteins in cotton rat (*Sigmodon hispidus*) was sufficient to induce proliferative suppression of lymphocytes (Niewiesk, Eisenhuth et al. 1997). The immunosuppression is

related to cell cycle retardation or arrest rather than apoptosis (Schnorr, Seufert et al. 1997; Engelking, Fedorov et al. 1999; Niewiesk, Ohnimus et al. 1999).

1.1.3.5. Surface receptor(s) involved in silencing of T cells

MV-induced immunosuppression requires the gp complex, which is also the ligand for cellular receptor CD150 and CD46. These are not required for T cell arrest, because this is not prevented by CD46 or CD150 specific antibodies (Erlenhoefer, Wurzer et al. 2001). Thus, it is generally agreed that gp complex interacts with receptor(s) other than CD46/CD150 in mediating immune suppression.

1.1.3.6. Signaling pathways targeted by MV

Activation of the phosphatidylinositol-3 kinase (PI3K) triggers Akt activation and subsequently cell cycle initiation in T cells. Phosphatidylinositol (3,4,5)-trisphosphate (PIP3)-dependent activated Akt is recruited into detergent-resistant membrane microdomains (DRMs) in close proximity to phosphoinositide-dependent kinase 1 (PDK1), which phosphorylates Akt (Waugh, Sinclair et al. 2009). The MV gp inhibited IL-2 or anti-CD3/CD28 driven Akt kinase activation (Avota, Avots et al. 2001; Avota, Muller et al. 2004) and hence stable expression of a catalytically active Akt prevented MV-induced negative signal to proliferation (Avota, Avots et al. 2001).

Dampening PI3K activity through phosphatase-mediated depletion of the PIP3 pool can negatively regulate lymphocyte activation. SIP110, an alternatively spliced mRNA isoform of the lipid phosphatase SHIP145, is found as a consequence of the interaction of MV-gp and T cells. When transiently expressed in primary or Jurkat T cells, SIP110 is constitutively localized at membrane independently of TCR activation (Avota, Harms et al. 2006). In addition, MV contact abrogates Rho kinases activation of the Rac1, Cdc42, but not of RhoA, thereby impeding actin cytoskeletal rearrangements in primary T cells upon TCR

activation. Consequently, filopodia and lamellopodia formation are completely altered, as are fibronectin adhesion and TCR-activated phosphorylation of ezrin/radixin/moesin (ERM). Strikingly, actin-based protrusion collapses on MV exposure (Muller, Avota et al. 2006). In summary, MV – through its gp complex – targets most survival initiation pathways, which renders T cell functionally and physically paralysed.

1.2. DC-T cell interaction

1.2.1. Immunological synapse

The term lymphocytic synapse was first coined by Norcross (1984) to describe the similarity between T cell-recognition activation process and cell-communication process found in the neuronal system. It was renamed immunological synapse (IS) by Monks, Freiberg et al. (1998) and Grakoui, Bromley et al. (1999). Literally, synapse is a Greek word meaning to fasten together. The word is thus used to illustrate the stable junctions of IS, in contrast to the promigratory junctions of kinapse (Dustin 2007). Due to limitation of imaging technologies, the IS first image was published more than a decade after the term was coined (Monks, Freiberg et al. 1998). In that image the three-dimensional contacting region between a T cell and an APC was revealed as a bulk's-eye-like structure containing dynamic but well-segregated receptor clusters. Anatomically, an IS consists of three distinguishable clusters including central-, peripheral- and distal-supramolecular activation cluster (c-, p- and d-SMAC, respectively) that physically and functionally promote T cell activation and differentiation (Figure 1-2).

A c-SMAC is comprised of central phosphorylated inactive TCR microclusters (MCs), CD28 and protein kinase C (PKC)-θ locating in close proximity to the p-SMAC (Figure 1-2). The continually formed nascent MCs move from d-SMAC towards c-SMAC in a F-actin-dependent manner and often end up in TCR signal termination (Varma, Campi et al. 2006).

Size exclusion of bulky molecules like CD45 occurs simultaneously with MC formation because of topological hindrance of TCR-pMHC interactions (Choudhuri, Wiseman et al. 2005; Varma, Campi et al. 2006).

An annular structure enclosing the c-SMAC is defined as p-SMAC, which constitutes of Leukocyte Function associated Antigen (LFA)-1, CD2 and the cytoskeletal linker talin (Figure 1-2). The interaction of LFA-1 with its ligand Inter-Cellular Adhesion Molecule (ICAM)-1 on an APC facilitates and enhances TCR-pMHC interactions (Bachmann, McKall-Faienza et al. 1997).

CD2 serves both as an intercellular adhesion and a signal transducer since some engagements of CD2 in combination with anti-CD3 enhance cytokine secretion and other engagements block conjugate formation between T cells and its ligand LFA-3 expressing cells (Zhu, Dustin et al. 2006; Espagnolle, Depoil et al. 2007).

The outermost region of SMAC was lately named d-SMAC, which is enriched for the large and bulky phosphatase CD45, (Figure 1-2) which dephosphorylates inhibitory tyrosine residue requiring for activating Lck and regulatory tyrosine residue.

The role of cytoskeleton has been recognized in cellular dynamics quite early. Together with microtubule network, it plays a crucial role in spatial organization of the IS as disruption or inhibition of filamentous actin impairs synapse formation and function (Gomez and Billadeau 2008). TCR-induced F-actin reorganization via LAT1 and SLP-6 recruits Vav1-driven activating Cdc42 and Rac1 which interact with WASp (Wiskott-Aldrich Syndrome protein) and WAVE2 complex, respectively. WASp/WAVE2-activated Arp2/3 (actin-related protein 2/3) coupling to talin and vinculin nucleates newly branched F-actin formation (Barda-Saad, Braiman et al. 2005; Nolz, Medeiros et al. 2007).

Table 1-1: Components of the IS

SMAC	T cell	APC
Central (c-SMAC), inner	TCR, LBPA*, ESCRT**	MHC-peptide
Central (c-SMAC), outer	PKC-θ, CD28	CD80/86
Peripheral (p-SMAC)	LFA-1, CD2, Talin, F-actin	ICAM-1, CD58
Distal (d-SMAC)	CD45, F-actin	

* LBPA: lysobisphosphatidic acid, a marker for multivesicular body (MBV) formation (Varma, Campi et al. 2006)

** ESCRT: endosomal sorting complex required for transport (Vardhana, Choudhuri et al. 2010)

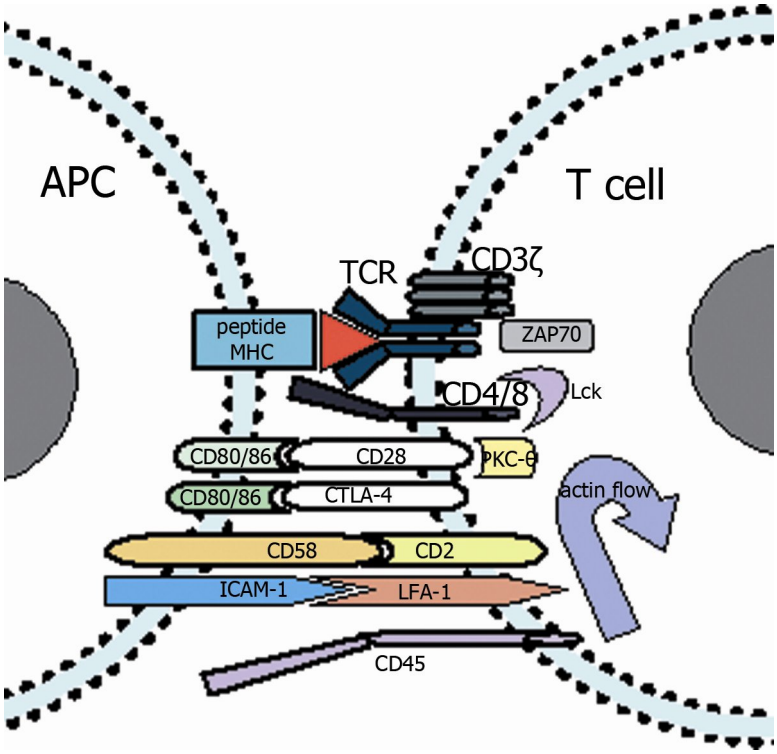

Figure 1-2: Anatomical view of a mature DC-T cell synapse.

The scheme depicts key molecules and ligand pairs that are involved in DC-T cell synapse formation. In descending order, the central region of the supra-molecular activation complex (c-SMAC) characterized by MHC-peptide-TCR complex, enhanced by CD4/8. The intracellular domain of TCR is associated with CD3ζ, which is phosphorylated via Lck-mediated ZAP70. An annular structure of CD28 interacting with CD80/86 is located at the outer c-SMAC, distinct from PKC-θ foci. CTLA-4 can compete with CD28 for CD80/86 binding. At the peripheral region of SMAC (p-SMAC), two ligand pairs of CD58-CD2 and ICAM-1-LFA-1 are located. The outmost of SMAC (d-SMAC) are occupied by CD45 and an actively maintained retrograde flow of actin. APC: antigen-presenting cell, TCR: T-cell receptor, MHC: major histocompatibility complex, ZAP70: ζ-chain associated protein 70, Lck: leukocyte-specific protein tyrosine kinase, PKC-θ: protein kinase C isoform θ, CTLA-4: cytotoxic T lymphocyte antigen 4, ICAM-1: intercellular adhesion molecule 1, LFA-1: leukocyte function-associated antigen 1.

1.2.2. Termination of immune response

Following expansion phase, antigen-driven T cell responses wane to maintain lymphocyte homeostasis. This contraction phase mainly results from "programmed cell death" or apoptosis of formerly activated lymphocytes. This also involves the extrinsic (death receptor) pathways, since previously activated lymphocytes highly express TNF- family receptors such as Fas, CD40 and RANK.

Recently, semaphorin3A (SEMA3A) has been implicated for promoting Fas translocation into DRMs and thus sensitizing leukemic T cells to Fas-mediated apoptosis. (Moretti, Procopio et al. 2008).

1.3. Semaphorins and their role in cell morphology and immune modulation

Since the identification of semaphorins as repulsive neuronal guidance cues in the early 1990s, more than 20 types of these proteins have been characterized which regulate neuronal outgrowth, cardiogenesis, angiogenesis, vasculogenesis, embryogenesis, immunomodulation and tumorigenesis (Neufeld and Kessler 2008; Suzuki, Kumanogoh et al. 2008).

Semaphorins (SEMAs) are secreted, transmembrane, and glycosylphosphatidylinositol [GPI]-linked proteins that are divided into 8 subclasses - two in invertebrates, five in vertebrates and one in viruses - based on their structural homology (1999). All SEMAs possess a highly distinct and conversed ~500 amino-acid extracellular (Sema) domain, which is also present in their primary receptor plexin family.

Most membrane-bound SEMAs use plexin for binding and signal transduction, whereas secreted SEMAs, in particularly the SEMA-3 subclass, require additionally neuropilin (NP) as an obligatory binding moiety (Takahashi, Fournier et al. 1999; Tamagnone, Artigiani et al. 1999). Furthermore, SEMA4A also interacts with TIM2 on T cells (Kumanogoh, Marukawa

et al. 2002), SEMA4D with CD72 (Kumanogoh, Watanabe et al. 2000) or SEMA5A with proteoglycans (Kantor, Chivatakarn et al. 2004).

1.3.1. SEMA receptors

1.3.1.1. The plex family

Nine members of plexins (plex) family constitute the major receptors for vertebrate SEMAs and are divided into 4 groups, designated with letters from A to D, which can be further subdivided eg. plexA4, plexB3, plexC1 and plexD1 (Figure 1-3).

A typical plexin molecule possesses, in addition to the Sema domain, three PSI domains and three IPT (Ig-like, plexins and transcription factors) domains. In its cytoplasmic tail, the molecule contains two GAP domains segmented by a Rho GTPase-binding domain (RBD) which is hidden in the non-signaling state and becomes conformationally changed upon SEMA binding (He, Yang et al. 2009; Tong, Hota et al. 2009). The RBD in B-type plexin is shown to physically interact with RhoD, Rhn1 and Rac1 (Tong, Chugha et al. 2007). The regulation of Rho GTPase is mediated through its C-terminal binding site including PDZ (PSD-95/Dlg/ZO-1)-RhoGEF and RhoGEF (LARG) (Perrot, Vazquez-Prado et al. 2002; Swiercz, Kuner et al. 2002).

1.3.1.2. The NP family

The NP family consists of two members, neuropilin-1 (NP-1) and neuropilin-2 (NP-2). The former was first identified as a neuronal recognition molecule (Takagi, Hirata et al. 1991) and lately as a co-receptor for the SEMA-3 subclass (He and Tessier-Lavigne 1997; Kolodkin, Levengood et al. 1997). These two members share about 44% homology in amino acid, and contain extracellularly two complement binding (CUB) domains (or a1 and a2 domains), two coagulation factor V/VIII homology-like domains (or b1 and b2 domains)

and a merphin A5 (MAM) domain (or c domain) (Figure 1-3). The a1/a2 and b1/b2 ectodomains mediate ligand binding, whereas the c domain is throught to mediate NP oligomerization (Kolodkin, Levengood et al. 1997).

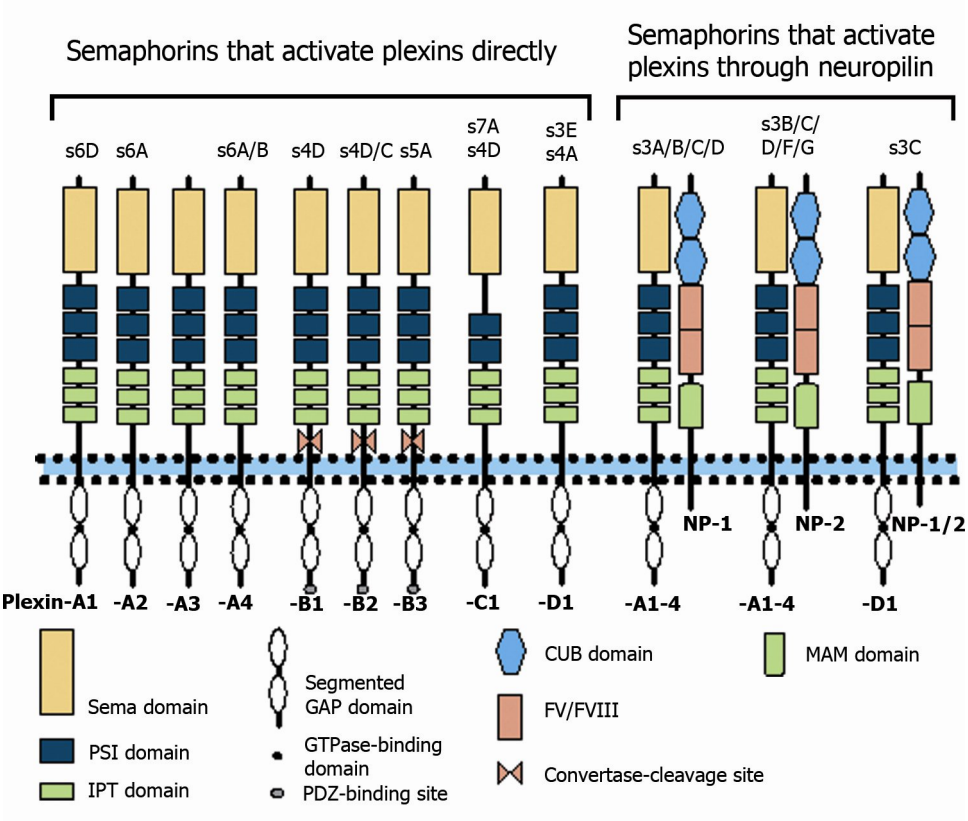

Figure 1-3: Semaphorin receptors.

In vertebrates, there are nine members of plexin and two of neuropilins (NP). The plexin consists of four A-types, three B-types, one C-type and one D-type. Plexins are transmembrane receptor characterized by a Sema domain, followed by three repeated PSI domains and three repeated IPT domains. The intracellular domain of plexin possesses a GAP domain which is segmented by a GTPase-binding domain. Some plexins also have PDZ binding sites and convertase-cleavage sites. Neuropilin is characterized by two CUB domains, two FV/FVIII domains and followed by a MAM domain. The interactive partner(s) of a particular semaphorin species can be plexin alone or neuropilin as coreceptor. s stands for semaphorin, the number signifies the subclass and the following letter specifies the subclass member.

1.3.2. Cellular morphology regulation

The hallmark of SEMAs as repulsive cues in neuronal development is well documented. However, depending on the target cell and receptors SEMAs also act as an attractive guidance molecule (Castellani, De Angelis et al. 2002; Chen, Sima et al. 2008) (Figure 1-4).

1.3.2.1. SEMA-mediated cellular detachment to ECM via plexin

In resting state, the Sema ectodomain of plexin auto-inhibits constitutive activation of plexA1. Upon SEMA3A binding via coreceptor NP-1, plexA1 undergoes a conformational change that releases inhibition (Takahashi and Strittmatter 2001), simutaneously with GEF FARF2 discharge. The binding promotes conversion of GTPase Rac1 to its active (GTP bound) state (Toyofuku, Yoshida et al. 2005). The recruiment of active Rac1 to the Rho GTPase binding site in the RGD in turn promotes translocation of the constitutively active GTPase Rnd1 to the Rho GTPase binding site where GTPase RhoD can also dock to and atagonizes the effect of plexA1-induced collapse (Zanata, Hovatta et al. 2002). Furthermore, the open conformation of GAP domains induces intrinsic function of the active integin-regulator-GTPase R-Ras that leads to GTP hydrolysis. SEMA4D ligation also induces integrin-mediated ERM detachment, similar to the mode of action of SEMA3A (Figure 1-4).

1.3.2.2. Induction of cytoskeletal dynamics by plexin-mediated SEMA

Engagement of SEMA to plexin also contributes to cytoskeletal dynamics including actin and microtubule organization in neuronal cells (Figure 1-4). SEMA-induced Rac1 activation spatially isolates phosphorylated PAK1 (p21- activated kinase 1) from its downstream effector, LIMK1, that decreases phosphorylated level of cofilin required for actin assembly. Moreover, SEMA ligation activates $p190^{RhoGAP}$ which in turn inactivates RhoA thus leading to Rho kinase inactivation. The inactive Rho kinase dephosphorylates cofilin via Rho-associated coiled-coil containing kinase (ROCK) and LIMK1 (Barberis, Casazza et al. 2005) both of which mediate cofilin-mediated actin diassembly.

In addition to actin, SEMA3A/4D also regulates microtubule dynamics by exploiting different signaling pathways. Cyclin-dependent kinase 5 (CDK5) is recuited to Fyn kinase upon plexA2 activation. The recruiment activates collapsin response mediating protein-2

(CRMP2), a downstream subtrate of CDK5, that leads to dissociation of CRMP2 with tubulin dimer and microtubules, thereby disrupting microtuble organization (Fukata, Itoh et al. 2002; Arimura, Menager et al. 2005; Uchida, Ohshima et al. 2005; Ito, Oinuma et al. 2006). A group of proteins, MICAL (molecule interacting with CasL) family, has also been implicated in SEMA class 3-mediated axonal guidance via CRMP2.

In contrast to plexA1, plexB1 does not recruit Fyn upon activation but R-Ras instead. R-Ras, in addtion to regulating integrin inside-out signaling, can activate PI3K/Akt pathway to negate GSK3β activity. Thus, inactivation of R-Ras via intrinsic function of plexin GAP attenuates PI3K/Akt pathway, thereby phosphorylates CRMP2 in GSK3β-dependent manner and consequently disassembes microtuble dynamics (Fukata, Itoh et al. 2002; Ito, Oinuma et al. 2006) (Figure 1-4).

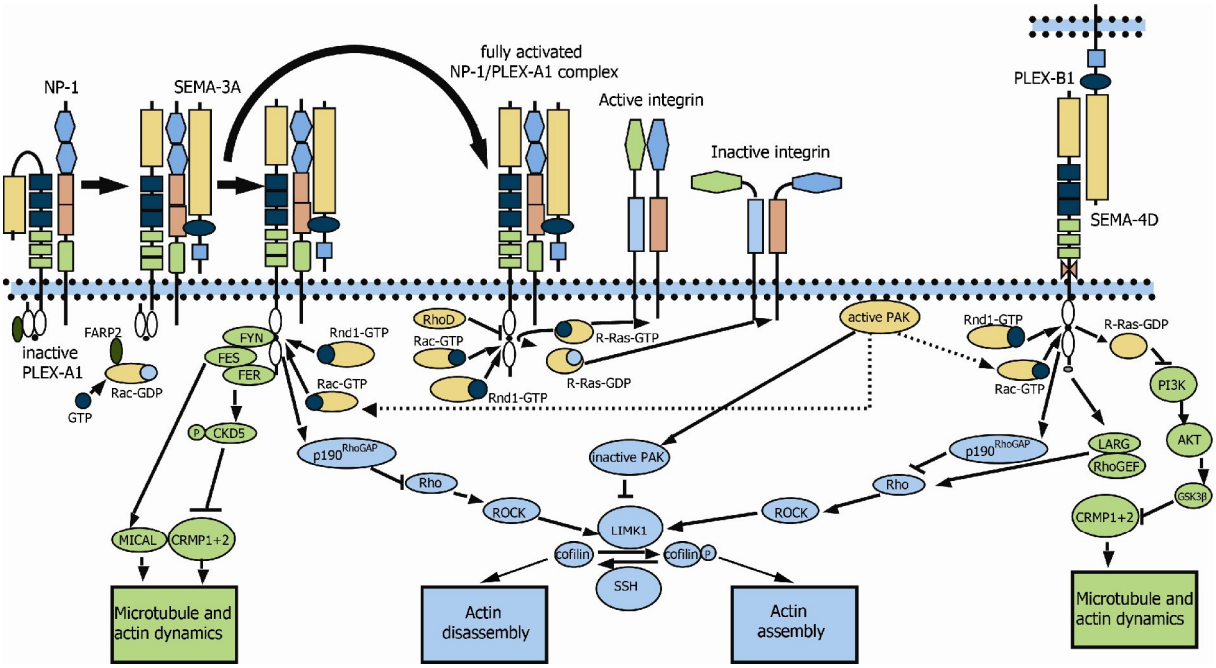

Figure 1-4: The molecular mechanism of SEMA3A induced cellular morphology.
Semaphorin can modulate cellular morphology via microtubule, actin dynamics or integrin affinity. In integrin-mediated detachment, the active GAP of plexA1 induces intrinsically enzymatic R-Ras, resulting in hydrolyzing of GTP-R-Ras, inactivating the regulator, and thus does not sustain inside-out signaling required for integrin-mediated adhesion to ECM. Alternatively, plexA1 or -B1 via its RBD domain inhibits actin assembly though Rho-ROCK-LIMK1 pathway. The inhibition exploits PAK or

$p190^{RhoGAP}$, which can be counteracted by LARG and RhoGEF via PDZ domain. The ligation of respective semaphorin to plexA1 or -B1 also affects microtubule organization. Although using CRMP-mediated microtuble pertubation, these plexins use distinct pathways eg. plexA1 exploits CDK5 and MICAL in contrast to PI3K/Akt/GSK3β in plexB1 action mode.

1.3.3. Immunomodulatory semaphorins

A gross body of evidence suggests an immunomodulatory role of SEMAs in the immune system. However, the mode of action, receptor usage as well as associated molecules are to some extent different from those in neuronal cells (Suzuki, Kumanogoh et al. 2008). Thus, further investigations are needed to shed light on the roles of immunomodulatory semaphorins.

1.3.3.1. Semaphorin in DC functions

Although plexins have been well documented in neuronal system, the role of the molecules in immune system is not fully elucidated. Recently, the important role of plexA1 has been deduced from study of class II transactivator (CIITA) where plexA1 was markedly reduced in DCs isolated from $CIITA^{-/-}$ mice in comparison to control littermates and the kinetic of plexA1 expression resembled that of MHC-II with some delay. PlexA1 has also been found accummulated in the murine IS. Genetic ablation of the molecule results in a poorly allostimulatory function of DCs in priming Ag-specific T cells without impairing their antigen processing capacity (Wong, Brickey et al. 2003). The effect is due to a reduction in actin polarization as well as RhoA activation in DCs that reduces T cell activation (Eun, O'Connor et al. 2006). The data clearly demostrate an important role of plexA1 on the IS formation and stability, at least on DC side.

1.3.3.2. Semaphorin-mediated T cell activation, differentiation and termination response

Recently, secreted SEMA3A has also been reported as a negative immunomodulator. This

repulsive ligand is secreted by human mature DCs, activated T cells at the late stage of an immune response (Lepelletier, Moura et al. 2006) as well as by tumor cells (Catalano, Caprari et al. 2006). SEMA3A exerts its proliferative inhibiton directly on T cells since it blocks actin cytoskeletal rearrangement, TCR polarization, and early signals of T cell activation such as ZAP-70 and FAK phosphotylation. Importantly, SEMA3A has been proposed to terminate normal T cell response by acting on DC-induced T cell proliferation, though receptors involved are not really known (Lepelletier, Moura et al. 2006). Hence, the data suggest that SEMA3A secretion is spatially and timely controlled for a normal immune response. The molecules are also attributed to T cell dysfunction exploiting by tumor cells since T cell proliferation and cytokine secretion are inhibited in the presence of SEMA3A, which accounts for mitogen-activated protein kinase (MAPK) signaling inhibition (Catalano, Caprari et al. 2006).

1.4. Aims

It has been shown that MV-exposed T cells aberrantly regulate actin binding proteins and this is associated with microvillar collapse. These cells show a marked reduction in phosphorylated levels of ERM and cofilin proteins, both of which are key mediators of actin reorganization. In line with this notion, when being analyzed by scanning EM, the majority of MV-exposed T cells do not show a typical finger-like projection surface and are unable to spread on stimulatory slide (Muller, Avota et al. 2006). Although immunological synapse (IS) structures formed between T cells and MV-infected DCs are indistinguishable from those of functional IS in term of CD3 clustering and MHC-II surface recruitment, the infected DCs do not support synapse stability as seen in a live cell imaging approach. The majority of analyzed conjugates are highly unstable, quickly dissolve within 2 minutes and fail to sustain T cell activation. MV glycoproteins on DC surface are most likely involved

since swapping of the glycoproteins with VSV-G partially rescues T cell activation (Shishkova, Harms et al. 2007). Thus, the data indicate that MV does strongly affect integrity of actin dynamics. Since this is a property of SEMA/plexins/NPs interactions which are known to regulate IS function and stability, it raises a question whether MV affects expression levels of SEMA receptors, in particular plexA1 and NP-1, and impairs IS recruitment of these receptors. The effects of MV infection on secretion of the repulsive plexin ligand, SEMA3A, are also of interest. To address these questions, the consequences of MV infection or exposure on plexA1/NP-1 expression on DCs and T cells, respectively, were investigated. The role of these molecules was analyzed regarding to IS recruitment and stability. In particular, the kinetics of SEMA3A secretion and the effects of this ligand on cell motility, cellular collapse and actin dynamics were also studied.

CHAPTER II
MATERIALS AND METHODS

2. General methodologies

2.1. Laboratory safety

All experimental procedures were subject to the safety regulations provided by Institut für Virologie und Immunbiologie (VIM) safety manual. Attendance at a safety course provided by VIM was annually compulsory. Protective gloves and a laboratory coat were worn when working with all toxic chemicals or biological agents. All procedures involving living uninfected and infected tissue culture cells and human blood samples were carried out in Class II laminar biological safety cabinet (NUAIRE Ltd, Germany). Liquid biological waste was inactivated with 5% (w/v) sodium hypochlorite overnight prior to disposal. Solid biological waste was placed into autoclave bags and inactivated by autoclaving. Radioactivity and ethidium bromide wastes were disposed according to Bayerische Julius-Maximilians-Universität Würzburg instructions.

2.2. Chemical reagents

The majority of chemicals used were of analytical or molecular biology grade and were obtained from Sigma Aldrich or Invitrogen Ltd., Germany. Organic solvents were obtained from A. Hartenstein, Germany.

2.3. Sterilization

Glassware and media were sterilized by autoclaving at 1.02 atm (15psi) for 15 minutes at 115-120^{0}C in a S300 autoclave (Münchener Medizin Mechanik GmbH, Germany). Heat labile solutions were sterilized by passage through a 0.22 μm Millex-GV filter sterilizing unit (Millipore Ltd., Billerica, USA).

2.4. Commonly used solutions and buffers

2.4.1. Water

Unless otherwise stated, solutions were prepared in distilled de-ionized water (ddH_2O). Deionization was achieved by passing distilled water through a Milli-Q2 system (Millipore Ltd., Billerica, USA).

2.4.2. Standard buffers

The pH of all solutions was ascertained using a pH meter (FE20 FiveEasy™ pH meter, Metteler Toledo Ltd., USA).

(i) Phosphate buffered saline complete (PBS) (0.136 mM NaCl, 2.7 mM KCl, 1.5 mM KH_2PO_4, 8 mM Na_2HPO_4, 1 mM $MgCl_2$, 1 mM $CaCl_2$) was sterilized at 115^0C.

(ii) Phosphate buffered saline minus (PBS -/-) was prepared as a complete PBS without $MgCl_2$ and $CaCl_2$ added.

2.5. Tissue Culture

2.5.1. Solutions and media

All media and tissue culture solutions were obtained from Invitrogen unless otherwise stated.

2.5.1.1. Growth media

The growth medium was supplemented with fetal calf serum (FCS), antibiotics (Penicillin and Streptomycin) and sodium hydro-carbonate as a pH indicator prior to use. The medium was stored at 4^0C and pre-warmed to 37^0C prior to use.

B95a and BJAB cells (section 2.6.1) were grown in RPMI 1640. Prior to use, the growth medium was supplemented with FCS, which was added to yield a final concentration of 10%

(RPMI-10) for BJAB and 5% (v/v) (RPMI-5) for B95a cell lines.

Human peripheral blood leukocytes (PBL) were maintained in RPMI-10. Additional cytokines were supplied if required.

All cells were incubated at 37^0C in a 5% (v/v) CO_2 humidified incubator with an appropriate cell density or until the required level of confluency was attained.

2.5.1.2. Serum

Fetal calf serum (FCS), which had been heat inactivated and screened for the presence of mycoplasma, was purchased from Invitrogen.

2.5.1.3. Anticoagulant solution

Anticoagulant solution was prepared by adding 0.14 M NaCl, 2.7 mM KCl, 1.5 mM KH_2PO_4, 4 mM Na_2HPO_4 and 0.54 mM disodium EDTA into ddH_2O and was filter sterilized.

2.5.1.4. Trypsin solution

A trypsin solution was prepared by addition of 0.14 M NaCl, 5.36 mM KCl, 5.55 mM Glucose, 0.32 mM EDTA, 6.54 mM $NaHCO_3$, 0.25% (w/v) trypsin powder (Sigma-Aldrich, Germany) and 0.2% (v/v) Penicillin/Streptomycin to 10 liters of deionized water. Phenol red indicator (Sigma-Aldrich) was added to a final concentration of 0.01% (v/v). The solution was filter sterilized and stored at -20^0C.

2.5.1.5. Freezing medium

Freezing medium was prepared by the addition of 10% (v/v) DMSO to FCS.

2.5.2. Miscellaneous

2.5.2.1. Poly-L-lysine

A 0.01% (w/v) solution of poly-L-lysine (PLL) was prepared from 0.1% (w/v) solution of PLL (Sigma) in HPLC grade water. This solution was filter sterilized and dispensed in 1 ml aliquots into cryotubes (Nunc, Denmark), which were stored at -20^{0}C. 12mm cover slip or 8-chamber slide was coated with 150 µl of PLL per slip or chamber, washed twice with an excess PBS, which was air-dried in a flow cabinet for 40 minutes.

2.5.2.2. Lubria-Bertani broth (LB broth)

Tryptone [1% (w/v)], NaCl [1% (w/v)], yeast extract [0.5% (w/v)], and casamino acids were dissolved in deionized water, adjusted to pH 7.0. LB was autoclaved and stored at 4^{0}C.

2.6. Tissue culture techniques

2.6.1. Cultured cell lines

2.6.1.1. B95a

The B95a cell line is an Epstein Barr virus-transformed marmoset B cell line (Kobune *et al.*, 1990) and was obtained from Prof. Dr. Jürgen Schneider-Schaulies, University of Würzburg, Germany.

2.6.1.2. BJAB

The BJAB is an Epstein-Barr virus (EBV)-negative lymphoblastoid cell line (LCL), establishing from an African Burkitt's lymphoma (BL). The cell line contains no detectable EBV and the EBV specified antigen EBNA and can be maintained in EBV-independent manner (Menezes, Leibold et al. 1975). The cells were obtained from Prof. Dr. Jürgen Schneider-Schaulies, University of Würzburg, Germany.

2.6.2. Maintenance and sub-culturing of B95a and BJAB

A confluent B95a cell monolayer cultured in a T-175 flask (Bio-Greiner, Germany) was trypsinized by first rinsing the cell monolayer with 5 ml of trypsin. After incubation for 20 seconds at room temperature, the trypsin was decanted into a waste container and another 5 ml of trypsin was added. The flask was incubated at 37^0C for 5 minutes. After the cells had detached from the plastic, growth medium (20 ml) was added to the cell suspension and the cell suspension was passed rapidly through a 10 ml pipette to produce a homogenous cell suspension. The cell suspension was equally divided into three T-175 flasks containing growth medium (20 ml).

For virus titration, $5x10^4$ B95a cells were seeded into half area 96-well plate (Costar, Corning, USA) one day prior to titration. All flasks and wells were incubated at 37^0C until the cells attained the required level of confluency.

A suspension of BJAB was cultured in T-175 flask (Bio-Greiner) and equally distributed into two T-175 flasks containing growth medium every two days of culturing.

2.6.3. Maintenance of stocks of frozen cells

Stocks of BJAB and B95a cells were stored in an -80^0C freezer. A stock of frozen homogenous cell suspension was prepared by adding an appropriate freeze medium (section 2.5.1.5). The cell suspension was aliquoted into cryotubes (1 ml per tube) (Nunc, Denmark), which were transferred to an -80^0C freezer.

2.6.4. Recovery of cells from storage at -80˚C

A cryotube (Nunc) containing cell suspension (1 ml) was removed from storage (section 2.2.2.6) and was quickly defrosted by incubation at 37^0C. This cell suspension was transferred to a T-75 tissue culture flask to which the appropriate growth medium (20 ml) was previously added. After 24 hours incubation at 37^0C the flask was examined by phase

contrast microscopy. Upon observing attachment of cells to the plastic for B95a and floating for BJAB, the growth medium was removed and replaced with additional growth medium (20 ml). The cells were incubated until the required level of confluency or density had been attained.

2.6.5. Cultured primary cells

Human blood obtained from healthy donors at the Institute for Transfusion medicine and Immune hematology, University hospital Würzburg served as a source for peripheral blood leukocyte (PBL) isolation. Human PBLs were obtained by density gradient centrifugation. Briefly, 10 ml of filter-condensed blood were diluted in 30 ml of anticoagulant solution. The mixture was overlaid to 9 ml of lymphocyte separation medium (PAA, Germany). Cell layer was obtained after 30 minutes centrifugation with low acceleration and de-acceleration. Separation medium and anticoagulant solution were removed by two additional PBS -/- wash steps before adhering on T-75 flask took place. Non-adherent cells were subjected to RPMI-5 equilibrated nylon wool for T cell enrichment. The adherent cells were cultured over night in RPMI-10 and served as a monocyte source.

2.6.5.1. Maintenance and sub-culturing of human T cells

Human primary T cells collected from enrichment step (section 2.6.5) were ascertained by flow cytometry using CD3 antibody as a T cell marker and were kept in RPMI-10 and used within 3 days.

2.6.5.2. Maintenance and sub-culturing of human monocyte-derived dendritic cells (MDDCs)

Supplemented RPMI-10 containing 250 U/ml IL-4 (Miltenyi Biotech, Germany) and 500 U/ml GM-CSF (Berlex, Germany) was added to monocytes (section 2.6.5). Freshly

supplemented RPMI-10 was replaced every two days of culturing. Immature DCs can be collected after 3 day culturing. Mature dendritic cells can be generated from immature monocyte derived dendritic cells by adding 100 ng/ml LPS (Sigma-Aldrich) to the culture and incubating for one more day. $CD11c^+$ immature and mature dendritic cells were ascertained by flow cytometry using CD83, HLA-DR, CD80 and CD86.

2.6.6. Culturing cells on coverslips

For immunocytochemistry of fixed cells, it was necessary to culture cells on 12 mm diameter borosilicate glass coverslips (A. Harstenstein, Germany). Coverslips were autoclaved and each one was placed into individual wells of a 24-well plate using a sterile forceps. A cell suspension of MDDCs (sections 2.6.5.2) was added to each well. The 24-well tray was placed into a humidified, airtight container and the atmosphere was adjusted to 5% (v/v) CO_2. The container was sealed and the cells were incubated at 37^0C until the required time point had been reached.

For scanning electron microscopy (SEM) of fixed cells, 12-mm glass coverslips were chemically modified as described (Crowley and Horwitz 1995). Coverslips were washed overnight in 20% H_2SO_4, rinsed three times in water, neutralized in 0.1 M NaOH, and dried for 30 minutes by leaning against the wall of a sterile tissue culture dish lid. The coverslips were incubated in 3-aminopropyltriethoxysilane (Sigma-Aldrich) for 10 minutes at room temperature, rinsed three times with deionized water, and then incubated in deionized water containing 0.5% glutaraldehyde (Sigma-Aldrich) for 30 minutes. The coverslips were rinsed in deionized water, placed on parafilm and conjugated with 100 µl of 20 µg/ml fibronectin (Sigma-Aldrich) for 1 hour at room temperature. The coverslips were then washed in PBS, blocked with 1% (w/v) BSA in PBS for 30 minutes at 37^0C, placed fibronectin side up in a 24-well plate and washed three times with sterile pre-warmed PBS before adding T cells or

MDDCs (section 2.6.5.1 and 2.6.5.2).

2.6.7. Trypan blue staining

Trypan blue was prepared by mixing trypan blue 0.4% (w/v) in PBS. Trypan blue is a vital stain used to selectively color dead tissues or cells blue. It is a diazo dye. Live cells or tissues with intact cell membranes are not colored. Since cells are very selective in the compounds that pass through the membrane, in a viable cell Trypan blue is not absorbed; however, it traverses the membrane of a dead cell. Hence, dead cells are shown in a distinctive blue color under a microscope. Since live cells are excluded from staining, this staining method is also described as a Dye Exclusion Method.

2.7. Viruses

2.7.1. Virus strains

The lymphotropic wild-type MV strain WTF was isolated in 1990 from peripheral blood mononuclear cells (PBMCs) of a patient suffering from acute measles in Germany (Rima, Earle et al. 1995), and propagated in the human B-cell line BJAB.

The lymphotropic wild-type MV strain IC-B was isolated in Japan during the outbreaks from 1984 to 1988 (Kobune, Sakata et al. 1990). The strain was recovered, tagged with enhanced enhanced green fluorescent protein (EGFP), thus designated as IC323-EGFP (Hashimoto, Ono et al. 2002), and propagated in the human B-cell line BJAB. This strain was provided by Prof. Yusuke Yanaki, Kyushu University, Japan.

2.7.2. Virus stock preparation

For primary infection, $5x10^7$ BJAB cells were cultured in a T-75 flask and the virus was added to the flask to get a multiplicity of infection (MOI) of 0.01. The flask was then placed onto a platform shaker for one hour at 37^0C to allow the virus to attach to cells. Following

this incubation, unbound virus was removed and growth medium was added. Virus-infected cells were incubated at 37^0C and regularly monitored by phase contrast microscopy for the development of cythopathic effect (CPE).

For main infection, two day infected BJAB cells in the T-75 flask above were equally distributed into ten flasks containing approximately 10^8 BJAB cells. Cell-associated virus was collected by centrifugation. After a quick freeze and thaw step, cell-associated virus was collected from the supernatant of thawed cells. The supernatant was aliquoted into cryotubes (1 ml per tube) (Nunc), which were transferred to an -80^0C freezer and served as virus stock.

Mock was prepared identical to virus infection except the cells were given an appropriate volume of PBS instead of virus.

2.7.3. Tissue culture infectious dose assay

Virus tires were obtained using the 50% tissue culture infectious dose assay (TCID50) using the Spearman–Karber method (Ballew 1992). A confluent B95a cell monolayer cultured in a T-75 flask was split into two 96-well microtitre plates, which were transferred to a 37^0C incubator for 24 hours. The 96-well trays were examined by phase contrast microscopy to ensure that a 90% confluent B95a cell monolayer was visible in a representative number of wells. The virus aliquot was diluted logarithmically (10^{-1} to 10^{-8}) in maintenance medium (RPMI) and was immersed into ice rack. After the growth medium was removed, each virus dilution (800 µl) was added to each of eight adjacent wells. Maintenance medium (800 µl) was added to eight adjacent wells as a negative control for cell viability. The microtitre plate was incubated at 37^0C for four days. After this time the number of wells showing CPE at each virus dilution was recorded, as were those not showing CPE. The proportion of infected to uninfected wells at each virus dilution was recorded and the titre of the virus

sample was taken as the reciprocal of the dilution which has infected 50% of the wells.

2.7.4. Inhibition of MV mediated cell-to-cell fusion

Fusion inhibitory peptide (Z-D-Phe-L-Phe-Gly-OH) (FIP) has previously been shown to inhibit cell-to-cell fusion in MV infected cells (Norrby 1971; Richardson and Choppin 1983). A 1000X stock solution of FIP (0.2 M) was prepared by dissolving FIP (0.5 g) (BACHEM, Germany) in DMSO (446 µl).

2.7.5. Infection of MDDCs

For the purpose of infection, MDDCs (section 2.6.5.2) were infected at an MOI of 1.0 for 1 hour at 37^0C. After this time, virus was removed and growth medium containing 250 U/ml IL-4 and 500 U/ml GM-CSF plus 200 µM FIP was added. Mock was used as a negative control. Cells were monitored by phase microscopy for morphology. At 28 h.p.i. and 48 h.p.i. supernatant from infected cells were collected, stored at -80^0C for further analysis. The cells then were stained and subjected to flow cytometry for surface marker detection (section 2.8.3).

2.7.6. Virus exposure assay

For exposure, UV inactivated virus ($1.5 J/cm^2$) was given to T cells at amounts corresponding to a live virus MOI of 0.5 for 2 hours at 4^0C. After this time, virus was removed and maintenance medium containing 200 µM FIP was added. Mock was used as a negative control. Under these conditions, infection of T cells throughout the experiment was completely abolished (Avota, Muller et al. 2004). The cells were used for further analysis (section 2.14).

2.8. Detection of molecules of interest by flow cytometry

2.8.1. Solutions

2.8.1.1. Paraformaldehyde (PFA) fixation buffer

Paraformaldehyde [4% (w/v)] was added to PBS and heated at 65^0C over night. The solution was cooled to room temperature and the pH was adjusted to 7.4 before use.

2.8.1.2. FACS buffer

BSA pH 7 fraction [0.5% (w/v)] was added to PBS -/- plus 0.02 % (w/v) sodium acid for longer storage. The pH was adjusted to 7.4

2.8.1.3. Saponin buffer

Permeabilized buffer was prepared by adding 0.33 % (w/v) saponin to FACS buffer pH 7.4.

2.8.2. Monoclonal antibodies and polyclonal antisera

All antibodies, antisera and dyes used, their specificity and the sources from which they were obtained are summarized below.

Table 2-1: List of antibodies using in this research

Antibody	Dilution	Isotype	Clone	Conjugate	Provider
CD3	1:50 (FACS)	Mouse IgG1, κ	UCHT1	PE	BD Pharmingen
CD11c	1:50 (FACS)	Mouse IgG1, κ	B-ly6	PE	BD Pharmingen
CD80	1:50 (FACS)	Mouse IgG1, κ	MAB104	PE	Immunotech, Beckman Coulter
CD86	1:50 (FACS)	Mouse IgG1, κ	2331 (FUN-1)	FITC	BD Pharmingen
MHCII	1:50 (FACS)	Mouse	B.8.12.2	FITC	Immunotech,

(HLA-DR)		monoclonal			Beckman Coulter
CD71	1:500 (IF)	Mouse IgG1	PAL-M1	none	Santa Cruz
PLEXA1 (23391)	1:50 (FACS, living cells)	Rabbit polyclonal		none	Abcam
PLEXA1 (32960)	1:50 (FACS, fixed cells) 1:500 (IF)	Rabbit polyclonal		none	Abcam
PLEXA1 (0.1 mg/ml)	1:20-50 (blocking)	Rabbit polyclonal		none	ECMbiosciences
PLEXA4 (39350)	1:50 (FACS) 1:500 (IF)	Rabbit polyclonal		none	Abcam
NP-1 (CD304)	1:50 (FACS) 1:250 (IF)	Mouse IgG1	AD5-17F6	none	Miltenyi Biotec
CD43	1:200 (IF)	Mouse IgG1	DF-T1	none	Santa Cruz
SEMA3A	1:100 (IP)	Rabbit polyclonal	H300	none	Santa Cruz
SEMA3A	1:500 (WB)	Mouse IgG2b	215803	none	R&D
Rabbit serum (0.1-0.2 mg/ml)	1:20-50 (FACS, blocking)	Rabbit polyclonal		none	Gibco, Invitrogen
Goat serum (0.1-0.2 mg/ml)	1:20-50 (FACS, blocking)	Goat polyclonal		none	Gibco, Invitrogen
Goat anti Mouse	1:250 (FACS)	Goat polyclonal		FITC	Immunotech, Beckman Coulter
Goat anti Mouse	1:1000 (IF)	Goat polyclonal		Alexa 488	
Goat anti Rabbit	1:500 (FACS) 1:1000 (IF)	Goat polyclonal		Alexa 488	Invitrogen

Chicken anti Rabbit	1:300 (FACS) 1:500 (IF)	Chicken polyclonal		Alexa 488	Invitrogen
DND99 (Lysotracker)	1:2000 (IF, living cells)				Invitrogen
Phaloidin	1:100 (IF)				Invitrogen
Anti-H (MV)	1:50 (FASC)	Mouse monoclonal	K83	none	Our lab.

FACS: Fluorescence activated cell sorting

IF: Immunofluorescence

IP: Immunoprecipitation

WP: Western blot

2.8.3. Immunofluorescent staining of primary T cells or MDDCs

2.8.3.1. Immunofluorescent staining of live cells

Living cells cultured on wells were collected, rinsed three 5-minute times with FACS buffer and then incubated in a primary antibody diluted in FACS buffer (50 µl) for 30 minutes at 4^0C. Cells were then rinsed for 5 minutes in FASC buffer to remove any non-specifically bound primary antibody. The cells were then incubated with the appropriate secondary antibody diluted in FACS buffer (50 µl) for 30 minutes at 4^0C. Following another 5-minute wash in FASC buffer to remove any non-specifically bound secondary antibody, cells were kept in FACS buffer and subjected to flow cytometry (Calibur, BD).

2.8.3.2. Immunoflourescent staining of fixed cells

Immature or mature MDDCs grown in 24-well plate were collected and directly applied 4% PFA (250 µl per well) to get the final of 2% for 15 minutes. Following fixation, cells were carefully washed twice with PBS (250 µl) for 5 minutes before they were stained.

Primary T cells (section 2.6.5.1) were collected and directly applied 4% PFA to get the final of 2% for 15 minutes. Following fixation, cells were carefully washed twice with PBS for 5

minutes before they were stained.

For extra-cellular staining, fixed cells above were incubated in a primary antibody diluted in FASC buffer (50 µl) for 30 minutes at 4^0C. Non-specifically bound primary antibody was removed during a 5-minute wash in FASC buffer. The cells were then incubated in the appropriate secondary antibody in FASC buffer (50 µl) for 30 minutes at 4^0C. At this point, non-specifically bound secondary antibody was removed by a 5-minute wash step in FASC buffer. The cells were kept in FACS buffer and subjected to flow cytometry (Calibur, Becton Dickinson).

For intra-cellular staining, fixed cells above were permeabilized in Saponin buffer for 10 minutes. The cells were then carefully washed twice with Saponin buffer for 5 minutes before they were stained using the same procedure as extra-cellular staining except that all steps were done in Saponin buffer at room temperature.

2.8.4. Immunocytochemical staining of human primary T cells or MDDCs

2.8.4.1. Paraformaldehyde fixation

Immature or mature MDDCs grown in 24-well plate were collected and spun onto PLL-coated chamber slides and were incubated for 30 minutes at 4^0C following by a direct application of 4% PFA (250 µl per well) solution to get the final of 2% for 15 minutes. After fixation, chamber slides were carefully washed twice with PBS (250 µl) for 5 minutes before they were stained or stored at 4^0C.

Primary T cells (section 2.6.5.1) were collected and spun onto PLL-coated chamber slides and were incubated for 30 minutes at 4^0C following by a direct application of 4% PFA solution to get the final of 2% for 15 minutes. After fixation, chamber slides were carefully washed twice with PBS for 5 minutes before they were stained or stored at 4^0C.

2.8.4.2. Immunocytochemical staining of fixed cells

Fixed cells cultured on a chamber slides were incubated in a primary antibody diluted in PBS (250 µl) containing 1.0% (w/v) BSA for one hour at 4^0C.

Non-specifically bound primary antibody was removed during three 5-minute washes in excess of PBS. The chamber slides was then incubated in the appropriate secondary antibody diluted in PBS (250 µl) containing 1.0% (w/v) BSA for 1 hour at 4^0C.

Non-specifically bound secondary antibody was removed by three 5-minute washes in excess of PBS. The chamber was removed and slides were mounted face down on a glass slide covered with Fluoromount-G (SoutherBiotech, Germany) and sealed with nail polish.

2.8.4.3. Detection of filamentous actin in fixed cells

Actin microfilaments were detected using Alexa 594-conjugated phallodin (Sigma), a fluorescently conjugated phallotoxin from *Amanita phalloides,* which specifically binds to F-actin.

Fixed cells cultured on a coverslip or wells after treatment (section 2.9) were incubated in 66 nM Alexa 594 conjugated phallodin (100 µl) in PBS containing 1% BSA (w/v) for 1 hour at 4^0C. Excess phallodin was removed by rinsing the cells three times for 5 minutes in excess PBS.

2.9. Tracker and inhibitors

Lysotracker® Red DND-99 (Invitrogen) was dissolved in DMSO and directly applied to living DCs at final concentration of 0.5µM for 5min at 37^0C. The cells were then fixed and stained with the molecules of interest as described (section 2.8.4)

Chloroquine(CQ)/phenylarsine oxide(PAO) (Sigma) was dissolved in water/DMSO and applied at final concentration of 50µM and 0.1µg/ml, respectively for 24 hrs at 37^0C. The cells were then stained with the molecules of interest as described (section 2.8.3.1)

2.10. Semaphorin treatment

Human recombinant SEMA3A fused to human Fc fragment (SEMA3A-Fc) and SEMA6A-Fc (R&D Systems) were dissolved in PBS containing 0.1% (w/v) BSA, aliquoted and kept at -20^{0}C. Upon treatment, semaphorins were reconstituted in serum-free medium (RPMI-0) at a concentration of 150 ng/ml. Human IgG was used as a negative control at the same concentration. Culture medium containing semaphorin was carefully added to the cells. After 15 minute- or 60 minute-period, cells were fixed with PFA at the final concentration of 2%. Three times of 5-minute PBS wash were performed and filamentous actins were stained using Alexa 594 conjugated phallodin as described (section 2.8.4.3).

2.11. Mixed leukocyte reaction (MLR)

In these assays, 96-well tissue culture plates (Falcon, CA) were used for co-culturing of DC and T cells (ratio 1:10). Cells were pre-incubated with antibodies (ECM Biosciences, USA). The culture was performed in the presence of blocking antibodies raised against synthetic peptide corresponding to a region within the semaphorin domain in human plexin-A1 (at various concentrations) with an appropriate isotype-matched control. After 5 days, allogeneic T lymphocyte proliferation was measured by thymidine incorporation after 18-h pulses with 1 μCi/well (0.037 MBq/well) [^{3}H]thymidine (Amersham). Cells were then harvested with a 96-well harvester (Pharmacia, Germany), collected on filters (Pharmacia), and the incorporation of [^{3}H]thymidine was measured using a β-plate microscintillation counter (Pharmacia)

2.12. Scanning electron microscopy

T cells were washed in PBS, resuspended in RPMI, transferred onto 12 mm glass coverslips chemically coated with human fibronectin (20 μg/ml in PBS) (section 2.6.6) and incubated

for 45 to 60 minutes at 37^{0}C. The cells treated with 150 ng/ml of human IgG served as negative control or chimeric human Fc-fused semaphorin-3A (Sema-3A) and Sema-6A for 15 minutes and 60 minutes. Following treatment, cells were subsequently fixed with 6.25 % glutaraldehyde in 50 mM phosphate buffer (pH 7.2) for 50 min at room temperature and subsequently stored at 4^{0}C overnight. After a washing step in phosphate buffer, samples were dehydrated stepwise in acetone, critical point dried, and sputtered with platin/paladium before analyzed on ascanning electron microscope (SEM) (Zeiss DSM 962).

2.13. Conjugate formation between DC and T cells

PLL-coated chamber slides were seeded with 10^5 DCs resuspended in 200 µl RPMI-0. Cells were incubated for 30 minutes at 4^{0}C. DCs were left untreated or pulsed with a superantigen solution [a combination of *Staphylococcus* enterotoxin A (SE-A) 5 µg/ml and SE-B 5 µg/ml in RPMI-10], incubated at 37^{0}C for 30 minutes. 4x10^5 allogenic or autologous T cells resuspended in culture medium or superantigen solution, respectively, were added to the DCs. Conjugation was performed by incubation for 30 minutes at 37^{0}C and stopped by fixation with 4% PFA at room temperature for 20 minutes. Cells were then washed twice with an excess PBS and blocked with 1.0% (w/v) BSA in PBS for 30 minutes at 4^{0}C. The fixed cells were incubated with primary antibody diluted in PBS (250 µl) containing 1.0% (w/v) BSA for one hour at 4^{0}C. Non-specifically bound primary antibody was removed during three 5-minute washes in excess PBS. The cells were then incubated with the appropriate secondary antibody diluted in PBS (250 µl) containing 1.0% (w/v) BSA for 1 hour at 4^{0}C. Non-specifically bound secondary antibody was removed by three 5-minute washes in excess PBS. The chambers were then mounted with 100 µl of Fluoromount-G (SoutherBiotech, Germany), covered by a glass slide and sealed with nail polish.

2.14. Pseudo immunological synapse formation using CD3/28 DYNAL® bead

The desired volume of Dynabeads® Human T-Activator CD3/CD28 was washed with an excess volume of PBS by keeping on a roller for 5 minutes. Beads were collected by centrifugation at 10,000 rpm for 2 minutes and resuspended in RPMI-10. A total of 10^7 T cells in RPMI-10 medium were stimulated by $2x10^5$ resuspended beads for 30 minutes at 37^0C in a water bath. The cell suspension was then seeded onto a PLL-coated chamber slide for 30 minutes at 4^0C. Cells were subsequently fixed using 4% (w/v) PFA in PBS at room temperature for 20 minutes. The fixed cells were washed twice with an excess PBS and blocked with 1.0 % (w/v) BSA in PBS for 30 minutes at 4^0C. The fixed cells were incubated with primary antibody diluted in PBS (250 µl) containing 1.0 % (w/v) BSA for one hour at 4^0C. Non-specifically bound primary antibody was removed during three 5-minute washes in excess PBS. The appropriate secondary antibody diluted in PBS (250 µl) containing 1.0% (w/v) BSA was then added to the chambers and incubated for 1 hour at 4^0C. Non-specifically bound secondary antibody was removed by three 5-minute washes in excess PBS. The chambers were mounted with 100 µl of Fluoromount-G (SoutherBiotech, Germany), covered by a glass slide and sealed with nail polish.

2.15. Western blotting

2.15.1. Sample preparation

Immunocomplex (section 2.23) was equally mixed with 2X of sodium dodecyl sulfate-polyacrylamide gel electrophoresis (SDS-PAGE) sample buffer. Samples were boiled in a dry heater for 5 minutes at 100^0C and were subjected to SDS-PAGE or stored at -20^0C.

2.15.2. Gel electrophoresis

Protein sample were loaded onto a 10% tricine gel, immersed in tricine running buffer and placed within a vertical electrophoresis unit (Hoefer, USA). The approximate size of bands was determined by the addition of PageRuler™ pre-stained markers (10 μl) onto either side of the tricine gel. Proteins were separated at a constant current of 45 mA for 3 hours. The tricine gel and nitrocellulose membrane (Protran, Whatman, GE) were transferred to a semi-dry transfer cassette (Hoefer, USA) and immersed in transfer buffer. Proteins were electro-blotted onto nitrocellulose membrane for 1 hour. After this time, the nitrocellulose was immersed in skim milk blocking buffer [5% (w/v) in PBS] for 20 minutes to reduce non-specific antibody binding. The nitrocellulose was rinsed twice for 5 minutes in excess PBS-T [PBS containing 0.1% (v/v) Tween 20]. The nitrocellulose was incubated overnight at 4^0C with the appropriate primary antibody. Following this incubation, non-specifically bound primary antibody was removed by rinsing the nitrocellulose three times for 5 minutes in excess PBS-T. The gel was then incubated for 1 hour at RT with the appropriate secondary antibody. After the gel was rinsed three times for 5 minutes in excess PBS-T, positive bands were visualized by immersing the membrane for 1 minute in developing substrate (Amersham Biosciences, GE). The bands were then recorded either by a sensitive chemiluminescent camera (LAS 3000, Fujifilm) or on an X-ray film (Fuji).

2.16. Amplification of Plasmids

2.16.1. Transformation

100 μl aliquot of *E. coli* competent cells (Top10 strain) was thawed on ice, then homogenously mixed with 50 ng of plasmid DNA and incubated for 5 minutes on ice. Transformation was perfomed by a heat shock step at 37^0C for 5 min followed by 5-minute incubation on ice. The bacteria were then resuspened in 1 ml LB-medium without

antibiotics. After 30-minute incubation at 37^0C, 100 µl of bacterial suspension were spread onto an agar plate with the appropriate antibiotic. The plate was incubated overnight at 37^0C and single colony was picked up for further mini or maxi cultivation.

2.16.2. Endo-free plasmid preparation

Maxi-preparation was performed according to the instruction from the Qiagen EndoFree Plasmid Maxi Kit (Qiagen, Germany). This method is to obtain endotoxin-free grade plasmid requiring for human-origin cell transfection. The DNA concentration was determined by a spectrophotometer.

2.17. Handling and disposal of ethidium bromide

A 100 mg ethidium bromide tablet (Sigma-Aldrich, Germany) was dissolved in 10 ml ddH_2O to give a solution with the final concentration of 10 mg/ml. The solution was stored at 4^0C and protected from light. Care was taken when handling and disposing of this chemical due to its carcinogenic properties. Solid waste contaminated with ethidium bromide was transferred to chemical waste bags for incineration.

2.18. Spectrophotometry

A spectrophotometer was used to determine the concentration and purity of double stranded DNA at the wavelength of 260 nm (BioPhotometer, Eppendorf). An absorbance reading of 1.0 is approximately equal to 50 µg/ml of double stranded DNA or 40 µg/ml of RNA. The A260/A280 ratio indicates the purity of isolated DNA. The range from 1.7 to 2.1 indicates a relatively pure and protein free DNA solution.

2.19. DNA gel electrophoresis

DNA molecules of different sizes were separated and visualized using gel electrophoresis.

Agarose gels were prepared by the addition of agarose [0.8% (w/v) A.Hartenstein, Germany] to 1X TAE buffer (100 ml). TAE buffer was prepared as a 10X concentrated solution using 48.4 g Tris, 20 ml of 0.5 M EDTA pH 8.0 and 11.42 ml glacial acetic acid dissolved in 1l ddH_2O. The agarose/buffer solution was heated to fully dissolve. The gel was cooled to 45^0C and 5 µl of ethidium bromide (section 2.17) was added. The liquid gel was poured into a casting cassette with a 14-well comb. After the gel solidified, it was horizontally placed in an electrophoresis tank (Model H5, Series 1087, Gibco BRL). TAE running buffer was added to the tank, submerging the gel by 2-3 mm. DNA samples were mixed with 1/6th volume of loading buffer [50% glycerol, 0.1% (w/v) bromophenol blue, 0.1% (w/v) xylene cyanol] and loaded into the well. DNA size markers (Fermentas, Germany) were added to the outermost lanes of the gel and the gel was electrophoresed at the current of 80 mA until the desired migration was reached.

2.20. Documentation of gel images

DNA fragments in agarose gels were stained by ethidium bromide, which intercalates into the double helix. The DNA bands were visualised on an U.V. transilluminator (Intas, Germany). The image was digitized using a high-resolution 12-bit CCD camera (Intas, Germany).

2.21. Preparation of total RNAs from MDDCs

MDDCs were culture as described (section 2.6.5.2). When indicated the cells were infected with IC323-EGFP strain at a MOI of 1.0. At 24 h.p.i, the cells were collected and washed once with PBS. RNA isolation was carried out using an RNeasy® isolation kit (Qiagen, Germany). Briefly, cells were lysed then the genomic DNA was sheared by passing through a 20-gauge needle. Total RNAs containing in the passed through solution was selectively adsorbed on silica-gel membrane. Contaminants were simply removed by sequential wash

steps. Optionally, DNase treatment can be added directly to the membrane for complete DNA removing. The RNA was then eluted from the membrane and purified RNA was quantified (section 2.18) and was stored at -70^{0}C.

2.22. RT-PCR amplification of SEMA3A

2.22.1. Primers

Primers were synthesised Sigma and were supplied in 100 µM solution stock.

β-actin primers were used as referential controls:

Forward 5'-GCA CTC TTC CAC CTT CCT TC-3'

Reverse 5'-TCA CCT TCA CCG TTC CAG TT-3'

The primer for SEMA3A gene was described elsewhere (Kigel, Varshavsky et al. 2008).

5'-AAC GGG GGC TTT TCA TCC-3'

5'-CCC TTC TCA CAT CAC TCA TGC T-3'

2.22.2. RT-PCR

The Transcriptor one-step RT-PCR kit (Roche, Switzerland) was used to amplify cDNA copies of the Sema-3A gene from total RNA extracted from MDDCs. 100ng of isolated RNA was used per 25 µl PCR reaction as followed.

5X buffer reaction	5 µl
Fwd primer	0.4 µM
Rev primer	0.4 µM
Transcriptor enzyme mix	1 µl
Template RNA	100 ng
Water, PCR grade	fill up to 25 µl

The RT-PCR reactions were performed as followed

1. Denaturation	94^{0}C, 30s
2. Annealing	55^{0}C, 30s
3. Elongation	72^{0}C, 60s
4. Denaturation	94^{0}C, 10s
5. Repeated cycles	35X
6. Final elongation	72^{0}C, 10min

PCR products were kept at 4^{0}C for subsequent analysis by agarose gel electrophoresis (section 2.19 and 2.20).

2.23. Immuno-precipitation of soluble SEMA3A in supernatants

Supernatants of DC or DC/T cell co-cultures were harvested at the time intervals indicated and immuno-precipitated using 2 µg/ml rabbit polyclonal anti-Sema-3A antibody (H300, Santa Cruz). Immune complexes were precipitated using 10 µl/ml protein A/G Plus-agarose 25% (Santa Cruz), then were washed sequentially in PBS plus protease inhibitors (Sigma) containing 0.5 M LiCl and 1% (v/v) Triton, PBS plus protease inhibitors containing 1% (v/v) Triton X100, PBS plus protease inhibitors and analyzed by Western blot (section 2.15) using 0.4 µg/ml mouse anti-Sema-3A mAb (R&D Systems) followed by an anti-mouse HRP-conjugated antibody (Dianova, Hamburg, Germany). Signals obtained after ECL development were digitalized and quantified using the AIDA software program.

2.24. Under agarose assay

2.24.1. Experimental setups

Under-agarose assays have been performed as described elsewhere (Lammermann, Renkawitz et al. 2009). Briefly, 2.5% UltraPure agarose (Invitrogen) in distilled water was heated and mixed with 56^{0}C prewarmed RPMI/20% FCS and 2X Hank buffered salt

solution (Sigma-Aldrich) at a 1:2:1 ratio, resulting in an agarose concentration of 6.25 mg/ml. 2 ml of warm agarose-medium mixture was cast in 3.5-cm cell-culture dishes (BD Falcon) and allowed to polymerize at room temperature. An attractor hole was punched into the agarose and a mixture 1:1 of 1.2 µg/ml CCL19 and 1.2 µg/ml CCL21 was filled into the attractor hole. After 30 minutes of equilibration at 37^0C, 5% CO_2, $1x10^4$ DC or $2x10^4$ T cell suspension (2 µl) was injected beneath the agarose with a fine pipette tip and 5mm away from the attractor hole. Time-lapse video microscopy recording started immediately.

2.24.2. Tracking and quantification of migrating cells

All moving cells in observed field were tracked using ImageJ software, plug-in Manual tracking. For DCs, the cells were monitored every one minute for 2 hrs. For T cells, the cells were monitored every 20 seconds for 30 mins. Tracked data were transformed into trajectory plots and speeds were calculated using plug-in Chemotaxis tool. Mean velocity plot and statistic were performed using Graphpad 4.0. Unpaired student t-test was applied, if not indicated otherwise.

2.25. FACS-based conjugate analysis

For conjugate formation analyses, DCs were labeled with 1 µM R18 dye in RPMI-5 for 20min at 37^0C in incubator. T cells were labeled with 1 µM CSFE in RPMI-5 for 5min at 37^0C in incubator. DCs and T cells were left untreated or treated with SEMA3A/6A (150 ng/ml) for 15min at 37^0C and human IgG at the same concentration was used as negative control. Treated DCs and T cells were used directly or washed prior to co-culture in a FACS tube. At indicated time points, co-culturing cells were fixed with PFA at the final concentration of 2% (w/v). The cells were washed once with FACS buffer in low speed centrifugation manner (400rpm) and subsequently analyzed by flow cytometry. A double positive population determined a conjugate.

Percent of control was calculated using one sample t-test with hypothetical value set as 100.

2.26. siRNA-mediated plexA1 knockdown

For silencing of plexA1, human T cells were transfected according to the manufacturer's protocol (DharmaFECT, Thermal Scientific) with siRNA targeting plexA1 (Santa Cruz) or, for control, a scrambled siRNA (Sigma, Germany). Two days post transfection, cells were recruited into the respective experiments. Aliquots of transfected cells were harvested for nucleic acid extraction (Qiagen, RNAeasy Kit) and subsequent RT-PCR analyses (section 2.21 and 2.22). Forward 5'-CTG CTG GTC ATC GTG GCT GTG CT-3' and reverse 5'-GGG CCC TTC TCC ATC TGC TGC TTG A-3' primers were used for specific plexA1 amplification (Kigel, Varshavsky et al. 2008). Signals obtained after electrophoresis were digitalized and quantified using the AIDA software program (Raytest, Straubenhardt, Germany).

2.27. Statistic

All statistics were performed using Graphpad 4.0. Unpaired student t-test was applied, if not indicated otherwise.

CHAPTER III
RESULTS

3. Results

3.1. Expression of SEMA3A prototypic receptors on human primary T cells is not grossly altered by MV exposure

It has been previously shown that MV induces microvillar loss on T cells and these cells do not respond to CD3/28 stimulation (Muller, Avota et al. 2006). Since SEMA/plexA1/NP-1 interactions are known to regulate actin dynamics and are implicated in IS function (Tordjman, Lepelletier et al. 2002; Eun, O'Connor et al. 2006), it raises a question whether these molecules may account for the loss of actin-based protrusion seen on MV-exposed T cells.

It has been suggested that the two prototypic receptors of SEMA3A, plexA1 and NP-1, are expressed by human primary T cells (Tordjman, Lepelletier et al. 2002; Catalano, Caprari et al. 2006) although plexA1 expression is not directly addressed (Tordjman, Lepelletier et al. 2002; Catalano, Caprari et al. 2006) and only being confimed on leukemic Jurkat T cells (Moretti, Procopio et al. 2008). Thus, the first aims were to confirm the expression profile of these molecules on human primary T cells and to analyze whether plex-A1/NP-1 can contribute to functional IS and are modulated by MV/MV-gp.

3.1.1. Expression profile of plexA1 and NP-1

In line with the published data, the expression level of NP-1 was low to negligible on freshly isolated human primary T cells (Figure 3-1B) as measured by flow cytometry. The expression of plexA1 was also low (Figure 3-1A). Interestingly, the expression pattern of plexA1, but not NP-1, drastically changed with differently assessed methods. The percentages of positive cells as well as mean fluorescent intensities (MFIs) increased upon fixation and permeabilization (Figure 3-1, middle and right panels) indicating plexA1 was

stored intracellularly. In contrast, NP-1 did not show a marked difference with the tested methods. Thus, the data indicate that plexA1 is mostly intracellularly located, where as NP-1 is not.

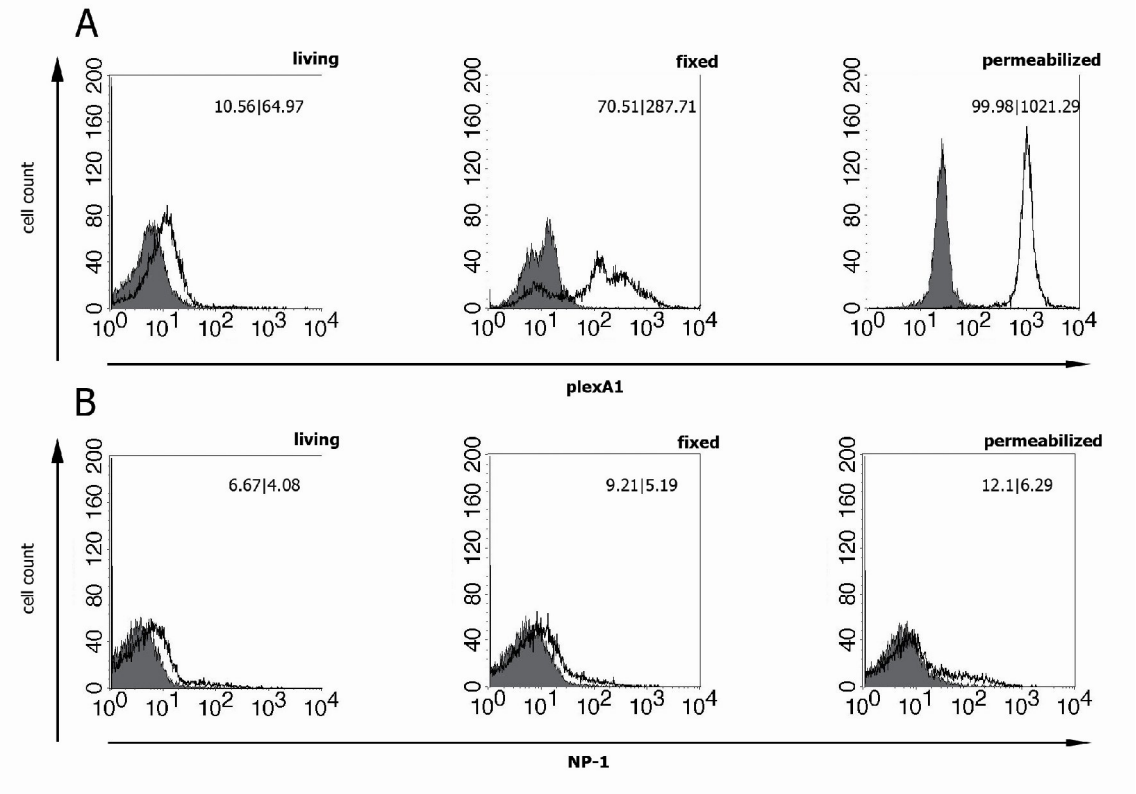

Figure 3-1: Semaphorin-3A prototypic receptors, plexA1 and NP-1, are expressed on human primary T cells.

Expression levels of plexA1 (A) or NP-1 (B) were analyzed on living human primary T cells by flow cytometry with different staining methods including living (left panel) fixed (middle panel) or permeabilized (right panel) cells. Insert numbers show the percentage of positive cells and mean fluorescent intensities (MFI) (percent|MFI). Filled histograms: isotype matched control, open histograms: specific antibodies.

3.1.2. PlexA1 and NP-1 expression patterns is not grossly altered by MV exposure

The next question was to investigate whether MV exposure affects surface expression levels of these molecules. To exclude MV-induced fusion and productive replication, UV-inactivated MV was used and the experiments were performed in the presence of fusion inhibitory peptide (FIP). Human primary T cells were exposed to UV-inactivated MV at 4°C

for 2 hrs in the presence of FIP. For control, mock extract was used. After extensive washing, the cells were analyzed by flow cytometry. As shown in Figure 3-2, expression levels of both plexA1 and NP-1 were not detectably affected within 2 hrs of MV exposure. Taken together, the data indicate that both plexA1 and NP-1 are expressed on human primary T cells and their expression levels are not altered by MV exposure.

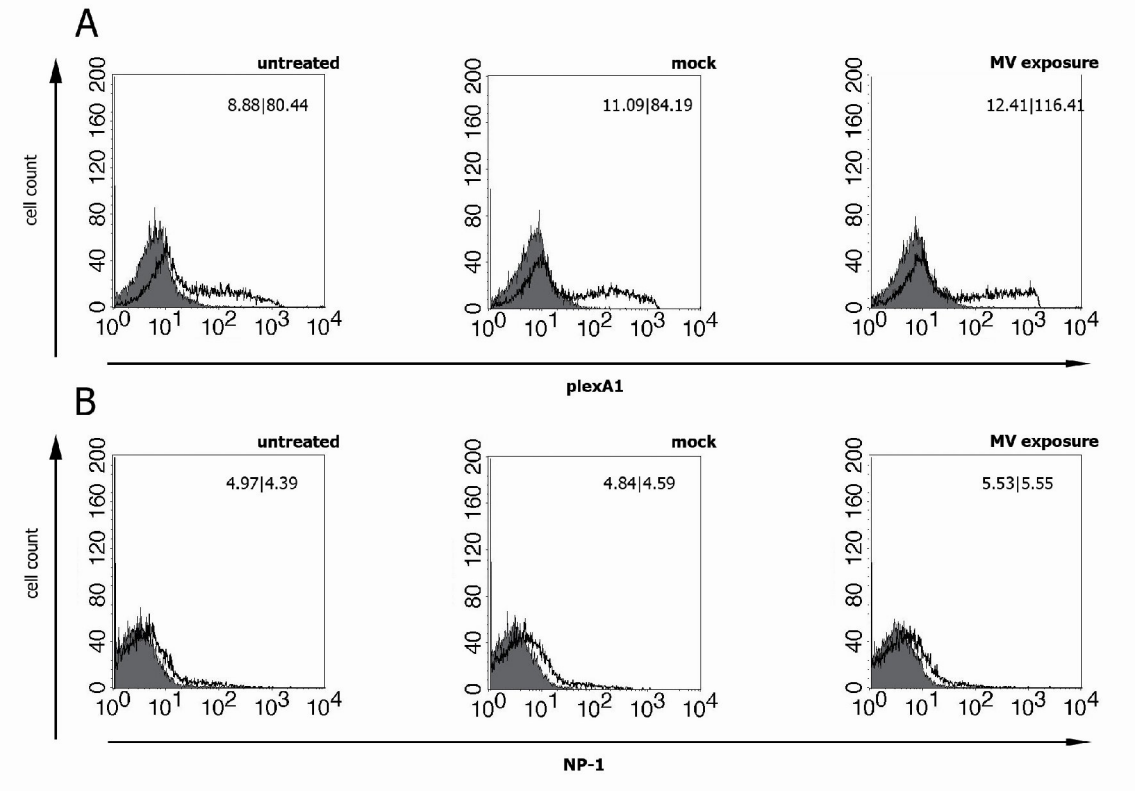

Figure 3-2: PlexA1 and NP-1 expression levels are not detectably affected upon UV-MV exposure

Expression levels of plexA1 (A) or NP-1 (B) were analyzed on living human primary T cells by flow cytometry after 2 hrs exposure to UV-inactivated MV at 4°C in the presence of FIP. Insert numbers show the percentage of positive cells and mean fluorescent intensities (MFI) (percent|MFI). Filled histograms: isotype matched control, open histograms: specific antibodies.

3.2. Polyclonal CD3/28 stimulation causes short-term translocation of plexA1 to the T cell surface and increases the percentage of plexA1 as well as NP-1 expressing cells on long-term culturing

As shown in Figure 3-1A, the plexA1 is mostly cytoplasmic and it raises a question whether it can be shifted to different locations such as the membrane surface. To ensure that all experimentally tested T cells were activated, polyclonal CD3/28 stimulation, which mimics an APC engagement to T cells, was used. The stimulation was monitored over a time course of 96 hrs.

Indeed CD3/28 ligation caused a transient shift of plexA1 to the cell surface indicated by MFI increase (Figure 3-3). 30-min stimulation led to a short-lived induction of plexA1 on the T cell surface (Figure 3-3A, second from the left). Interestingly, the percentage of plexA1 expressing cells was drastically elevated to up to 40% 96 hrs post activation which was not seen after 72 hrs (Figure 3-3B). The kinetic expression of NP-1 on T cells is similar to that of plexA1 despite it is initially nearly undetectable as determined by immunofluorescent staining (Figure 3-3C).

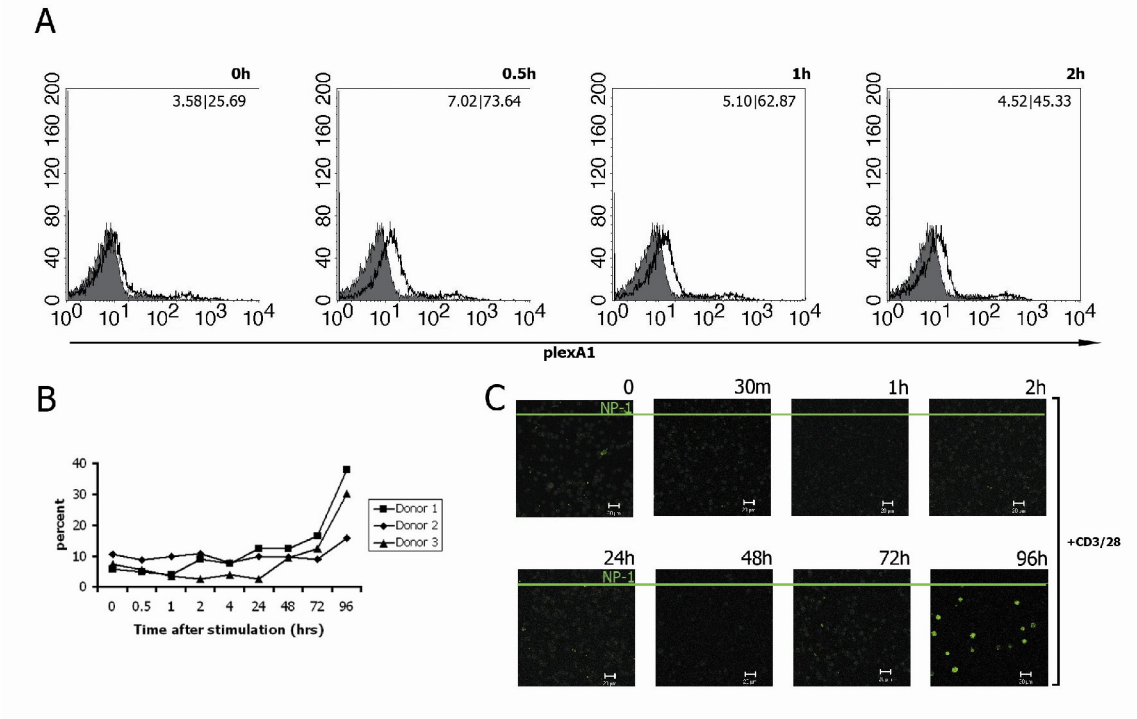

Figure 3-3: CD3/28 ligation causes a translocation of plexA1 to the T cell surface in short-term and increases the percentage of plexA1 as well as NP-1 in long-term culture.
(A) Human primary T cells were assessed by flow cytometry for their surface expression of plexA1 after CD3/28 cross-linking for 0 hour (left), 0.5 hour (second), 1 hour (third) and 2 hours (right). Insert numbers show the percentage of positive cells and mean fluorescent intensities (MFI) (percent|MFI). Filled histogram: isotype matched control, open histogram: specific antibodies.
(B) Surface expression of plexA1 of T cells was monitored over a time-course of 96 hours. Percentage of positive cells following subtraction of isotype control values is shown.
(C) CD3/28 cross-linked T cells were captured on PLL-coated-slides and stained for NP-1 with various intervals indicated.
Experiments were performed in triplicates and one representative out of three experiments is shown.

3.3. PlexA1 is involved in DC-induced T cell proliferation

The engagement of CD3/28 causes a transient shift of plex-A1 to the cell surface (Figure 3-3) indicating the role of this molecule for T cell activation. The importance of plexA1/NP-1 in IS function has predominantly been addressed in murine cells (Wong, Brickey et al. 2003; Eun, O'Connor et al. 2006). Given its important role in the IS function, blockage or interference with its expression and distribution could show an effect on

synapse formation, stability or function. To this end, the molecule was manipulated by several modes such as exogenous blocking, genetic knock-down and overexpression.

3.3.1. Exogenous blockage of plexA1 directly inhibits T cell proliferation

As shown in Figure 3-5, plexA1 staining reveals that both DC and T cells express the molecule. This raises a question whether plexA1 plays a role in IS function.

To answer the question, T cells and DCs were pretreated with different concentrations of neutralizing antibodies prior to onset of the MLR. A rabbit polyclonal serum was used as control. As shown in Figure 3-4A, immature DCs stimulated T cells not as efficiently as LPS-matured DCs (white and black bar, respectively). The presence of rabbit polyclonal serum decreased T cell proliferation but not that pronounced as plexA1 blocking antibodies did, albeit with differential efficiency.

3.3.2. siRNA-mediated knockdown of plexA1 significantly decreases T cell proliferation

To further strengthen the important role of plexA1 in T cell expansion, human primary T cells were transfected for two days with siRNA targeting plexA1 or, for control, a scrambled siRNA. The knockdown efficiency was evaluated by RT-PCR with specific primers for plexA1 (section 2.26) as shown in the insert. About 50% of plexA1 mRNA was reduced by specific, but not scrambled siRNA two days post transfection. The T cells were then used for a functional assay in MLR (Figure 3-4B).

Scrambled siRNA transfected T cells showed a decrease in proliferation to some extent, however, plexA1 silencing significantly strengthened the effect. These data clearly show that plexA1 played an important role in the IS, at least on the T cell side.

3.3.3. Ectopic expression of cytoplasmic tailless, but not full length, plex-A1 reduces T cell proliferation

To extend our results, human primary T cells were transfected with VSV-G-tagged full length plexA1 or a dominant negative version, which lacks the cytoplasmic domain. Transfection efficiency was assessed using a VSV-G-specific antibody as shown in the insert (about 25%). Similar to siRNA-mediated silencing, ectopic expression of cytoplasmic tailless but not the full length of plexA1 abrogated allogeneic T cell expansion to 70%. Although overexpression of native plexA1 slightly decreased T cell proliferation, the effect is not significantly different from T cells transfected with GFP-coding plasmic used as a control.

Taken together, the data demonstrated that plexA1 on T cells had an important role in DC-T cell interaction as siRNA-mediated knockdown, exogenous blockage or ectopic expression of dominant negative of plexA1 reduced the efficiency of T cell expasion.

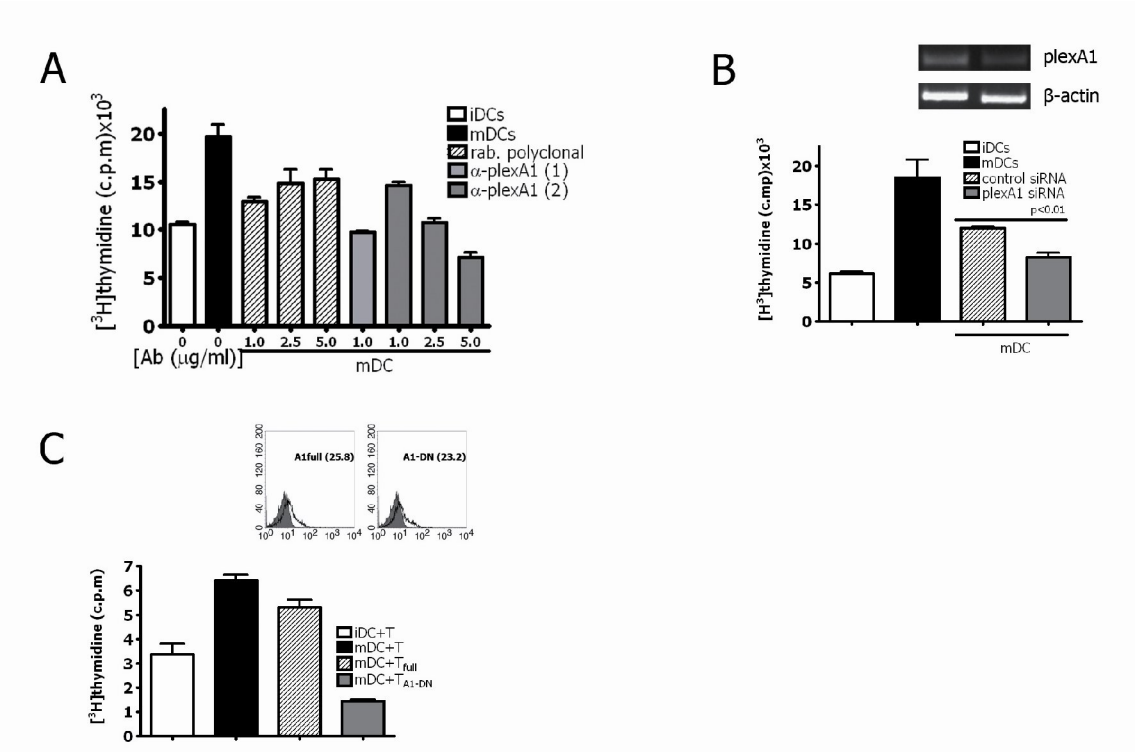

Figure 3-4: PlexA1 is involved in T cell proliferation assessed by MLR.

(A) MLR assays were performed using T cells co-cultured with mDCs left untreated (black bar), exposed to a rabbit polyclonal serum (hatched bars) or plexA1 neutralizing antibodies (grey bars) at the concentrations indicated for 30 mins at 4^0C.

(B) T cells were transfected with scrambled (inset RT-PCR, left lane, and graph, hatched bar) or plexA1-specific siRNA (inset RT-PCR, right lane, and graph grey bar) 48 hrs prior to co-culture with allogenic mDCs.

(C) T cells were used for co-cultures with mDCs 6 hrs following transfection of plasmids encoding for GFP (black bar), or VSV-G tagged full length (hached bar) or DN plexA1 (grey bar) (see inset for flow cytometry using VSV-G by specific (open histograms) or an isotype (filled histograms) with the respective percentage of expression indicated),

A to C: iDCs co-cultured with unmodified T cells (each white bar) were also included into the MLRs where T cell proliferation was determined by ^{3}H-thymidine incorporation. Experiments were performed in triplicates and means and SEM are indicated. For each, one representative out of three experiments is shown.

3.4. PlexA1 and NP-1 are recruited to the IS

The role of plexA1 and NRP-1 on immune cells, in particular T cells and DCs, is not well understood. They are implicated in T cell activation by murine or human DCs (Tordjman, Lepelletier et al. 2002; Wong, Brickey et al. 2003; Eun, O'Connor et al. 2006) as also evident from their recruitment to the IS.

As having shown in the previous experiments, plexA1 surface expression is transiently increased upon CD3/28 ligation, peaks at 30min and is sustained for up to 2 hrs. The following experiments were performed to address the fate of plexA1 involved in the synapse formation.

3.4.1. PlexA1 translocates towards the interface formed between T cells and DCs

On murine DCs, plexA1 has been first documented to polarize to the DC-T cell interface with a non-punctate distribution (Eun, O'Connor et al. 2006). In line with this finding, immunofluorescent staining of autologous/allogeneic DC-T conjugates revealed that there was a strong accumulation of plexA1 at the IS between T cell and DCs (Figure 3-5).

Immature DCs infrequently conjugated to T cells and immature synapses were characterized by a homogeneous distribution of TCR (Figure 3-5A-B, upper panels), and by diffuse location of plexA1 in DCs and T cells. In contrast, mature DCs established, with allogeneic T cells, efficiently ISs where plexA1 strongly co-localized (about 80% of analyzed conjugates) at the contact plane and with CD3 as depicted in the histogram plot (Figure 3-5A, right).

In an autologous system, IS formation is rare in the absence of super-antigen (SA). On mature DC pulsed with SA, plexA1 and CD3 co segregation was identical to that seen in the allogeneic system (Figure 3-5B).

Because both T cells and DCs express plexA1 (Figure 3-5), it is hard to discriminate whether the molecule locates to the T cell or DC side. Thus anti-CD3/28 coated beads were used to mimic antigen presenting cells (APCs). Evidently, plexA1 was translocated to the stimulatory interfaces between T cells and conjugating beads (Figure 3-5C, left), indicating that plexA1 in the IS is at least from the T cell side (Figure 3-5A-B).

3.4.2. NP-1 on T cells is recruited to the IS

It has been shown that NP-1 is polarized to the IS on T cells and DCs, and this is beneficial for DC-induced proliferation of resting T cell (Tordjman, Lepelletier et al. 2002). In agreement with that finding, NP-1 on T cells was seen translocated to the contact plane formed between these cells and pseudo APCs, anti-CD3/28 coated beads, (Figure 3-5C, right) and co-detected with its co-receptor plex-A1 (Figure 3-5D) in allogenic DC co-cultures. Furthermore, fluorescent staining revealed DCs do express NP-1, also confirmed by flow cytometry (section 3.6), the molecule did not translocate towards the contact plane (Figure 3-5D).

Altogether, plexA1 as well as NP-1 is recruited to the stimulatory interfaces in T cells and this may potentially play a role in synapse stability and function.

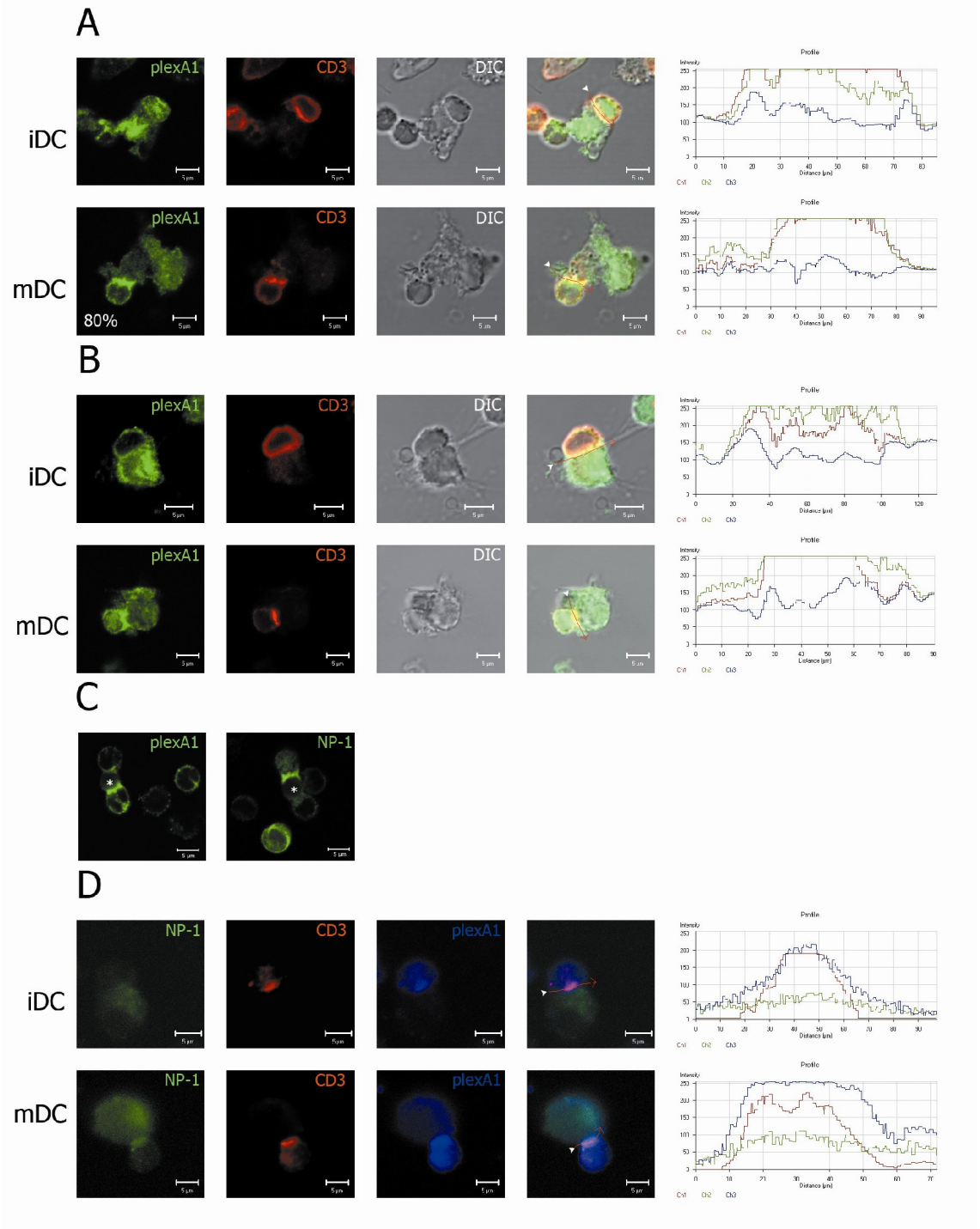

Figure 3-5: PlexA1, but not NP-1 on DC side, translocates towards the immunological synapse (IS).

Immunofluorescent staining of plexA1 labeled in green, and CD3 labeled in red on allogenic (A) and SA-pulsed autologous (B) fixed synapses. The intensity profiles for distribution are shown in right histograms (red line, indicated by white arrows). The frequency of conjugates revealing IS translocation of plexA1 in mDC/T cell conjugates was 80% of a total of 35 conjugates analyzed.
Immunofluorescent staining of plexA1 (C, left) or NP-1 (C, right) on T cells activated by CD3/28 beads (indicated by asterisks).
(E) Immunofluorescent staining of NP-1 (labeled in green), CD3 (labeled in red), and plexA1 (labeled in pseudo color blue) of allogenic fixed synapses. The intensity profiles for distribution are shown in right histograms (red line, indicated by white arrows). One out of 20 conjugates analyzed is shown.
Scale bar, 5 μm. Magnification, 40X.

3.5. MV-driven abrogation of plexA1/NP-1 translocation to the IS

It has already been shown that MV exposure prevents cytoskeletal rearrangement in T cells and this is thought to contribute to IS instability (Muller, Avota et al. 2006). PlexA1 and NP-1 are translocated towards the IS (section 3.3), playing a crucial role in DC-T cell interaction (section 3.3), it raises a question whether plexA1/NP-1 translocation in T cells is modulated by MV.

To this end, MV-exposed T cells were stimulated with CD3/28 coated beads and the translocation of plexA1/NP-1 to the stimulatory interface formed between cells and the beads was assessed (Figure 3-6). The plexA1/NP-1 induced shift was scored into three different categories. In a nonpolarized-pattern, plexA1/NP-1 showed a rather diffuse staining with barely detectable accumulation at the stimulatory interface. In a polarized-pattern, the molecules depicted a strong accumulation at the interface and the partial-pattern is an intermediate phenotype. In untreated T cells, the majority of cells showed a polarized-pattern of plexA1. In stark contrast, MV-exposed cells mainly had an unpolarized-pattern. Although mock treatment had an effect on plexA1 redistribution, this was not pronounced (Figure 3-6A, plot). Similarly, NP-1 distribution on MV-exposed T cells mainly exhibited a nonpolarized-pattern in comparison to untreated and mock-exposed T cells (Figure 3-6B, plot).

Altogether, MV exposure abrogates plexA1/NP-1 translocation towards the stimulatory interface in T cells.

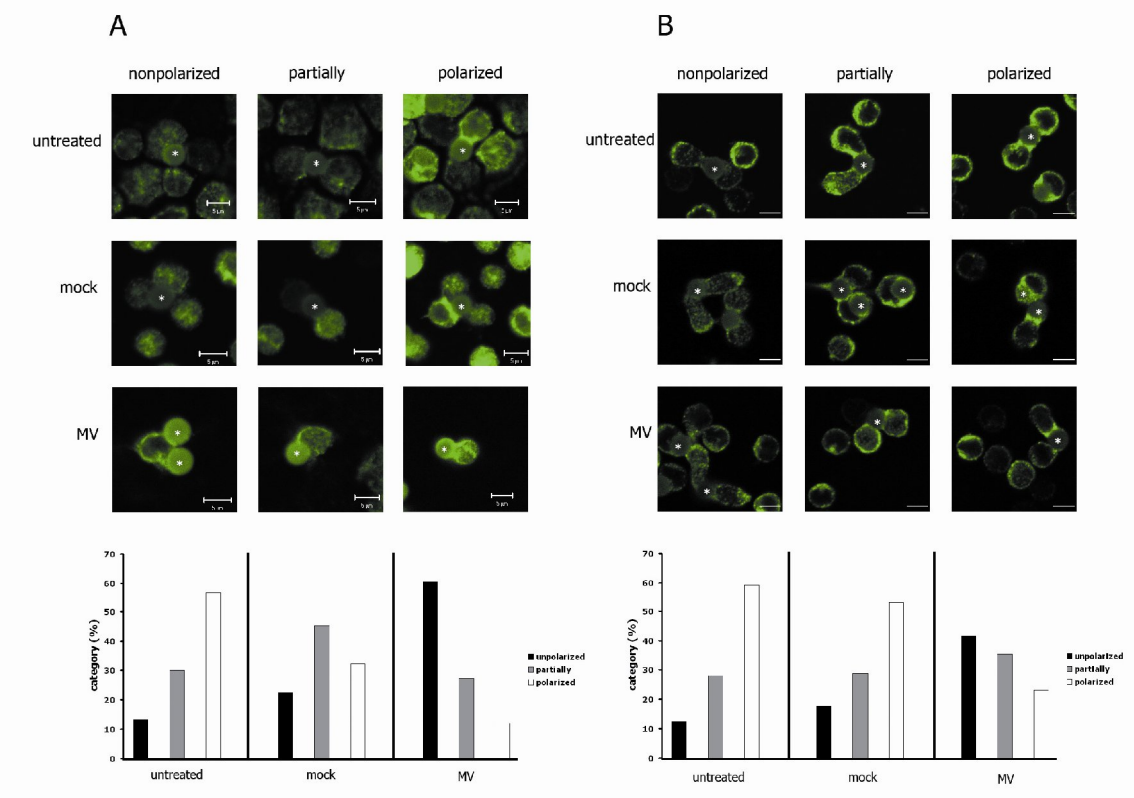

Figure 3-6: Recruitment of plexA1 and NP-1 to stimulatory interfaces are affected by MV exposure to T cells.

MV exposure T cells were activated with CD3/28 beads for 30min, and then stained for plexA1 (A) or NP-1 (B). Asterisks indicated beads. Scale bar, 5 μm. Magnification, 40X.

Quantitative analysis of plexA1 (A, bottom graph) or NP-1 (B, bottom graph) translocation in T cells treated as described above. Cells were scored into three staining patterns (black bar: nonpolarized, grey bar: partially, white bar: polarized). At least, 30 cells were counted for each experiment.

3.6. PlexA1 and NP-1 surface expression on maturing DCs is regulated by endocytosis

Aberrant signaling by DCs is thought to account for MV T cell silencing during immunosuppression. To analyse as to whether in addition to prevent plexA1/NP-1 IS recruitment on T cells, MV infection of DCs impairs T cell activation at the level of semaphorin receptors as well, the expression profiles of plexA1/NP-1 on DCs were first analysed. Expectedly NP-1 (Tordjman, Lepelletier et al. 2002; Chabbert-de Ponnat, Marie-

Cardine et al. 2005) (in around 60%) and, so far only described to be expressed on murine DCs (Eun, O'Connor et al. 2006), plexA1 were readily detectable on the surface of about 45% of iDCs (with MFIs of 41.61 and 85.84, respectively), and both were downregulated within 24 hrs on LPS maturation (Figure 3-7A). Interestingly, mock or MV-infection caused moderate (for plexA1) or no (for NP-1) downregulation confirming earlier observations that DC maturation by MV may not be complete (Servet-Delprat, Vidalain et al. 2000). To address the mechanisms underlying LPS-dependent plexA1 and NP-1 downregulation, markers for endo/lysosomal compartments iDCs and mDCs were used. In iDCs, plexA1 and NP-1 localized both at the cell surface and in cytosolic compartments not labeled by lysotracker (Figure 3-7B, upper row). In mDCs, NP-1, but not plexA1, efficiently co-localized with lysotracker indicating that its surface downregulation may involve lysosomal degradation (Figure 3-7B, middle row). In line with this hypothesis, chloroquine (CQ) present during LPS maturation partially rescued surface detection of NP-1 as detected also by flow cytometry (in a typical example, percentages of iDCs, mDCs and mDCs+CQ were 40.1, 13.8 and 23.6, respectively). In contrast, partial co-localization of plexA1 with CD71 in iDCs was strongly enhanced in mDCs, indicating surface expression of plexA1 is regulated by shuttling through recycling endosomal compartments (Figure 3-7C). Thus, inclusion of PAO stabilized and even enhanced surface expression of plexA1, but not NP-1, on mDCs (51.3, 12.0, 75.4% on iDCs, mDCs and mDCs+PAO, respectively). Altogether, LPS but not MV infection (Figure 3-7D) downregulates surface expression of both plexA1 and NP-1 on DCs by endocytosis.

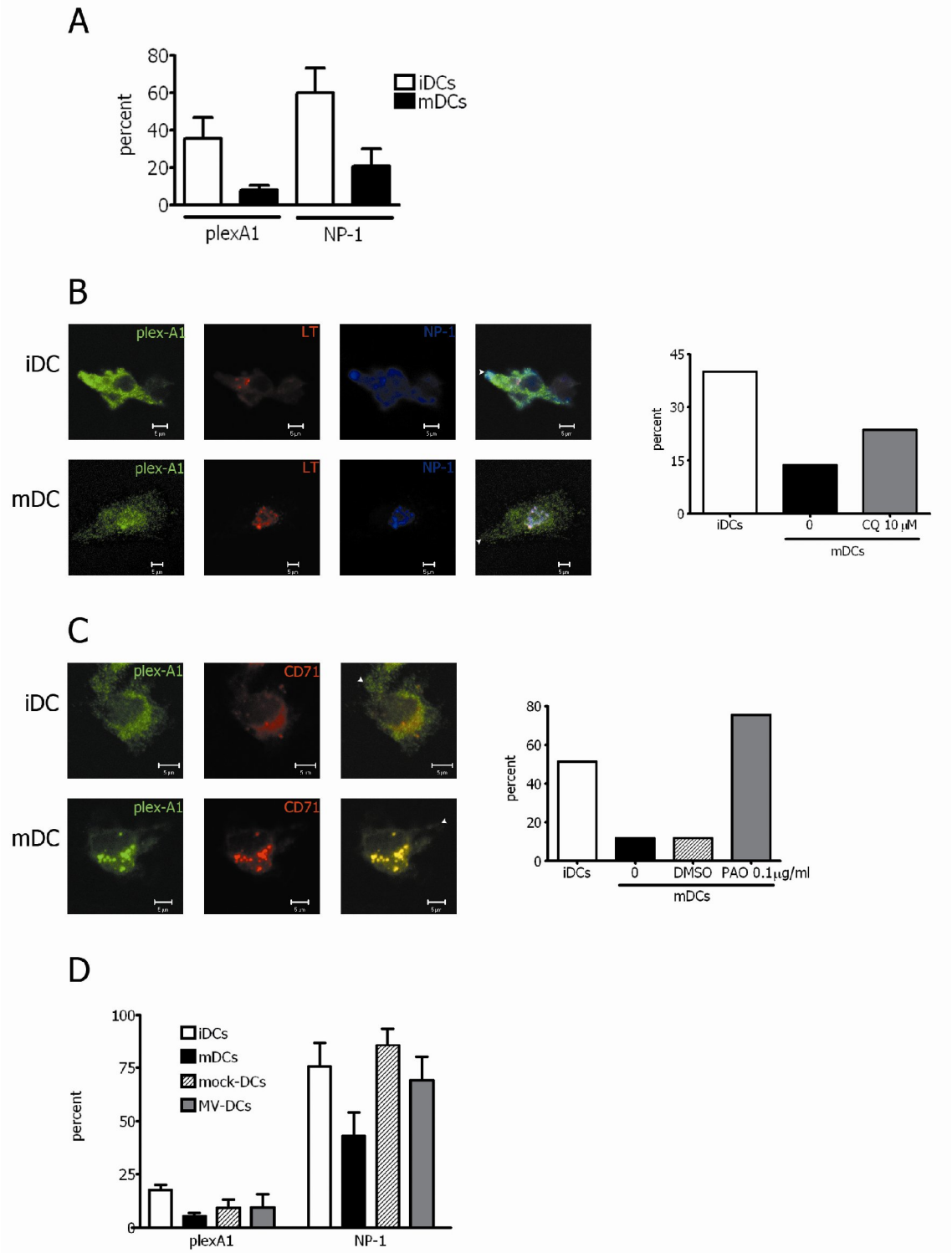

Figure 3-7: Both plexA1 and NP-1 are down modulated on LPS-matured DCs.

(A) Surface expression of plexA1 and NP-1 on MDDCs was assessed 24-hour post LPS maturation. Percentage of positive cells following subtraction of isotype control values are means of three independent experiments with SEMs.

(B) Immunofluorescent staining of NP-1 (labeled in pseudo color blue), plexA1 (labeled in green) and lysosomal compartments (labeled in red) in DCs 24-hour post LPS maturation. Right graph:

chloroquine (CQ, 10 μM) was simultaneously applied to LPS-containing medium and surface expression of NP-1 on DCs was assessed 24-hour post treatment.
(C) Immunofluorescent staining of plexA1 (labeled in green) and recycling compartments (CD71, labeled in red) in DCs 24-hour post LPS maturation. Right graph: phenylarsine oxide (PAO, 0.1 μg/ml) was simultaneously applied to LPS-containing medium and surface expression of plexA1 on DCs was assessed 24-hour post treatment. DMSO served as vehicle control.
(D) Surface expression of plexA1 (first bar each pair) or NP-1 (second bar each pair) on immature (i), mature (m), mock or MV-infected DCs was assessed after 24 hrs.
Scale bar, 5μm. Magnification, 40X. Data are representative of 3 independent experiments.

3.7. Upregulation and early secretion of SEMA3A by MV-DCs

The plexA1/NP-1 ligand SEMA3A released late after activation of T cells or DCs or in DC/T cell cocultures acts to block T cell proliferation, and has thus been proposed to avoid overactivation or to terminate T cell responses (Lepelletier, Moura et al. 2006). Therefore, it's worth investigating whether MV-DCs could differ from mDCs with regard to SEMA3A production. As revealed by RT-PCR experiments, MV-DCs upregulated transcripts encoding for SEMA3A over time, and these, though not quantitatively determined, accumulated somewhat more efficiently than in LPS-matured cells (Figure 3-8A). Supernatants from the very same cultures were used for immunoprecipitation to determine levels of secreted SEMA3A (sSEMA3A). Except for iDCs, all cultures produced within 48 hrs the 110 kD sSEMA3A species (Figure 3-8B) representing the repulsive isoform. In addition, a lower molecular weight species was also detected the nature of which is unknown as, unlike for other SEMAs (Adams, Lohrum et al. 1997), production of isoforms differing in activity has not been described for SEMA3A as yet. Production of sSEMA3A from MV-DCs, however, by far exceeded that by mDCs both with regard to kinetics and magnitude, with high levels produced already after 24 hrs levels that were not reached by mDCs within the entire observation period (Figure 3-8B, bottom graph). To reveal if early sSEMA3A secretion also occurred in co-cultures involving MV-DCs, these (as were the

control DC cultures) were extensively washed prior to addition of allogenic T cells and levels of sSEMA3A were determined over time. Indeed, 110 kD sSEMA3A was detectable already 6 hrs after onset of the MV-DC/T cell co-culture, and continuously rose until 48 hrs where it entered a plateau phase, while, in agreement with published observations, release of sSEMA3A in LPS-DC/T cell cultures was seen only after 72 hrs (Figure 3-8C). For unknown reasons, the mock prepation also caused some sSEMA3A production from DCs (Figure 3-8B and C). Collectively, MV infection of DCs promotes early overproduction of a repulsive plexA1/NP-1 ligand SEMA3A, especially in the presence of allogenic T cells.

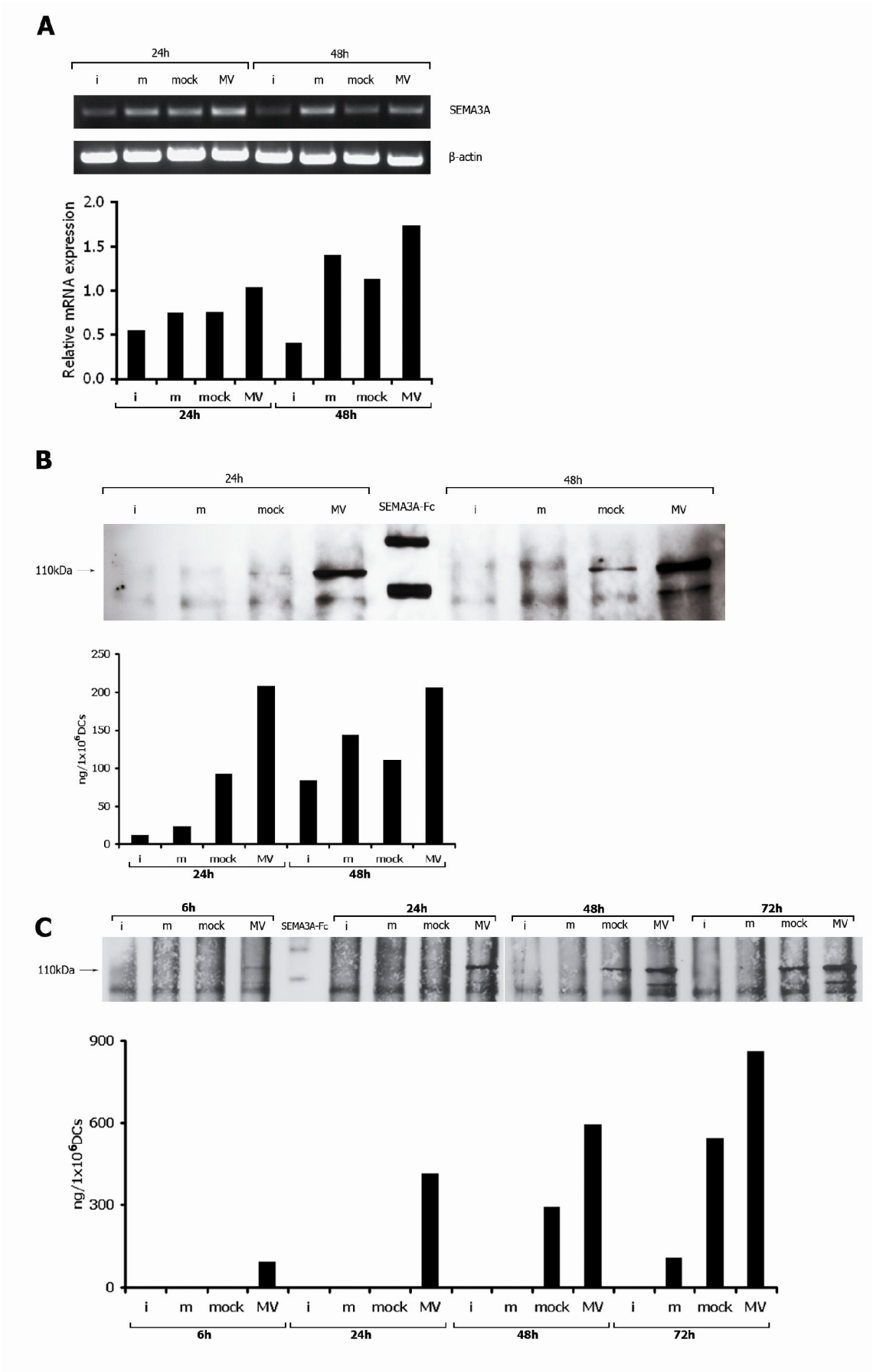
A
24h
48h
i
m
mock
MV
SEMA3A
β-actin
Relative mRNA expression
2.0
1.5
1.0
0.5
0.0
B
SEMA3A-Fc
110kDa
ng/1x10^6DCs
250
200
150
100
50
0
C
6h
72h

Figure 3-8: MV infected DCs promote early production of soluble SEMA3A, particularly in the presence of allogeneic T cells.
A. RT-PCR analysis of SEMA3A transcripts (or, for normalization, β-actin).
B. SEMA3A (110 kD; indicated by the arrows) was detected in immunoprecipitates of supernatants of the different DC species (MV infection was 65% after 48 hrs). Quantification of SEMA3A secretion was determined by comparison of band intensities to a defined SEMA3A-fused-Fc protein.
C. SEMA3A (110 kD; indicated by the arrows) was detected in immunoprecipitates of pooled supernatants of three independent co-cultures of the indicated allogeneic DC species and T cells. Infection levels for MV-DCs ranged between 60 and 80% after 48 hrs. Data were quantified as in B.
A-C. Lanes represent iDCs alone (each lane 1), or exposed to LPS (mDCs; each lane 2), mock (each lane 3) or MV (each lane 4) analyzed at the time intervals indicated. Quantifications were done using AIDA software (each bottom graphs). In A and B, each one out of three independent experiments is shown.

3.8. SEMA3A and, to a greater extent, SEMA6A causes a transient loss of F-actin and microvillar extension in T cells

So far, SEMA3A-induced collapse has been described only for neuronal outgrowth (Aizawa, Wakatsuki et al. 2001; Brown and Bridgman 2009). Recently, interference with TCR polarization and early signal transduction has indicated SEMA3A-dependent inhibiton of actin cytoskeleton reorganization (Lepelletier, Moura et al. 2006). Therefore, it remains to be determined whether a similar effect as already seen in neuronal system does apply to T cells.

3.8.1. SEMA3A and -6A cause a transient loss of F-actin, while front-rear polarization remains unaffected

To answer this question, FN seeded T cells were exposed for various intervals to IgG (included for control) or recombinant SEMA3A (SEMA3A-Fc) and analysed F-actin content of the cells. SEMA3A, but not IgG significantly decreased the average mean intensity of F-actin in T cells within 15 mins which then returned to normal within 60 mins (Figure 3-9A upper row, and graph). Strikingly, T cells exposed to recombinant SEMA6A

(SEMA-6A-Fc), initially included as a further negative control, also revealed a transient loss in F-actin, identical to that induced by SEMA3A (Figure 3-9A, bottom row and graph). SEMA6A binds plexA4 rather than plex-A1, and in line with its biological effect in our system, we readily detected expression of plexA4 on a substantial fraction of primary human T cells (Figure 3-9A, bottom left panel).

The next step was to analyze the front-rear polarized phenotype of SEMA-treated T cells since transient defect on F-actin could lead to a mislocalization of receptors required for cellular function. After application of SEMAs for different intervals, FN seeded T cells were stained for F-actin and CD43, to visualize lamellipodia and uropods, respectively. Despite SEMA treatment caused a temporal loss of F-actin, the treatment had no effect on front-rear formation in FN-seeded T cells (Figure 3-9B).

3.8.2. SEMA3A and SEMA-6A cause transient loss of microvillar extensions in T cells

The data presented in Figure 3-9A raises a question whether a transient effect on F-actin content correlates with an alteration in actin-based protrusion. To obtain higher resolution for image documentation, treated cells were analyzed by scanning electron microscopy. This method revealed that, in agreement with immunofluorescent staining, SEMA3A and SEMA6A exposure did not interfere with the ability of T cells to retain their polarized phenotype on the FN substrate (Figure 3-9C, upper right graph). However, in accordance to their loss of F-actin (Figure 3-9A), the integrity of their microvillar extensions was effectively lost with 15 mins, which fully recovered within 60 mins (Figure 3-9C, lower right graph). Thus, ligation of SEMA3A and -6A receptors on T cells causes a rapid, transient loss of actin-based protrusions.

Taken together, ligation of SEMA3A and -6A receptors on T cells affects actin turnover and dynamics in T cells transiently causing loss of membrane protrusions, yet not of front-rear polarization on FN.

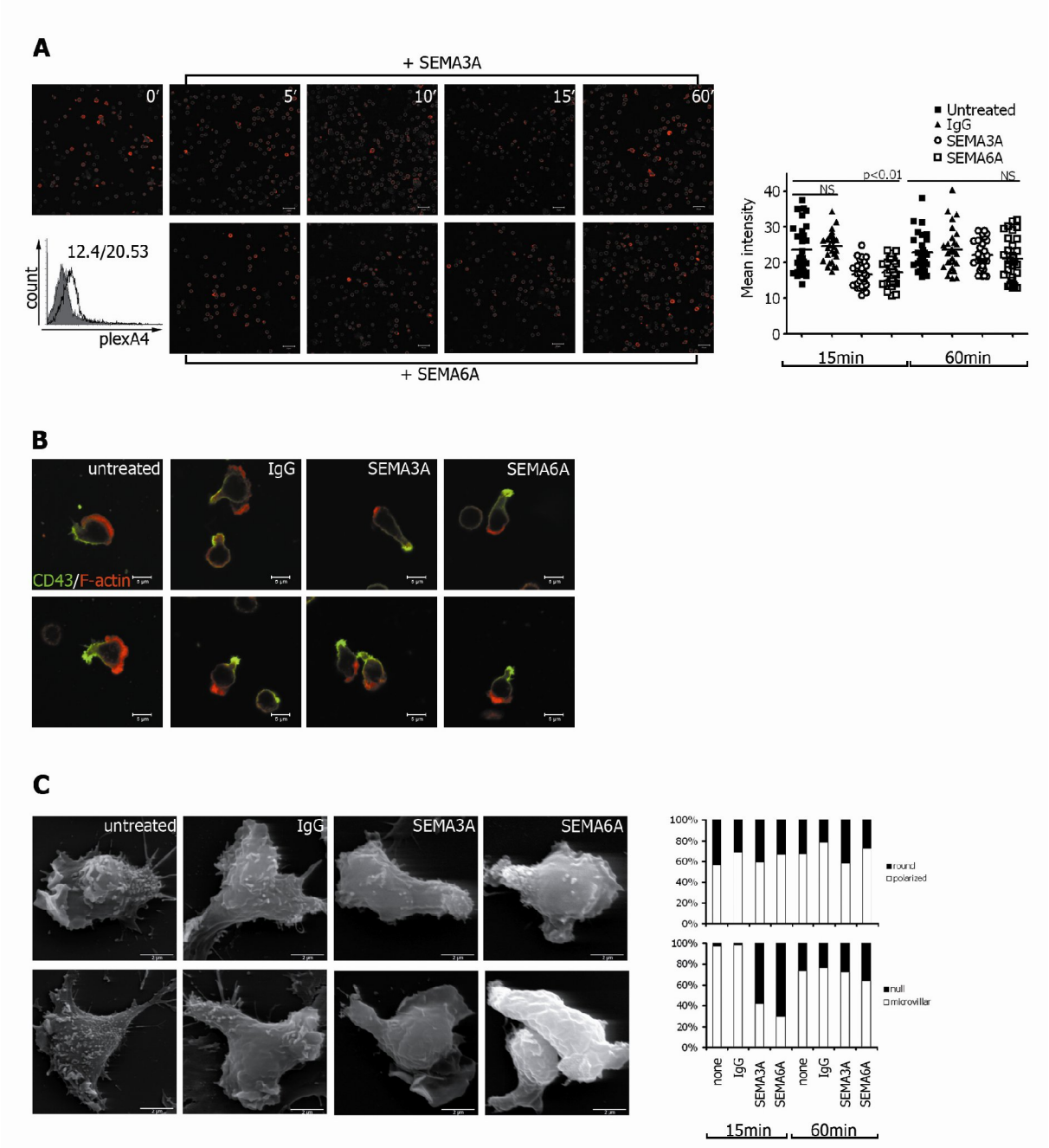

Figure 3-9: SEMA3A and SEMA6A cause transient loss of F-actin and microvillar extensions in T cells.

A. T cells seeded onto FN-coated slides were exposed to SEMA3A (left panel, upper row), SEMA6A (left panel, bottom row) or, for control, IgG, for the time intervals indicated, fixed and stained for F-actin using binding phalloidin-Alexa 594. Scale bar, 5 μm. Magnification, 40X. In addition, plexA4 was

detected on living, primary T cells by flow cytometry (filled histogram; open histogram showing the isotype control antibody staining; left bottom panel). Quantification of F-actin intensity was performed using ImageJ software, function Measure (right panel). At least, 30 cells were counted for each experiment. p values from Student's unpaired t-test are indicated.

B. One hour following seeding onto FN, T cells were left untreated (left panels) or exposed to IgG (second panels), SEMA3A (third panels) or SEMA6A (right panels) for 15 (upper row) or 60 (bottom row) mins prior to fixation and detection of F-actin and CD43. Representative examples of each 20 analyzed are shown. Scale bar, 5 μm. Magnification, 63X.

C. T cells seeded onto FN-coated slides were fixed after 15 mins (left panels and right graph) or 60 mins exposure to SEMA3A, SEMA6A or IgG (right graph) and analyzed by SEM. Cells (examples are shown in the left panels) were scored into morphological categories (round versus polarized and null versus microvillar). Each 100 cells were recruited into the analysis (right graph). Scale bar, 2 μm. Magnification, 5000X.

3.9. SEMA3A reduces the mean velocities of DCs but not T cells under "semi-3D" migratory condition

It has been shown that leukocyte migration can be integrin-dependent or -independent. In a semi-3D setup, migratory leukocytes are solely driven by an anterior actin flow. The data presented above show a transient loss of F-actin and microvilli upon SEMA treatment. Therefore, it raises a question whether this impairs the migratory capacity of treated cells. To answer this question, SEMA-preincubated DC/T cells were injected under an agarose layer (Figure 3-10A), triggered active movement using chemokines, CCL19 and CCL21, and monitored the movement of cells for 30 mins (T cells) or 2 hrs (DCs). As a control, we used IgG-treated cells.

Although pretreatment with IgG reduced the mean velocities of DCs (Figure 3-10B, bottom graph, black triangles) and T cells (Figure 3-10C, bottom graph, black triangles), the reduction is not significant in comparison to untreated cells (Figure 3-10B-C, bottom graph, black squares). Both SEMA3A and-6A treatments led to a significant reduction of DC speed (Figure 3-10B, bottom graph, open circles and diamonds), with a greater extent on SEMA6A treatment (Figure 3-10B, bottom graph, open diamonds). Similarly, SEMA6A

treated T cells also showed a marked retardation in mean velocity (Figure 3-10C, bottom graph, open diamonds). Unexpectedly, SEMA3A pretreated T cells, which transiently lost F-actin, did not dectectably reduce speed, though the differed significantly from untreated cells (Figure 3-10C, bottom graph, open circles). Hence, SEMA treatment reduces the mean velocities of DCs but not T cells treated with SEMA3A under semi-3D migratory condition.

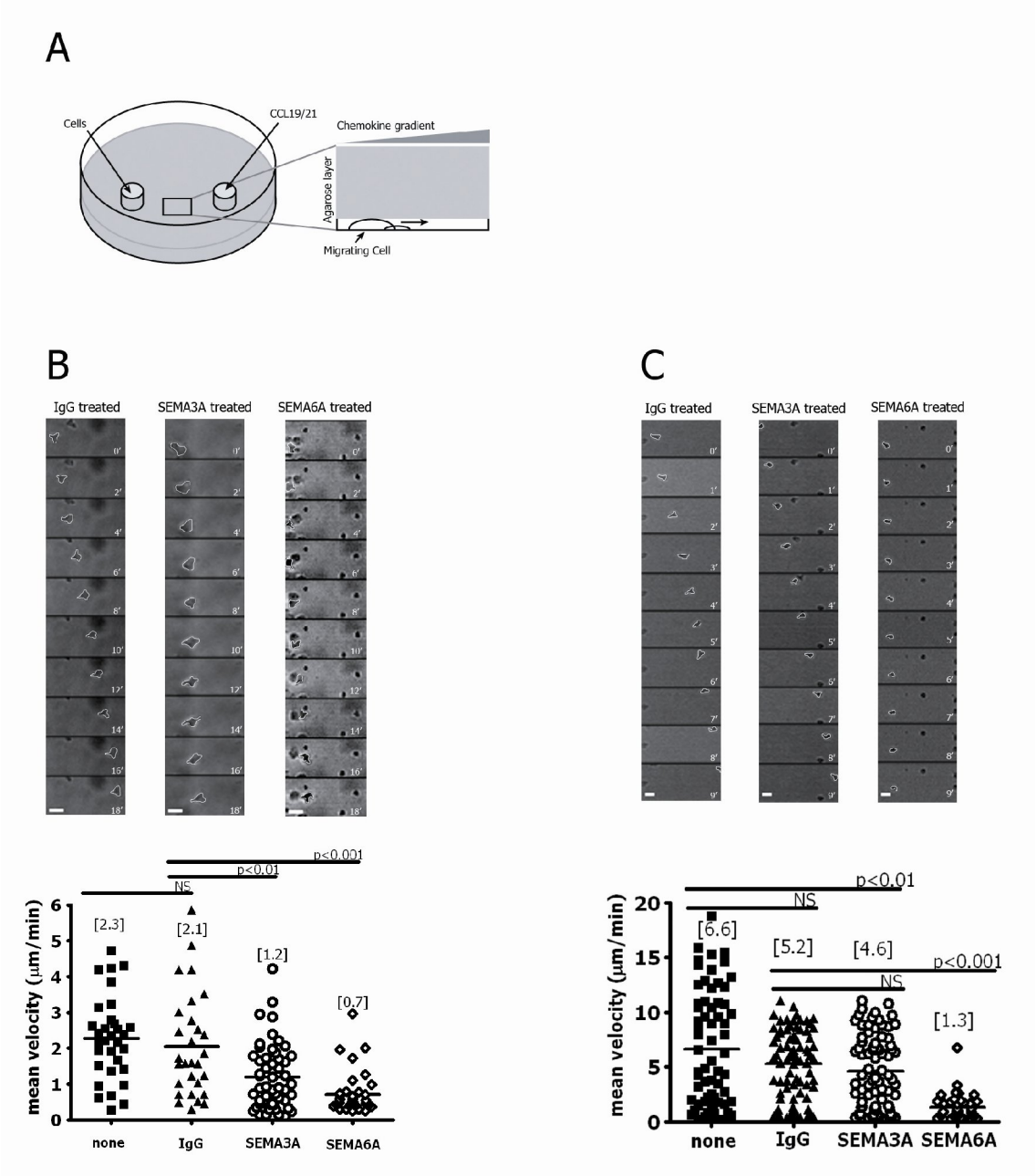

Figure 3-10: SEMA3A and SEMA6A affect on DC migration but not T cells.

A. Schematic set-up of under agarose assay, adapted from (Renkawitz, Schumann et al. 2009)

B. Montage micrographs obtained in under agarose migration assays depicting migrating T cells left untreated (bottom panels, black squares) or pre-exposed to IgG (bottom panels, black trinagles), SEMA3A (bottom panel, open circles) or SEMA6A (bottom panels, open diamonds) for 15 mins under agarose within the indicated time schedule (mins) in response to CCL19/21(each at 1.25 μg/ml). Cells (at least, 30 to 90 cells for each experiment) were traced using ImageJ, plugin Manual tracking, and mean velocities were calculated using ImageJ, plugin Chemotaxis tool. Graphs showed the speed of tracked DCs (B, bottom graph) or T cells (C, bottom graph), with mean velocities indicated [X] in μm/min. One representative out of three independent experiments is shown. Scale bar, 10 μm. Magnification, 10X.

3.10. DC/T cell conjugate formation decreases in the presence of SEMAs

SEMA3A secretion has been shown to inhibit early events in TCR-induced signaling via the interference with actin cytoskeletal rearrangement and kinase phosphorylation (Lepelletier, Moura et al. 2006). It's worth determining whether this negative regulation could result in a decrease in DC-T cell conjugate frequency. To address this question, R18 labeled DCs and CSFE-labeled T cells were pre-exposed to IgG (served as control) and SEMA3A or -6A for 15 min and set up an allogenic reaction with or without a washing step. Conjugate formation was determined by flow cytometry gated on the DC population which is simultaneously positive for CSFE. IgG treated cells were set as 100%.

Over time, the frequency of the double positive population increased, reaching the plateau at 20 min. The difference between treatments was only visible at 30-min time point (Figure 3-11A-C, all left graphs). At this point, the presence of SEMA3A or, with a greater extent, SEMA6A significantly inhibited conjugate formation ($p<0.005$) (Figure 3-11A, right graph). Although DCs or T cells only pretreated with SEMA3A/6A slightly decreased in the percentage of conjugate, it did not receive statistically relevance as compared to the IgG control (Figure 3-11B-C). Strikingly, the presence of SEMA6A but not SEMA3A in DC-T cell co-culture significantly inhibited a MRL and the effect was not synergistic when these two SEMAs were combined (Figure 3-11D).

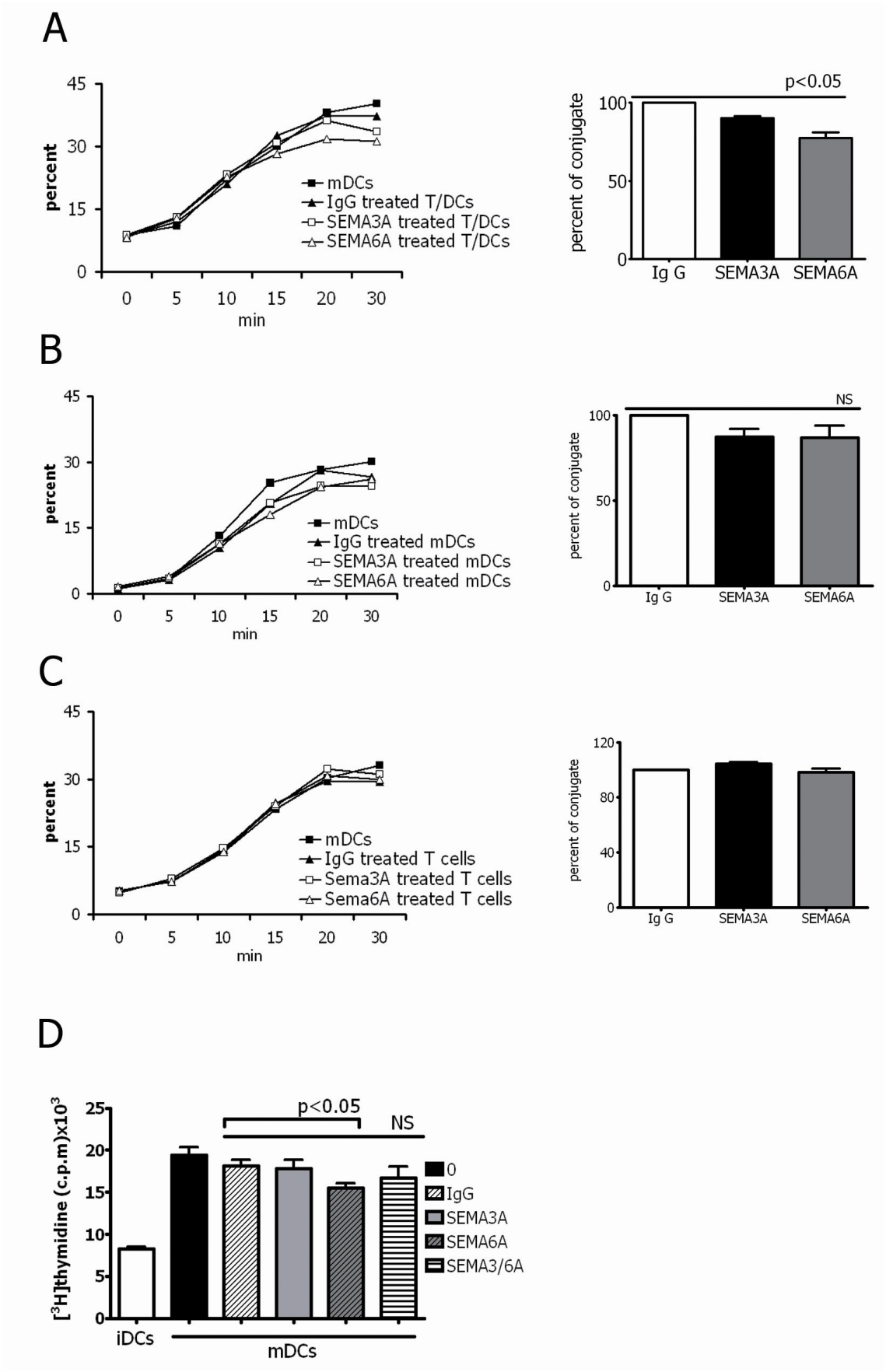
A
percent
min
mDCs
IgG treated T/DCs
SEMA3A treated T/DCs
SEMA6A treated T/DCs
p<0.05
percent of conjugate
Ig G
SEMA3A
SEMA6A
B
percent
min
mDCs
IgG treated mDCs
SEMA3A treated mDCs
SEMA6A treated mDCs
NS
percent of conjugate
Ig G
SEMA3A
SEMA6A
C
percent
min
mDCs
IgG treated T cells
Sema3A treated T cells
Sema6A treated T cells
percent of conjugate
Ig G
SEMA3A
SEMA6A
D
[3H]thymidine (c.p.m)x10³
p<0.05
NS
0
IgG
SEMA3A
SEMA6A
SEMA3/6A
iDCs
mDCs

Figure 3-11: SEMA3A and SEMA6A affect DC/T cell conjugate formation and only SEMA6A has an effect on MLR.

A. Conjugate formation between CFSE-labeled T cells and R18-labeled DCs pre-exposed to for 15 mins and in the presence of IgG (right panel, black triangles, left panel, white bar), SEMA3A (right graph, open squares, left graph, black bar) or SEMA6A (right graph, open triangles, left graph, grey bar) for the time intervals indicated was determined after fixation by flow cytometry (gating of double positive DCs) (left graph). For quantification, IgG treated controls were set as 100% (right graph).

Either R18-labeled DCs (B) or CFSE-labeled T cells (C) was pre-exposed for 15 mins to IgG (right graph, black triangles, left graph, white bar), SEMA3A (right graph, open squares, left graph, black bar) or SEMA6A (right graph, open triangles, left graph, grey bar). The cells were extensively washed and conjugate formation with indicated time intervals was determined after fixation by flow cytometry (gating of double positive DCs) (left graph). For quantification, IgG treated controls were set as 100% (right graph).

D. T cells were co-cultured with mDCs (m) in the absence (black bar) or presence of IgG (hatched bar), SEMA3A (grey bar), SEMA6A (hatched grey bar) or combination of SEMA3A/6A (striped bar). iDCs (i) co-cultured with T cells (white bar) were also included into the MLRs where T cell proliferation was determined by ^{3}H-thymidine incorporation.

Experiments were performed in triplicates and means and SEMs are indicated for each one representative out of three experiments. p values (student's unpaired t-test) are indicated.

CHAPTER IV
DISCUSSION

4. Discussion

It has been shown that T cells which have been exposed to MV do not expand on stimulatory slides and lack surface microvillar structures (Muller, Avota et al. 2006). DCs infected with MV do not support synapse stability and are thus unable to sustain T cell activation (Shishkova, Harms et al. 2007). This suggests that MV strongly affects the integrity of actin dynamics. But the cellular mechanism by which MV alters actin dynamics is incompletely understood.

Bridging innate and adaptive immunity, DCs are able to mount and determine viral immune responses, but also to support viral transmission to T cells and to be targets for viral immunomodulation, thereby being thought to be the first targets conveying MV to lymphoid tissues. Albeit only subtly different from LPS-matured DCs with regard to integrin activation, morphological and adhesive properties (Shishkova, Harms et al. 2007), MV-infected DCs show a functional impairment (Klagge, ter Meulen et al. 2000; Servet-Delprat, Vidalain et al. 2000; Abt, Gassert et al. 2009). Recently, it has been shown that mature DCs alone release repulsive SEMA3A and this secretion is delayed in the presence of allogenic T cells (Lepelletier, Moura et al. 2006).

Since interference with actin dynamics is a property of SEMA/plexin/NP interactions which are known to regulate IS function and stability, it raised a question whether plexA1/NP-1 could contribute to MV-induced collapse of T cell protrusion. To address this question, the first aims were to understand the mode of regulation and basic functions of the two receptors - plexA1 and NP-1 - in IS formation and function by analyzing their expression profile on T cells and DCs. Then the next questions were to investigate on how MV modulates these two receptors in T cells after exposure to the virus and whether MV infection modifies the kinetic of secretion of repulsive plexA1/NP-1 ligand, SEMA3A.

4.1. Basic regulation of plexA1 and NP-1

4.1.1. Basic regulation of plexA1 and NP-1 in T cells

To approach these questions, the expression patterns and basic regulations of plexA1 and NP-1 in T cells and DCs were first investigated. Although there are some indirect evidences of plexins being expressed on primary T cells and it is also shown on leukemic Jurkat T cells that plexA1 is expressed at least at mRNA level, the expression patterns of plexA1 has not been directly studied (Catalano, Caprari et al. 2006; Moretti, Procopio et al. 2008). In this present study, the data indicated that plexA1 was expressed on human primary T cells (Figure 3-1A) although its expression patterns were different from those generated by other methods such as fixation or permeabilization. On living cells, the expression of the molecule was low, while expression levels in fixed cells were high. This indicated that the majority of plexA1 was stored intracellularly (Figure 3-1A).

So far, little is known about the role of plexA1 in the function of T cells. The presented data are now showed that plexA1 was an important component of IS function. By using CD3/28 ligation activation, it demonstrated that this molecule translocated transiently to the surface of T cells. The translocation exhibited a peak at 30 min after activation (Figure 3-3). The localization of plexA1 was further investigated using allogenic DCs. This interaction showed an accumulation of plexA1 at the stimulatory interface between T cells and DCs. To corroborate that plexA1 was indeed contributed by T cells, we used CD3/28 coated beads, which mimic antigen-presenting cells - (APCs). This method showed that plexA1 is also accumulated at the interface between T cells and the beads (Figure 3-5). Due to technical limitation, spatial location of this molecule within IS, however, could not be elucidated, so that it remains elusive whether it is part of the c-SMAC or p-SMAC. Furthermore, the disruption of T cell expansion via several methods including siRNA-mediated knockdown,

exogeneous blockage or overexpression of dominant negative version of plexA1 (Figure 3-4) indicated the important role of plexA1 in IS stability and function. This study is the first to document the important role of plexA1 in human primary T cells.

The importance of NP-1 in the IS has been established in murine and human system. In line with published data, surface expression level of NP-1 remained very low (Figure 3-1B) and NP-1 was co-detected with CD3 at the interface between human T cells and DCs, as well as between human T cells and stimulatory beads (Figure 3-5). Unlike murine system, NP-1 on human T cells is not a Treg marker since it can be upregulated on up to 20% of cells after 24-48 hrs of CD3/28 or PMA/ionomycin activation [Milpied, Renand et al. (2009), and unpublished observations]. Notably, both plexA1 and NP-1 were upregulated at very late stage of CD3/28 activation on T cells (Figure 3-3) which timely coincided with the secretion of the plexA1/NP-1 ligand SEMA3A (Lepelletier, Moura et al. 2006). Since the repulsive role of SEMA3A in IS formation has been suggested (Lepelletier, Moura et al. 2006), it seems that the late upregulation of plexA1/NP-1 on activated T cells plays a role in terminating a normal immune response.

Accumulating evidence suggests that semaphorin receptors, plexA1/NP-1, known to act as guidance cues in neuronal pathfinding, play an important role in regulating immune functions, especially at the level of the IS (Takahashi, Fournier et al. 1999; O'Connor and Ting 2008). Due to their ability to regulate adhesion, their expression profiles and ligands determine if they have a stabilizing or repulsive activity and, for immune cells, this is of particular importance in cell migration and conjugate formation, efficiency and duration (Casazza, Fazzari et al. 2007). This has been specifically highlighted for the plexA1/ NP-1 complex for which a dual role in the IS has been evidenced, generally by supporting initial formation and IS function, potentially by self-interactions or with unknown ligands (Ohta, Mizutani et al. 1995; Tordjman, Lepelletier et al. 2002), while, at late stages, as receptors for

the repulsive ligand SEMA3A which has been linked to termination of T cell activation (Catalano, Caprari et al. 2006; Lepelletier, Moura et al. 2006).

The self-interactions of NP-1 has been proposed and experimentally proven. This is thought to mediate the interactions between human DCs and T cells that are essential for initiation of the primary immune response (Tordjman, Lepelletier et al. 2002) or between murine iDCs and Treg during antigen recognition leading to a "default" suppression of immune response in the absence of danger signals (Sarris, Andersen et al. 2008). In contrast to the murine system, NP-1 in humans is not restricted to Treg (Milpied, Renand et al. 2009) and in agreement with this the molecules was found expressed low to negligible in 3 to 5 % of freshly isolated T cells (Figure 3-1).

Like NP-1, plexA1 expression was also low (Figure 3-1), ranging between 4 to 10% of human PBLs. The molecule was expressed on both T cells and DCs, and translocated towards the interfacial plane of DC/T cell interactions. Because it has already been shown in neuronal cells that plexA1 is homotypic interactions (Ohta, Mizutani et al. 1995), this raises a question whether plexA1 could, like NP-1, self-interact to support initial formation and IS function.

4.1.2. Basic regulation of plexA1 and NP-1 in DCs

Similar to the murine system, plexA1 was expressed on human DCs (Figure 3-7) although the expression pattern was quite different. In murine DCs, the molecule is detected as cytoplamic protein in immature DCs and becomes primarily membrane located upon TNF-α maturation (Eun, O'Connor et al. 2006) that is in contrast to what has been seen in this study. In humans, LPS-maturated DCs downmodulated plexA1 (Figure 3-7). This difference could be species or methodology specific. In the favor of the latter explanation, this study was performed to measure the surface expression of plexA1, but not the total

level like it was done in the study of Eun, O'Connor et al. (2006). Moreover, the expression level drastically increased when fixation was applied (data not shown). Despite being downmodulated from the cell surface on mDCs, plexA1 was not subjected to protein degradating but to recycling compartments, suggesting that the molecule might be needed for mDC function and can shuttle back to the membrane upon DC-T cell interactions. Hence, it remains elusive why mDCs downmodulate plexA1 after LPS treatment.

It has been shown that NP-1 is expressed on human DCs (Tordjman, Lepelletier et al. 2002; Chabbert-de Ponnat, Marie-Cardine et al. 2005). However, the fate of this molecule after DC maturation or upon pathogen encounter has not been fully characterized. LPS-driven maturation promoted the downregulation of NP-1 from DC surface (Figure 3-7), which is in contrast to what has been observed by Tordjman (2002). The disagreement between the presented data and theirs could be due to methodological differences since in Tordjman's study, mature DCs were generated using TNF-α/IL-1β while LPS was used in this study instead. This raises a question whether NP-1 plays a redundant role in IS stability and function since DCs generated by both methods seem to be stimulatory. In stark contrast to plexA1, NP-1 on mDCs was routed to lysosomes for protein degradation (Figure 3-7C), supporting the idea of the redundant role of this molecule.

4.2. MV-driven modulation and consequences

Given the importance of plexA1 in T cell activation, the finding that its recruitment to interfaces with stimulator beads is impaired is likely to efficiently interfere with IS efficiency as well. The inability of MV-exposed T cells to organize a correct synapse architecture has previously been described (Muller, Avota et al. 2006) and the established interference of MV signaling with actin cytoskeletal dynamics expectedly accounts for aberrant sorting of receptors probably also including plexA1/NP-1 to this structure (Figure 3-6). This could,

however, not directly be confirmed in conjugates between MV-DCs and T cells because the majority of these is highly unstable (Muller, Avota et al. 2006; Shishkova, Harms et al. 2007).

A role for SEMA3A in termination of DC/T cell interactions by repulsive destabilization of the conjugates on NP-1 interaction has been proposed in the study of Lepelletier, Moura et al. (2006). In agreement with this notion, the kinetic secretion of SEMA3A was at a late stage after onset of an allogenic MLR, about 72-96 hrs (Figure 3-8), when its receptors, plexA1/NP-1, were also upregulated (Figure 3-3). Thus, the timely coordination between the ligand and its receptors seem to control a normal immune response. Notably, MV-DCs alone or, especially, in co-cultures with allogenic T cells promoted early (within few hours) and over secretion of the repulsive SEMA3A (Figure 3-8), by far exceeding those determined to actively inhibit T cell expansion stimulated by allogenic LPS-DCs or on TCR-induced activation. The secreted SEMA3A then could act on T cells in paracrine fashion or on DCs in para-/autocrine manner. It has been shown that MV-DCs resemble a mature phenotype (Shishkova, Harms et al. 2007), these DCs, however, retain plexA1/NP-1 on their surface (Figure 3-7D). Thus, it remains to be determined whether MV impairs DC functions via the alteration the expression pattern of these two receptors.

In axon guidance, plexA1/NP-1/SEMA3A signaling modifies the growth cone cytoskeleton by causing retraction of filopodia and lamellopodia and rearrangement of the actin cytoskeleton (Casazza, Fazzari et al. 2007). The kinetics of actin rearrangement is dependent on the mode of application, gradient or bath. In gradient application, growth cones show a prolonged collapse phase. Bath application, however, induces a brisk but transient collapse and the growth cones eventually return to normal growth cone structure (Brown and Bridgman 2009). In line with this observation, bath application of SEMA3A and also SEMA6A depolymerizes F-actin of T cells (Figure 3-9), peaking at 15 mins. However, the effect is transient since the cells gained their F-actin content after 1hr (Figure 3-9). This

could be due to the receptor desensitization or degradation of SEMAs in bath application mode (Brown and Bridgman 2009). The transient abrogation of the integrity of the actin cytoskeleton as reflected by the loss of actin content correlates with the loss of microvillar extensions (Figure 3-9) which is similar to that in MV-exposed T cells (Muller, Avota et al. 2006). Correlating with this effect, the phosphorylation level of both actin binding and connecting proteins, ERM and cofilin, is reduced in CD3/28 stimulated T cells pre-exposed to MV. Similarly, SEMA treated neuronal cells also reduce p-ERM and p-cofilin levels (Mintz, Carcea et al. 2008; Shimizu, Mammoto et al. 2008). Furthermore, MV-H protein shows highly structural similar to Sema domain (unpublished analysis). Thus, it remains to be determined whether MV binds to plexA1/NP-1 to induce the collapse or to unidentified receptor(s) which share a common pathway with SEMA receptors. Interestingly, SEMA-mediated cytoskeletal interference did not affect overall β1-integrin-stimulated front-rear polarization or receptor-segregation (Figure 3-9) thereby essentially differing from actin cytskeletal paralysis induced on MV exposure of these cells (Gassert, Avota et al. 2009). In line with hypothesis, induction of ceramides as found relevant for MV actin interference was not detectable on SEMA3A/6A exposure of T cells (data not shown) indicating the SEMA-induced signaling may not involve SMase activation.

In contrast to earlier studies (Catalano, Caprari et al. 2006; Lepelletier, Moura et al. 2006), SEMA6A was at least as efficient at interfering with IS stability and function as SEMA3A (Figure 3-11). IgG control did not have any effect on all parameters determined except for T cell motility (Figure 3-10). PlexA4 is known to prevent mossy fibers from entering Sema6A-expressing regions (Suto, Tsuboi et al. 2007) and to negatively regulate T cell responses (Yamamoto, Suzuki et al. 2008). Furthermore, the molecule is readily detectable on a substantial fraction of freshly isolated human T cells (Figure 3-9), thus the activity of SEMA6A in the assay is considered as specific and thus, the obvious discrepancy cannot be

explained at present, and needs further experimentation to identify of the cellular source of SEMA6A.

Similar to plexA1, plexA4 was found expressed in T cells and DCs and the molecule was translocated to the stimulatory interface between T cells and DCs as well as CD3/28 coated beads (data not shown). However, the role of the molecule in the IS could not further be investigated since reagents such as siRNA or neutralizing antibodies are not commercially available yet. Thus, it remains unclear whether human plexA4, like its member subclass plexA1, is required for IS formation and stability or, like its murine counterpart, negatively controls T cell responses (Yamamoto, Suzuki et al. 2008).

Recently, it has been reported that SEMA6A expression is restricted to Langerhans cells (LC) and that SEMA6A protein *in vivo* is only detectable under pathological conditions such as LC histiocytosis or dermatopathic lymphadenitis (Gautier, de Saint-Vis et al. 2006). The upregulation of this molecule is only observed after IFN (interferon)-γ stimulation but not other stimuli such as IL-4, IL-10, IFN-α/β or LPS. In line with this notion, neither immature/mature nor MV-infected DCs express SEMA6A at least at transcriptional level (data not shown).

It has been shown that migration of leukocyte under agarose layer, a semi-3D migratory mode, is dependent on anterior actin-based flow and myosin-II mediated contraction (Lammermann, Bader et al. 2008). Despite of a transient loss of F-actin in T cells (Figure 3-9), SEMA3A treatment did not detectably affect on the actin-based migration of the cells. In contrast, SEMA6A treatment showed a pronounced effect on the mean velocities of treated T cells (Figure 3-10). Although did not address directly, mislocation of chemokine receptor could be excluded since SEMA-mediated cytoskeletal interference did not affect overall β1-integrin-stimulated front-rear polarization or receptor-segregation (Figure 3-9).

By contrast to T cells, both SEMA3A and -6A application reduced the mean velocities of the treated DCs, with a greater extent for SEMA6A treatment (Figure 3-10). It has been recently proposed that plexA1 on murine DCs acts as posterior contractile mediator to squeeze its rigid nucleus through narrow gaps of lymphatic vessels (Takamatsu, Takegahara et al. 2010). It remains to be clarified in human DCs whether spatial distribution or surface levels of plexA1 determine the effect of SEMA-3A treatment since in this study, mature DCs downmodulated surface expression of plexA1 (Figure 3-5A). Notably, SEMA treatment retarded the mean velocities of migrating DCs. At the first glimpse, it seems to contradict Takamatsu's study in which SEMA3A treated murine DCs show an indistinguishabe speed. However, this is likely due to the fact that Takamatsu's experiments are designed to investigate integrin-dependent mode of migration while this present study examined actin-dependent migration.

Even though similar to LPS-matured DCs with regard to integrin activation, morphological and adhesive properties, MV-infected DCs showed a failure in chemotaxis which may result in prolongation of tissue residency and impairment of lymph node homing (Shishkova, Harms et al. 2007; Abt, Gassert et al. 2009). In this present study, SEMA-treated DCs showed impaired chemotaxis towards CCL19/21, the major chemokine sources found in lymph nodes (Luther, Bidgol et al. 2002). In addition, MV- infected DCs early secreted SEMA3A at the concentration (200ng/1x10^6 DCs) by far exceed the amount using in under agarose assay. Thus, SEMA3A probably accounts for the impairment of lymph node homing of MV-infected or bystander DCs.

As reported, inhibition of actin cytoskeletal rearrangement on NP-1 interaction with SEMA3A (the latter produced from mesenchymal stem cells or DCs late after activation) has been linked to human T cell immunosuppression (Lepelletier, Moura et al. 2006; Lepelletier, Lecourt et al. 2009). A role for SEMA3A in termination of DC/T cell

interactions by repulsive destabilization of the conjugates on NP-1 interaction has been proposed. Although exogenous addition of SEMA3A blocks actin and TCR polarization in DC/T cell interfacial zone and ZAP-10 and FAK phosphorylation, it does not affect on DC/T cell conjugates (Lepelletier, Moura et al. 2006). In contrast, lower frequencies of stable conjugates were observed on exogenous addition of SEMA3A (and also SEMA6A) (Figure 3-11A). These, however, do not fully correlate with the MRL results (Figure 3-11D) which are in contrast to what has seen in the study of Lepelletier (2006). The disagreement between the present data and theirs could be due to methodological differences as discussed above.

While abrogation of NP-1/SEMA3A interaction reportedly significantly improved allogenic T cell expansion driven by LPS-DCs, this and conjugate stability in MV-DC/T cell co-cultures could not detectably be rescued by SEMA-neutralizing antibodies (data not shown). This is, however, not surprising since the presence of the MV glycoprotein complex on the DC surface within the DC/T cell interface has previously been linked to IS destabilization and contact-mediated inhibition of T cell expansion (Schlender, Schnorr et al. 1996; Klagge, ter Meulen et al. 2000; Muller, Avota et al. 2006; Shishkova, Harms et al. 2007). It is also because MV particles displaying the inhibitory complex were likely present in conditioned supernatants of MV-DCs or MV-DC/T cell co-cultures containing high levels of SEMA3A that we did not directly prove their activity on anti-CD3/CD28-stimulated T cell expansion.

In addition to adding to the current view on the role and regulation of human semaphorin receptors in the IS in general (such as plexA1 IS recruitment and its importance for IS function in T cells, plexA4 expression in human T cells, plexA1/NP-1 turnover in maturing DCs, SEMA3A and SEMA6A in regulation of T cell protrusions and chemotactic migration), this study is the first to address regulation of those by a pathogen and their importance in the established MV interference with IS function. Recruitment to and

concentration of semaphorin receptors to the IS might, however, also be of relevance for viral transmission there as indicated by the function of NP-1 as physical and functional partner of HTLV env proteins during transmission in the virological synapse (Tordjman, Lepelletier et al. 2002; Ghez, Lepelletier et al. 2006).

5. Summary

Measles virus (MV) infection causes approximately 164,000 deaths per year worldwide (WHO, 2008). The main cause of death is MV-induced immunosuppression but the underlying mechanisms are not fully understood. It has been suggested that MV renders T cells dysfunctional by disrupting the integrity of actin dynamics while MV infection of dendritic cells results in their inability to sustain T cell activation. During neuronal development, semaphorins (SEMAs), especially SEMA3A, induce a collapse of growing dendrites via the binding to plexin-A1 (plexA1) and its coreceptor neuropilin-1 (NP-1). The collapse results from a disruption of actin dynamics. In this study, the roles of these three molecules were investigated in human immune cells and their possible role in MV induced immunosuppression.

The present data have shown that plexA1 is an important component of human immunological synapse (IS). It translocated transiently to the surface of T cells after CD3/28 ligation and accumulated at the stimulatory interface between T cells and DCs (or CD3/28 coated beads). When plexA1 expression was inhibited (RNAi) or its function was disrupted (exogenous blocking or dominant negative expression), T cell expansion was reduced.

Upon MV exposure, translocation of plexA1 and NP-1, another important component of IS, towards the stimulatory interface in T cells was abrogated. Moreover, MV infection interfered with plexA1/NP-1 turnover in maturing DCs and promoted early and substantial release of SEMA3A from these cells, particularly in the presence of allogenic T cells. As revealed by scanning electron microscopy, the release of SEMA3A caused a transient loss of actin-based protrusions on T cells. SEMA3A affected chemotactic migration of T cells and DCs, and reduced formation of allogenic DC/T cell conjugates.

In conclusion, MV targeted SEMA receptor function both by disrupting their recruitment to the IS and by promoting a premature release of their repulsive ligand, SEMA3A. Both of which could contribute to MV-induced immunosuppression.

6. Zusammenfasung

Jährlich gehen ca. 164000 Todesfälle (WHO, 2008) auf eine Infektion mit Masernviren (MV) zurück. Die Hauptursache für den tödlichen Verlauf der Krankheit ist die MV-induzierte Immunsuppression, deren zugrunde liegende Mechanismen noch nicht völlig aufgeklärt sind. Es gibt Hinweise darauf, dass MV einerseits die Funktionalität von T-Zellen beeinträchtigt, indem es die Aktindynamik behindert, und andererseits dendritische Zellen (DC) infiziert, was dazu führt, dass sie T-Zellen nicht mehr vollständig aktivieren können. Während der Entwicklung bzw. des Wachstums von Neuronen kommt es zum Kollaps wachsender Dendriten, wenn Semaphorine (insbesondere SEMA3A) an den Rezeptor Plexin-A1 (plexA1) und seinem Korezeptor Neuropilin-1 (NP-1) binden. Dieser Kollaps wird durch interferenz mit der Aktindynamik verursacht. In dieser Studie wurde die Funktion dieser drei Moleküle in Immunzellen bzw. ihre Rolle in der MV-induzierten Immunsuppression untersucht.

Es konnte gezeigt werden, dass plexA1 eine wichtige Komponente der humanen immunologischen Synapse (IS) ist. Nach CD3/CD28-Ligation kommt es zur transienten Translokation zur T-Zelloberfläche und zur Akkumulation an der Kontaktfläche zwischen T-Zelle und DC bzw. α-CD3/CD28 beschichteten Mikropartikeln. Wird die plexA1-Expression inhibiert (RNAi) oder die plexA1-Funktion gestört (exogenes Blockieren oder Expression einer dominant negativen Mutante), ist die T-Zellexpansion reduziert.

Nach MV-Exposition ist die Translokation von plexA1 und NP-1, ebenfalls einem wichtigen Bestandteil der immunologischen Synapse, zur Kontaktfläche auf T-Zellseite gestört. Des Weiteren behindert eine MV-Infektion den plexA1/NP-1-Metabolismus in reifenden DC und führt zusätzlich zu einer frühen und starken Ausschüttung von SEMA3A durch DC, insbesondere in Gegenwart allogener T-Zellen. Durch

rasterelektronenmikroskopische Aufnahmen wurde gezeigt, dass SEMA3A einen transienten Verlust aktinbasierter Zellfortsätze bei T-Zellen zur Folge hat. Zusätzlich reduziert SEMA3A das chemotaktische Migrationsverhalten von DC und T Zell und die Frequenz ihrer Konjugat-Bildung.

Zusammenfassend stellt sich die Situation so dar, dass MV die Semaphorinrezeptorfunktion zum einen dadurch beeinträchtigt, dass es die Rekrutierung der Rezeptoren zur IS verhindert und zum anderen zur verfrühten Ausschüttung des kollapsinduzierenden Liganden SEMA3A führt. Beide Phänomene könnten einen wichtigen Beitrag zur MV-induzierten Immunsuppression leisten.

7. Reference

(1999). "Unified nomenclature for the semaphorins/collapsins. Semaphorin Nomenclature Committee." Cell 97(5): 551-552.

Abt, M., E. Gassert, et al. (2009). "Measles virus modulates chemokine release and chemotactic responses of dendritic cells." J Gen Virol 90(Pt 4): 909-914.

Adams, R. H., M. Lohrum, et al. (1997). "The chemorepulsive activity of secreted semaphorins is regulated by furin-dependent proteolytic processing." EMBO J 16(20): 6077-6086.

Aizawa, H., S. Wakatsuki, et al. (2001). "Phosphorylation of cofilin by LIM-kinase is necessary for semaphorin 3A-induced growth cone collapse." Nat Neurosci 4(4): 367-373.

Arimura, N., C. Menager, et al. (2005). "Phosphorylation by Rho kinase regulates CRMP-2 activity in growth cones." Mol Cell Biol 25(22): 9973-9984.

Avota, E., A. Avots, et al. (2001). "Disruption of Akt kinase activation is important for immunosuppression induced by measles virus." Nat Med 7(6): 725-731.

Avota, E., H. Harms, et al. (2006). "Measles virus induces expression of SIP110, a constitutively membrane clustered lipid phosphatase, which inhibits T cell proliferation." Cell Microbiol 8(11): 1826-1839.

Avota, E., N. Muller, et al. (2004). "Measles virus interacts with and alters signal transduction in T-cell lipid rafts." J Virol 78(17): 9552-9559.

Bachmann, M. F., K. McKall-Faienza, et al. (1997). "Distinct roles for LFA-1 and CD28 during activation of naive T cells: adhesion versus costimulation." Immunity 7(4): 549-557.

Ballew, H. C. (1992). "Neutralization." Clinical virology manual In S. Specter and G. Lancz (ed.): 229-241

Bankamp, B., S. M. Horikami, et al. (1996). "Domains of the measles virus N protein required for binding to P protein and self-assembly." Virology 216(1): 272-277.

Bankamp, B., S. P. Kearney, et al. (2002). "Activity of polymerase proteins of vaccine and wild-type measles virus strains in a minigenome replication assay." J Virol 76(14): 7073-7081.

Barberis, D., A. Casazza, et al. (2005). "p190 Rho-GTPase activating protein associates with plexins and it is required for semaphorin signalling." J Cell Sci 118(Pt 20): 4689-4700.

Barda-Saad, M., A. Braiman, et al. (2005). "Dynamic molecular interactions linking the T cell antigen receptor to the actin cytoskeleton." Nat Immunol 6(1): 80-89.

Baron, M. D. and T. Barrett (2000). "Rinderpest viruses lacking the C and V proteins show specific defects in growth and transcription of viral RNAs." J Virol 74(6): 2603-2611.

Bartz, R., U. Brinckmann, et al. (1996). "Mapping amino acids of the measles virus hemagglutinin responsible for receptor (CD46) downregulation." Virology 224(1): 334-337.

Bartz, R., R. Firsching, et al. (1998). "Differential receptor usage by measles virus strains." J Gen Virol 79 (Pt 5): 1015-1025.

Bellini, W. J., G. Englund, et al. (1986). "Matrix genes of measles virus and canine distemper virus: cloning, nucleotide sequences, and deduced amino acid sequences." J Virol 58(2): 408-416.

Bellini, W. J., G. Englund, et al. (1985). "Measles virus P gene codes for two proteins." J Virol 53(3): 908-919.

Bellini, W. J., J. S. Rota, et al. (1994). "Virology of measles virus." J Infect Dis 170 Suppl 1: S15-23.

Bieback, K., C. Breer, et al. (2003). "Expansion of human gamma/delta T cells in vitro is differentially regulated by the measles virus glycoproteins." J Gen Virol 84(Pt 5): 1179-1188.

Bieback, K., E. Lien, et al. (2002). "Hemagglutinin protein of wild-type measles virus activates toll-like receptor 2 signaling." J Virol 76(17): 8729-8736.

Biellik, R., S. Madema, et al. (2002). "First 5 years of measles elimination in southern Africa: 1996-2000." Lancet 359(9317): 1564-1568.

Billeter, M. A., R. Cattaneo, et al. (1994). "Generation and properties of measles virus mutations typically associated with subacute sclerosing panencephalitis." Ann N Y Acad Sci 724: 367-377.

Bolt, G., I. R. Pedersen, et al. (1999). "Processing of N-linked oligosaccharides on the measles virus glycoproteins: importance for antigenicity and for production of infectious virus particles." Virus Res 61(1): 43-51.

Brown, J. A. and P. C. Bridgman (2009). "Disruption of the cytoskeleton during Semaphorin 3A induced growth cone collapse correlates with differences in actin organization and associated binding proteins." Dev Neurobiol 69(10): 633-646.

Browning, M. B., J. E. Woodliff, et al. (2004). "The T cell activation marker CD150 can be used to identify alloantigen-activated CD4(+)25+ regulatory T cells." Cell Immunol 227(2): 129-139.

Calain, P. and L. Roux (1993). "The rule of six, a basic feature for efficient replication of Sendai virus defective interfering RNA." J Virol 67(8): 4822-4830.

Casasnovas, J. M., M. Larvie, et al. (1999). "Crystal structure of two CD46 domains reveals an extended measles virus-binding surface." EMBO J 18(11): 2911-2922.

Casazza, A., P. Fazzari, et al. (2007). "Semaphorin signals in cell adhesion and cell migration: functional role and molecular mechanisms." Adv Exp Med Biol 600: 90-108.

Castellani, V., E. De Angelis, et al. (2002). "Cis and trans interactions of L1 with neuropilin-1 control axonal responses to semaphorin 3A." EMBO J 21(23): 6348-6357.

Catalano, A., P. Caprari, et al. (2006). "Semaphorin-3A is expressed by tumor cells and alters T-cell signal transduction and function." Blood 107(8): 3321-3329.

Cathomen, T., B. Mrkic, et al. (1998). "A matrix-less measles virus is infectious and elicits extensive cell fusion: consequences for propagation in the brain." EMBO J 17(14): 3899-3908.

Cathomen, T., H. Y. Naim, et al. (1998). "Measles viruses with altered envelope protein cytoplasmic tails gain cell fusion competence." J Virol 72(2): 1224-1234.

Cattaneo, R., K. Kaelin, et al. (1989). "Measles virus editing provides an additional cysteine-rich protein." Cell 56(5): 759-764.

Chabbert-de Ponnat, I., A. Marie-Cardine, et al. (2005). "Soluble CD100 functions on human monocytes and immature dendritic cells require plexin C1 and plexin B1, respectively." Int Immunol 17(4): 439-447.

Chen, G., J. Sima, et al. (2008). "Semaphorin-3A guides radial migration of cortical neurons during development." Nat Neurosci 11(1): 36-44.

Choudhuri, K., D. Wiseman, et al. (2005). "T-cell receptor triggering is critically dependent on the dimensions of its peptide-MHC ligand." Nature 436(7050): 578-582.

Colf, L. A., Z. S. Juo, et al. (2007). "Structure of the measles virus hemagglutinin." Nat Struct Mol Biol 14(12): 1227-1228.

Crowley, E. and A. F. Horwitz (1995). "Tyrosine phosphorylation and cytoskeletal tension regulate the release of fibroblast adhesions." J Cell Biol 131(2): 525-537.

Das, T., A. Schuster, et al. (1995). "Involvement of cellular casein kinase II in the phosphorylation of measles virus P protein: identification of phosphorylation sites." Virology 211(1): 218-226.

de Swart, R. L. (2009). "Measles studies in the macaque model." Curr Top Microbiol Immunol 330: 55-72.

de Swart, R. L., M. Ludlow, et al. (2007). "Predominant infection of CD150+ lymphocytes and dendritic cells during measles virus infection of macaques." PLoS Pathog 3(11): e178.

de Witte, L., M. Abt, et al. (2006). "Measles virus targets DC-SIGN to enhance dendritic cell infection." J Virol 80(7): 3477-3486.

de Witte, L., R. D. de Vries, et al. (2008). "DC-SIGN and CD150 have distinct roles in transmission of measles virus from dendritic cells to T-lymphocytes." PLoS Pathog 4(4): e1000049.

Dowling, P. C., B. M. Blumberg, et al. (1986). "Transcriptional map of the measles virus genome." J Gen Virol 67 (Pt 9): 1987-1992.

Dubois, B., P. J. Lamy, et al. (2001). "Measles virus exploits dendritic cells to suppress CD4+ T-cell proliferation via expression of surface viral glycoproteins independently of T-cell trans-infection." Cell Immunol 214(2): 173-183.

Dustin, M. L. (2007). "Cell adhesion molecules and actin cytoskeleton at immune synapses and kinapses." Curr Opin Cell Biol 19(5): 529-533.

Engelking, O., L. M. Fedorov, et al. (1999). "Measles virus-induced immunosuppression in vitro is associated with deregulation of G1 cell cycle control proteins." J Gen Virol 80 (Pt 7): 1599-1608.

Erlenhoefer, C., W. J. Wurzer, et al. (2001). "CD150 (SLAM) is a receptor for measles virus but is not involved in viral contact-mediated proliferation inhibition." J Virol 75(10): 4499-4505.

Erlenhofer, C., W. P. Duprex, et al. (2002). "Analysis of receptor (CD46, CD150) usage by measles virus." J Gen Virol 83(Pt 6): 1431-1436.

Espagnolle, N., D. Depoil, et al. (2007). "CD2 and TCR synergize for the activation of phospholipase Cgamma1/calcium pathway at the immunological synapse." Int Immunol 19(3): 239-248.

Eun, S. Y., B. P. O'Connor, et al. (2006). "Cutting edge: rho activation and actin polarization are dependent on plexin-A1 in dendritic cells." J Immunol 177(7): 4271-4275.

Forthal, D. N., S. Aarnaes, et al. (1992). "Degree and length of viremia in adults with measles." J Infect Dis 166(2): 421-424.

Fournier, P., N. H. Brons, et al. (1997). "Antibodies to a new linear site at the topographical or functional interface between the haemagglutinin and fusion proteins protect against measles encephalitis." J Gen Virol 78 (Pt 6): 1295-1302.

Fukata, Y., T. J. Itoh, et al. (2002). "CRMP-2 binds to tubulin heterodimers to promote microtubule assembly." Nat Cell Biol 4(8): 583-591.

Gassert, E., E. Avota, et al. (2009). "Induction of membrane ceramides: a novel strategy to interfere with T lymphocyte cytoskeletal reorganisation in viral immunosuppression." PLoS Pathog 5(10): e1000623.

Gautier, G., B. de Saint-Vis, et al. (2006). "The class 6 semaphorin SEMA6A is induced by interferon-gamma and defines an activation status of langerhans cells observed in pathological situations." Am J Pathol 168(2): 453-465.

Gerlier, D., G. Varior-Krishnan, et al. (1995). "CD46-mediated measles virus entry: a first key to host-range specificity." Trends Microbiol 3(9): 338-345.

Ghez, D., Y. Lepelletier, et al. (2006). "Neuropilin-1 is involved in human T-cell lymphotropic virus type 1 entry." J Virol 80(14): 6844-6854.

Gomez, T. S. and D. D. Billadeau (2008). "T cell activation and the cytoskeleton: you can't have one without the other." Adv Immunol 97: 1-64.

Grakoui, A., S. K. Bromley, et al. (1999). "The immunological synapse: a molecular machine controlling T cell activation." Science 285(5425): 221-227.

Griffin, D. E. and B. J. Ward (1993). "Differential CD4 T cell activation in measles." J Infect Dis 168(2): 275-281.

Grosjean, I., C. Caux, et al. (1997). "Measles virus infects human dendritic cells and blocks their allostimulatory properties for CD4+ T cells." J Exp Med 186(6): 801-812.

Harty, R. N. and P. Palese (1995). "Measles virus phosphoprotein (P) requires the NH2- and COOH-terminal domains for interactions with the nucleoprotein (N) but only the COOH terminus for interactions with itself." J Gen Virol 76 (Pt 11): 2863-2867.

Hashiguchi, T., M. Kajikawa, et al. (2007). "Crystal structure of measles virus hemagglutinin provides insight into effective vaccines." Proc Natl Acad Sci U S A 104(49): 19535-19540.

Hashimoto, K., N. Ono, et al. (2002). "SLAM (CD150)-independent measles virus entry as revealed by recombinant virus expressing green fluorescent protein." J Virol 76(13): 6743-6749.

He, H., T. Yang, et al. (2009). "Crystal structure of the plexin A3 intracellular region reveals an autoinhibited conformation through active site sequestration." Proc Natl Acad Sci U S A 106(37): 15610-15615.

He, Z. and M. Tessier-Lavigne (1997). "Neuropilin is a receptor for the axonal chemorepellent Semaphorin III." Cell 90(4): 739-751.

Horikami, S. M. and S. A. Moyer (1995). "Structure, transcription, and replication of measles virus." Curr Top Microbiol Immunol 191: 35-50.

Hsu, E. C., F. Sarangi, et al. (1998). "A single amino acid change in the hemagglutinin protein of measles virus determines its ability to bind CD46 and reveals another receptor on marmoset B cells." J Virol 72(4): 2905-2916.

Huber, M., R. Cattaneo, et al. (1991). "Measles virus phosphoprotein retains the nucleocapsid protein in the cytoplasm." Virology 185(1): 299-308.

Ito, Y., I. Oinuma, et al. (2006). "Sema4D/plexin-B1 activates GSK-3beta through R-Ras GAP activity, inducing growth cone collapse." EMBO Rep 7(7): 704-709.

Kantor, D. B., O. Chivatakarn, et al. (2004). "Semaphorin 5A is a bifunctional axon guidance cue regulated by heparan and chondroitin sulfate proteoglycans." Neuron 44(6): 961-975.

Kigel, B., A. Varshavsky, et al. (2008). "Successful inhibition of tumor development by specific class-3 semaphorins is associated with expression of appropriate semaphorin receptors by tumor cells." PLoS One 3(9): e3287.

Klagge, I. M., V. ter Meulen, et al. (2000). "Measles virus-induced promotion of dendritic cell maturation by soluble mediators does not overcome the immunosuppressive activity of viral glycoproteins on the cell surface." Eur J Immunol 30(10): 2741-2750.

Kobune, F., H. Sakata, et al. (1990). "Marmoset lymphoblastoid cells as a sensitive host for isolation of measles virus." J Virol 64(2): 700-705.

Kolodkin, A. L., D. V. Levengood, et al. (1997). "Neuropilin is a semaphorin III receptor." Cell 90(4): 753-762.

Krantic, S., C. Gimenez, et al. (1995). "Cell-to-cell contact via measles virus haemagglutinin-CD46 interaction triggers CD46 downregulation." J Gen Virol 76 (Pt 11): 2793-2800.

Kruse, M., E. Meinl, et al. (2001). "Signaling lymphocytic activation molecule is expressed on mature CD83+ dendritic cells and is up-regulated by IL-1 beta." J Immunol 167(4): 1989-1995.

Kumanogoh, A., S. Marukawa, et al. (2002). "Class IV semaphorin Sema4A enhances T-cell activation and interacts with Tim-2." Nature 419(6907): 629-633.

Kumanogoh, A., C. Watanabe, et al. (2000). "Identification of CD72 as a lymphocyte receptor for the class IV semaphorin CD100: a novel mechanism for regulating B cell signaling." Immunity 13(5): 621-631.

Laine, D., J. M. Bourhis, et al. (2005). "Measles virus nucleoprotein induces cell-proliferation arrest and apoptosis through NTAIL-NR and NCORE-FcgammaRIIB1 interactions, respectively." J Gen Virol 86(Pt 6): 1771-1784.

Laine, D., M. C. Trescol-Biemont, et al. (2003). "Measles virus (MV) nucleoprotein binds to a novel cell surface receptor distinct from FcgammaRII via its C-terminal domain: role in MV-induced immunosuppression." J Virol 77(21): 11332-11346.

Lammermann, T., B. L. Bader, et al. (2008). "Rapid leukocyte migration by integrin-independent flowing and squeezing." Nature 453(7191): 51-55.

Lammermann, T., J. Renkawitz, et al. (2009). "Cdc42-dependent leading edge coordination is essential for interstitial dendritic cell migration." Blood 113(23): 5703-5710.

Lepelletier, Y., S. Lecourt, et al. (2009). "Galectin-1 and Semaphorin-3A are two soluble factors conferring T cell immunosuppression to bone marrow mesenchymal stem cell." Stem Cells Dev.

Lepelletier, Y., I. C. Moura, et al. (2006). "Immunosuppressive role of semaphorin-3A on T cell proliferation is mediated by inhibition of actin cytoskeleton reorganization." Eur J Immunol 36(7): 1782-1793.

Luther, S. A., A. Bidgol, et al. (2002). "Differing activities of homeostatic chemokines CCL19, CCL21, and CXCL12 in lymphocyte and dendritic cell recruitment and lymphoid neogenesis." J Immunol 169(1): 424-433.

Maisner, A., J. Alvarez, et al. (1996). "The N-glycan of the SCR 2 region is essential for membrane cofactor protein (CD46) to function as a measles virus receptor." J Virol 70(8): 4973-4977.

Maisner, A., J. Schneider-Schaulies, et al. (1994). "Binding of measles virus to membrane cofactor protein (CD46): importance of disulfide bonds and N-glycans for the receptor function." J Virol 68(10): 6299-6304.

Manchester, M., M. K. Liszewski, et al. (1994). "Multiple isoforms of CD46 (membrane cofactor protein) serve as receptors for measles virus." Proc Natl Acad Sci U S A 91(6): 2161-2165.

McQuaid, S. and S. L. Cosby (2002). "An immunohistochemical study of the distribution of the measles virus receptors, CD46 and SLAM, in normal human tissues and subacute sclerosing panencephalitis." Lab Invest 82(4): 403-409.

Menezes, J., W. Leibold, et al. (1975). "Establishment and characterization of an Epstein-Barr virus (EBC)-negative lymphoblastoid B cell line (BJA-B) from an exceptional, EBV-genome-negative African Burkitt's lymphoma." Biomedicine 22(4): 276-284.

Milpied, P., A. Renand, et al. (2009). "Neuropilin-1 is not a marker of human Foxp3+ Treg." Eur J Immunol 39(6): 1466-1471.

Minagawa, H., K. Tanaka, et al. (2001). "Induction of the measles virus receptor SLAM (CD150) on monocytes." J Gen Virol 82(Pt 12): 2913-2917.

Mintz, C. D., I. Carcea, et al. (2008). "ERM proteins regulate growth cone responses to Sema3A." J Comp Neurol 510(4): 351-366.

Moll, M., H. D. Klenk, et al. (2001). "A single amino acid change in the cytoplasmic domains of measles virus glycoproteins H and F alters targeting, endocytosis, and cell fusion in polarized Madin-Darby canine kidney cells." J Biol Chem 276(21): 17887-17894.

Moll, M., H. D. Klenk, et al. (2002). "Importance of the cytoplasmic tails of the measles virus glycoproteins for fusogenic activity and the generation of recombinant measles viruses." J Virol 76(14): 7174-7186.

Monks, C. R., B. A. Freiberg, et al. (1998). "Three-dimensional segregation of supramolecular activation clusters in T cells." Nature 395(6697): 82-86.

Moretti, S., A. Procopio, et al. (2008). "Semaphorin3A signaling controls Fas (CD95)-mediated apoptosis by promoting Fas translocation into lipid rafts." Blood 111(4): 2290-2299.

Muller, N., E. Avota, et al. (2006). "Measles virus contact with T cells impedes cytoskeletal remodeling associated with spreading, polarization, and CD3 clustering." Traffic 7(7): 849-858.

Naniche, D., T. F. Wild, et al. (1992). "A monoclonal antibody recognizes a human cell surface glycoprotein involved in measles virus binding." J Gen Virol 73 (Pt 10): 2617-2624.

Neufeld, G. and O. Kessler (2008). "The semaphorins: versatile regulators of tumour progression and tumour angiogenesis." Nat Rev Cancer 8(8): 632-645.

Niewiesk, S., I. Eisenhuth, et al. (1997). "Measles virus-induced immune suppression in the cotton rat (Sigmodon hispidus) model depends on viral glycoproteins." J Virol 71(10): 7214-7219.

Niewiesk, S., H. Ohnimus, et al. (1999). "Measles virus-induced immunosuppression in cotton rats is associated with cell cycle retardation in uninfected lymphocytes." J Gen Virol 80 (Pt 8): 2023-2029.

Nolz, J. C., R. B. Medeiros, et al. (2007). "WAVE2 regulates high-affinity integrin binding by recruiting vinculin and talin to the immunological synapse." Mol Cell Biol 27(17): 5986-6000.

Norcross, M. A. (1984). "A synaptic basis for T-lymphocyte activation." Ann Immunol (Paris) 135D(2): 113-134.

O'Connor, B. P. and J. P. Ting (2008). "The evolving role of semaphorins and plexins in the immune system: Plexin-A1 regulation of dendritic cell function." Immunol Res 41(3): 217-222.

Ohta, K., A. Mizutani, et al. (1995). "Plexin: a novel neuronal cell surface molecule that mediates cell adhesion via a homophilic binding mechanism in the presence of calcium ions." Neuron 14(6): 1189-1199.

Okada, H., T. A. Sato, et al. (2001). "Comparative analysis of host responses related to immunosuppression between measles patients and vaccine recipients with live attenuated measles vaccines." Arch Virol 146(5): 859-874.

Ono, N., H. Tatsuo, et al. (2001). "Measles viruses on throat swabs from measles patients use signaling lymphocytic activation molecule (CDw150) but not CD46 as a cellular receptor." J Virol 75(9): 4399-4401.

Ono, N., H. Tatsuo, et al. (2001). "V domain of human SLAM (CDw150) is essential for its function as a measles virus receptor." J Virol 75(4): 1594-1600.

Peltola, H., O. P. Heinonen, et al. (1994). "The elimination of indigenous measles, mumps, and rubella from Finland by a 12-year, two-dose vaccination program." N Engl J Med 331(21): 1397-1402.

Perrot, V., J. Vazquez-Prado, et al. (2002). "Plexin B regulates Rho through the guanine nucleotide exchange factors leukemia-associated Rho GEF (LARG) and PDZ-RhoGEF." J Biol Chem 277(45): 43115-43120.

Plemper, R. K., A. L. Hammond, et al. (2001). "Measles virus envelope glycoproteins hetero-oligomerize in the endoplasmic reticulum." J Biol Chem 276(47): 44239-44246.

Plemper, R. K., A. L. Hammond, et al. (2002). "Strength of envelope protein interaction modulates cytopathicity of measles virus." J Virol 76(10): 5051-5061.

Radecke, F. and M. A. Billeter (1996). "The nonstructural C protein is not essential for multiplication of Edmonston B strain measles virus in cultured cells." Virology 217(1): 418-421.

Rager, M., S. Vongpunsawad, et al. (2002). "Polyploid measles virus with hexameric genome length." EMBO J 21(10): 2364-2372.

Ravanel, K., C. Castelle, et al. (1997). "Measles virus nucleocapsid protein binds to FcgammaRII and inhibits human B cell antibody production." J Exp Med 186(2): 269-278.

Renkawitz, J., K. Schumann, et al. (2009). "Adaptive force transmission in amoeboid cell migration." Nat Cell Biol 11(12): 1438-1443.

Richardson, C. D. and P. W. Choppin (1983). "Oligopeptides that specifically inhibit membrane fusion by paramyxoviruses: studies on the site of action." Virology 131(2): 518-532.

Rima, B. K., J. A. Earle, et al. (1995). "Measles virus strain variations." Curr Top Microbiol Immunol 191: 65-83.

Ryon, J. J., W. J. Moss, et al. (2002). "Functional and phenotypic changes in circulating lymphocytes from hospitalized zambian children with measles." Clin Diagn Lab Immunol 9(5): 994-1003.

Santiago, C., M. L. Celma, et al. (2010). "Structure of the measles virus hemagglutinin bound to the CD46 receptor." Nat Struct Mol Biol 17(1): 124-129.

Sarris, M., K. G. Andersen, et al. (2008). "Neuropilin-1 expression on regulatory T cells enhances their interactions with dendritic cells during antigen recognition." Immunity 28(3): 402-413.

Sato, T. A., T. Kohama, et al. (1988). "Intracellular processing of measles virus fusion protein." Arch Virol 98(1-2): 39-50.

Schlender, J., J. J. Schnorr, et al. (1996). "Interaction of measles virus glycoproteins with the surface of uninfected peripheral blood lymphocytes induces immunosuppression in vitro." Proc Natl Acad Sci U S A 93(23): 13194-13199.

Schneider-Schaulies, J., J. J. Schnorr, et al. (1996). "Receptor (CD46) modulation and complement-mediated lysis of uninfected cells after contact with measles virus-infected cells." J Virol 70(1): 255-263.

Schneider-Schaulies, S., K. Bieback, et al. (2002). "Regulation of gene expression in lymphocytes and antigen-presenting cells by measles virus: consequences for immunomodulation." J Mol Med 80(2): 73-85.

Schneider-Schaulies, S., H. W. Kreth, et al. (1991). "Expression of measles virus RNA in peripheral blood mononuclear cells of patients with measles, SSPE, and autoimmune diseases." Virology 182(2): 703-711.

Schnorr, J. J., M. Seufert, et al. (1997). "Cell cycle arrest rather than apoptosis is associated with measles virus contact-mediated immunosuppression in vitro." J Gen Virol 78 (Pt 12): 3217-3226.

Servet-Delprat, C., P. O. Vidalain, et al. (2000). "Measles virus induces abnormal differentiation of CD40 ligand-activated human dendritic cells." J Immunol 164(4): 1753-1760.

Seya, T., A. Hirano, et al. (1999). "Human membrane cofactor protein (MCP, CD46): multiple isoforms and functions." Int J Biochem Cell Biol 31(11): 1255-1260.

Shaffer, J. A., W. J. Bellini, et al. (2003). "The C protein of measles virus inhibits the type I interferon response." Virology 315(2): 389-397.

Sheppard, R. D., C. S. Raine, et al. (1986). "Rapid degradation restricts measles virus matrix protein expression in a subacute sclerosing panencephalitis cell line." Proc Natl Acad Sci U S A 83(20): 7913-7917.

Shimizu, A., A. Mammoto, et al. (2008). "ABL2/ARG tyrosine kinase mediates SEMA3F-induced RhoA inactivation and cytoskeleton collapse in human glioma cells." J Biol Chem 283(40): 27230-27238.

Shishkova, Y., H. Harms, et al. (2007). "Immune synapses formed with measles virus-infected dendritic cells are unstable and fail to sustain T cell activation." Cell Microbiol 9(8): 1974-1986.

Suryanarayana, K., K. Baczko, et al. (1994). "Transcription inhibition and other properties of matrix proteins expressed by M genes cloned from measles viruses and diseased human brain tissue." J Virol 68(3): 1532-1543.

Suto, F., M. Tsuboi, et al. (2007). "Interactions between plexin-A2, plexin-A4, and semaphorin 6A control lamina-restricted projection of hippocampal mossy fibers." Neuron 53(4): 535-547.

Suzuki, K., A. Kumanogoh, et al. (2008). "Semaphorins and their receptors in immune cell interactions." Nat Immunol 9(1): 17-23.

Swiercz, J. M., R. Kuner, et al. (2002). "Plexin-B1 directly interacts with PDZ-RhoGEF/LARG to regulate RhoA and growth cone morphology." Neuron 35(1): 51-63.

Takagi, S., T. Hirata, et al. (1991). "The A5 antigen, a candidate for the neuronal recognition molecule, has homologies to complement components and coagulation factors." Neuron 7(2): 295-307.

Takahashi, T., A. Fournier, et al. (1999). "Plexin-neuropilin-1 complexes form functional semaphorin-3A receptors." Cell 99(1): 59-69.

Takahashi, T. and S. M. Strittmatter (2001). "Plexina1 autoinhibition by the plexin sema domain." Neuron 29(2): 429-439.

Takamatsu, H., N. Takegahara, et al. (2010). "Semaphorins guide the entry of dendritic cells into the lymphatics by activating myosin II." Nat Immunol 11(7): 594-600.

Tamagnone, L., S. Artigiani, et al. (1999). "Plexins are a large family of receptors for transmembrane, secreted, and GPI-anchored semaphorins in vertebrates." Cell 99(1): 71-80.

Tatsuo, H., N. Ono, et al. (2001). "Morbilliviruses use signaling lymphocyte activation molecules (CD150) as cellular receptors." J Virol 75(13): 5842-5850.

Tong, Y., P. Chugha, et al. (2007). "Binding of Rac1, Rnd1, and RhoD to a novel Rho GTPase interaction motif destabilizes dimerization of the plexin-B1 effector domain." J Biol Chem 282(51): 37215-37224.

Tong, Y., P. K. Hota, et al. (2009). "Structure and function of the intracellular region of the plexin-b1 transmembrane receptor." J Biol Chem 284(51): 35962-35972.

Topley, W. W. C., G. S. S. Wilson, et al. (2005). Topley & Wilson's microbiology & microbial infections. London, Hodder Arnold.

Tordjman, R., Y. Lepelletier, et al. (2002). "A neuronal receptor, neuropilin-1, is essential for the initiation of the primary immune response." Nat Immunol 3(5): 477-482.

Toyofuku, T., J. Yoshida, et al. (2005). "FARP2 triggers signals for Sema3A-mediated axonal repulsion." Nat Neurosci 8(12): 1712-1719.

Uchida, Y., T. Ohshima, et al. (2005). "Semaphorin3A signalling is mediated via sequential Cdk5 and GSK3beta phosphorylation of CRMP2: implication of common phosphorylating mechanism underlying axon guidance and Alzheimer's disease." Genes Cells 10(2): 165-179.

Valsamakis, A., H. Schneider, et al. (1998). "Recombinant measles viruses with mutations in the C, V, or F gene have altered growth phenotypes in vivo." J Virol 72(10): 7754-7761.

Vardhana, S., K. Choudhuri, et al. (2010). "Essential role of ubiquitin and TSG101 protein in formation and function of the central supramolecular activation cluster." Immunity 32(4): 531-540.

Varma, R., G. Campi, et al. (2006). "T cell receptor-proximal signals are sustained in peripheral microclusters and terminated in the central supramolecular activation cluster." Immunity 25(1): 117-127.

Vidalain, P. O., O. Azocar, et al. (2000). "Measles virus induces functional TRAIL production by human dendritic cells." J Virol 74(1): 556-559.

Wardrop, E. A. and D. J. Briedis (1991). "Characterization of V protein in measles virus-infected cells." J Virol 65(7): 3421-3428.

Waugh, C., L. Sinclair, et al. (2009). "Phosphoinositide (3,4,5)-triphosphate binding to phosphoinositide-dependent kinase 1 regulates a protein kinase B/Akt signaling threshold that dictates T-cell migration, not proliferation." Mol Cell Biol 29(21): 5952-5962.

Weidmann, A., C. Fischer, et al. (2000). "Measles virus-induced immunosuppression in vitro is independent of complex glycosylation of viral glycoproteins and of hemifusion." J Virol 74(16): 7548-7553.

Weidmann, A., A. Maisner, et al. (2000). "Proteolytic cleavage of the fusion protein but not membrane fusion is required for measles virus-induced immunosuppression in vitro." J Virol 74(4): 1985-1993.

WHO (2009). "Measles." (Factsheet N-286).

Wong, A. W., W. J. Brickey, et al. (2003). "CIITA-regulated plexin-A1 affects T-cell-dendritic cell interactions." Nat Immunol 4(9): 891-898.

Yamamoto, M., K. Suzuki, et al. (2008). "Plexin-A4 negatively regulates T lymphocyte responses." Int Immunol 20(3): 413-420.

Yokota, S., H. Saito, et al. (2003). "Measles virus suppresses interferon-alpha signaling pathway: suppression of Jak1 phosphorylation and association of viral accessory proteins, C and V, with interferon-alpha receptor complex." Virology 306(1): 135-146.

Young, D. F., L. Didcock, et al. (2000). "Paramyxoviridae use distinct virus-specific mechanisms to circumvent the interferon response." Virology 269(2): 383-390.

Zanata, S. M., I. Hovatta, et al. (2002). "Antagonistic effects of Rnd1 and RhoD GTPases regulate receptor activity in Semaphorin 3A-induced cytoskeletal collapse." J Neurosci 22(2): 471-477.

Zhu, D. M., M. L. Dustin, et al. (2006). "Mechanisms of Cellular Avidity Regulation in CD2-CD58-Mediated T Cell Adhesion." ACS Chem Biol 1(10): 649-658.

8. Publication

Paper

Conferences

Annual measles virus meeting, Würzburg, 2007
Localization and function of adhesion/repulsion receptors in the immunological synapse.

Annual measles virus meeting, Würzburg, 2008
Localization and function of adhesion/repulsion receptors in the IS formed between T cells and mature or infected DCs.

Annual measles virus meeting, Würzburg, 2009
Regulation of plexins on DCs and T cells, and their role in immunological synapse (IS) architecture and function.

Posters

Wü-Erl-Tüb Immunology training network, Rotherburg a.d. Tauber, 2008
Localization and function of adhesion/repulsion receptors in the IS formed between T cells and mature or infected DCs.

Wü-Erl-Tüb Immunology training network, Schöntal, 2009
Regulation of plexins on DCs and T cells, and their role in immunological synapse (IS) architecture and function.